SEPARATION PROCESSES IN MICROALGAE BIOREFINING

Claudia Nurra

Separation processes in microalgae biorefining

Dissertation presented by

Claudia Nurra

To obtain the degree of:

"Doctor per la Universitat Rovira i Virgili"

Department of Chemical Engineering

Universitat Rovira i Virgili

UNIVERSITAT ROVIRA I VIRGILI

Tarragona, Spain, September 2014

Author: Claudia Nurra

PhD Thesis, Universitat Rovira i Virgili

Spain, September 2014

Separation processes in microalgae biorefining

Dissertation presented by

Claudia Nurra

To obtain the degree of:

"Doctor per la Universitat Rovira i Virgili"

Department of Chemical Engineering

Universitat Rovira i Virgili

UNIVERSITAT ROVIRA I VIRGILI

Tarragona, Spain, September 2014

Thesis supervised by Dr. Carles Torras Font

UNIVERSITAT ROVIRA I VIRGILI
SEPARATION PROCESSES IN MICROALGAE BIOREFINING
Claudia Nurra

This thesis has been approved by the supervisor:

Dr. Carles Torras Font

Composition of the Examination Committee:

Prof. Dr. Joan Salvadó, Rovira i Virgili, Spain, Tarragona (president)

Prof. Dr. Albert Ibarz, Universitat de Lleida, Spain, Lleida (secretary)

Prof. Dr. Ir. Michiel Makkee, Delft University of Technology, The Netherlands, Delft (tribunal member)

Prof. Dr. Xavier Farriol, Rovira i Virgili, Spain, Tarragona (substitute)

Prof. Dr. Jorge Gascon, Delft University of Technology, The Netherlands, Delft (substitute)

Prof. Dr. Jordi Pagán-Gilabert, Universitat de Lleida, Spain, Lleida (substitute)

External evaluators:

Prof. Dr. Jorge Gascon, Delft University of Technology, The Netherlands, Delft

Prof. Dr. Clemens Posten, Karlsruhe Institute of Technology, Germany, Karlsruhe

The research reported in this thesis was conducted in the Bioenergy and Biodiesel division of the Catalonia Institute for Energy Research (IREC) of Tarragona.

PhD Thesis, Universitat Rovira i Virgili

With summary in Spanish

UNIVERSITAT ROVIRA I VIRGILI
SEPARATION PROCESSES IN MICROALGAE BIOREFINING
Claudia Nurra

Institut de Recerca en Energia de Catalunya
Catalonia Institute for Energy Research

I STATE that the present study entitled

"Separation process in microalgae biorefining"

Presented by *Claudia Nurra* for the award of the degree of Doctor, has been developed under my supervision in the Bioenergy and Biofuels division of the Catalonia Institute for Energy Research (IREC) and that it fulfills the requirements to be eligible for the degree of Doctor (PhD) in Chemical Environmental and Process Engineering and for the International Mention.

Tarragona, 8th September 2014

Doctoral Thesis Supervisor

Dr. Carles Torras Font
Researcher, IREC

UNIVERSITAT ROVIRA I VIRGILI
SEPARATION PROCESSES IN MICROALGAE BIOREFINING
Claudia Nurra

To my family

UNIVERSITAT ROVIRA I VIRGILI
SEPARATION PROCESSES IN MICROALGAE BIOREFINING
Claudia Nurra

CONTENTS

UNIVERSITAT ROVIRA I VIRGILI
SEPARATION PROCESSES IN MICROALGAE BIOREFINING
Claudia Nurra

LIST OF FIGURES

UNIVERSITAT ROVIRA I VIRGILI
SEPARATION PROCESSES IN MICROALGAE BIOREFINING
Claudia Nurra

LIST OF TABLES

UNIVERSITAT ROVIRA I VIRGILI
SEPARATION PROCESSES IN MICROALGAE BIOREFINING
Claudia Nurra

ABBREVIATIONS

ABS: Acrylonitrile-butadiene-styrene

AFM: Atomic force microscopy

CA: Cellulose acetate

CMR: Catalytic membrane reactor

CSPM: Corrugated pore structure model

DAF: Dissolved air flottation

DCM: Dichloromethane

DG: Diglycerides

DMA: Dimethylacetamide

DMF: N,N-dimethylformamide

DSC: Differential scanning calorimetry

EDL: electrical double layer

ESEM: Environmental scanning electron microscopy

FAME: Fatty acid methyl esters

FESEM: Field emission scanning electron microscopy

GC: Gas chromatography

MF: Microfiltration

MG: Monoglycerides

NF: Nanofiltration

NMP: 1-Methyl-2-pyrrolidone

P: Permeation constant

PAN: Polyacrylonitrile

PETG: Glycol-modified polyethylene terephthalate

PES: Polyethersulfone

PLA: PolyLactic Acid

PSD: Pore size distribution

PSf: Polysulfone

SEM: Scanning elector microscopy

SHC: Solid heterogeneous catalyst

SrO: Strontium oxide

TEM: Transmission electron microscopy

TG: Triglycerides

THF: Tetrahydrofuran

TMP: Transmembrane pressure

UF: Ultrafiltration

VFR: Volumetric flux reduction

VSEP: Vibratory shear enhanced process

SUMMARY

This thesis focuses on the development of new approaches for separation processes in biodiesel production from microalgae by membrane technology. Biodiesel production from microalgae is a subject being developed in the last years that still needs more investigation in order to reduce its costs. Among all steps involved in the process, this thesis focuses on harvesting, in particular to the investigation of the microalgae dewatering by using several membrane filtration techniques, and on the transesterification by using a catalyzed membrane reactor. Harvesting step is one of the major step responsible of the final cost of microalgae biodiesel, and the transesterification reaction needs the utilisation of large quantity of water and many stages that both make it unfeasible for this application. Improvements are needed in this sense, starting from the research of cheaper methods for the first process to simpler configurations for the latter one.

To reach these goals specific studies have been performed for this application on: (i) new materials in membrane filtration, from polymers already known to polymers usually not employed in membrane industry; (ii) new technologies in microalgae dewatering, as vibrating cross-flow filtration system; (iii) new perspectives in the transesterification reaction, with the utilization of heterogeneous catalyst immobilized on a membrane.

The cost is the first inconvenience for microalgae biodiesel production feasibility and harvesting step is the major contributor, as commented previously. Therefore, this work has

been primarily addressed to the first two studies. The replacement of centrifugation with membrane filtration has been considered as a solution to make harvesting cheaper.

In a first stage, an in-depth study in membrane materials have been performed, first with polymers commonly used in membrane industry (ceramic, PSf, PAN), later with ones generally commercialized in the packaging industries (ABS, PETg, PLA) and finally one polymer coming from sawdust of Pinus sp. (CA). In this sense one of the scopes of the work presented involves the study of the synthesis of polymeric membranes and their characterization.

Membrane technology is successfully used in many applications, but its weak point is cake formation and fouling. To decrease these phenomena vibrating cross flow filtration performances have been studied, in a second stage, as alternative of conventional one with different species of microalgae and different membrane cut-off and polymeric materials. Considerable attention has been dedicated to the complete understanding of membrane filtration technology in this application from the laboratory to the pilot plant scale.

In a third stage transesterification process in a membrane reactor has been studied. The aim was to substitute homogeneous catalyst with heterogeneous one and immobilizing it in/on a polymeric membrane. To achieve this objective various catalysts and immobilization techniques were studied.

For the evaluation of fouling phenomena, permeability is the most studied parameter in membrane filtration technology. This parameter depends from many variables and its study

is particularly important when synthesized membranes with unknown characteristics are used. To simply its attainment a final theoretical study has been carried out on membrane permeability prediction by the development of a model conceived for porous membranes.

UNIVERSITAT ROVIRA I VIRGILI
SEPARATION PROCESSES IN MICROALGAE BIOREFINING
Claudia Nurra

RESUMEN (SPANISH VERSION)

Esta tesis se centra en el desarrollo de nuevos enfoques para procesos de separación en la producción de biodiesel a partir de microalgas mediante tecnología de membranas. La producción de biodiesel a partir de microalgas es un tema que se está desarrollando en los últimos años y que todavía necesita más investigación con el fin de reducir sus costos. Entre todas las etapas implicadas en el proceso, esta tesis se centra en la recolección, en particular en la investigación de la deshidratación mediante el uso de microalgas mediante varias técnicas de filtración de membrana, y en la transesterificación mediante el uso de un reactor de membrana catalítico. La etapa de cosechado es una de los principales responsables del coste final de biodiesel de microalgas, y la reacción de transesterificación necesita la utilización de demasiada cantidad de agua, uso de reactivos, y diversas etapas. Se necesitan mejoras en este sentido, a partir de la investigación de métodos más económicos para el primer proceso a configuraciones más eficientes para el último.

Para alcanzar estos objetivos se han realizado estudios específicos para esta aplicación en: (i) nuevos materiales en la filtración por membrana, a partir de polímeros ya conocidos (PSf, PAN) a polímeros generalmente no empleados en la industria de la membrana (ABS, PETG, CA de serrín); (ii) nuevas tecnologías en la deshidratación de las microalgas, como sistema de filtración vibratorio; (iii) nuevas perspectivas en la reacción de transesterificación, con la utilización de catalizador heterogéneo inmovilizado en una membrana polimérica.

El coste es el primer inconveniente en la producción del biodiesel de microalgas y el cosechado es uno de los principales contribuyentes, como se ha comentado anteriormente. Por lo tanto, este trabajo se ha dirigido a los dos primeros estudios en su mayor parte. La sustitución de centrifugación con filtración por membrana ha sido considerada como una solución para hacer el cosechado más barato.

En una primera etapa, se han realizado un profundo estudio de los materiales de membrana, primero con polímeros de uso común en la industria de la membrana (PSf, PAN), después con los comerciales generalmente usados en las industrias de envasado (ABS, PETG) y, finalmente, un polímero procedente de aserrín de Pinus sp. (CA). En este sentido, uno de los ámbitos del trabajo presentado implica el estudio de la síntesis de membranas poliméricas y su caracterización.

La tecnología de membrana se utiliza con éxito en muchas aplicaciones, pero su punto débil es la formación de la torta en su superficie y su ensuciamiento. Para disminuir estos fenómenos, se ha estudiado el proceso de filtración vibratorio, como alternativa a la filtración convencional. Fueron utilizadas diferentes especies de microalgas y diferentes membranas con distintos cortes y materiales. Una considerable atención se ha dedicado a la comprensión completa de la tecnología de filtración por membrana en esta aplicación desde la escala laboratorio hasta la escala de planta piloto.

En una tercera etapa, se ha estudiado el proceso de transesterificación en un reactor de membrana. El objetivo era sustituir el catalizador homogéneo, usualmente utilizado, por uno

heterogéneo y inmovilizarlo en una membrana polimérica. Para lograr este objetivo diversos catalizadores y técnicas de inmovilización fueron estudiados.

Por último, la permeabilidad es el parámetro más estudiado en la tecnología de filtración por membrana. Este parámetro depende de muchas variables y su estudio es particularmente importante cuando se utilizan membranas sintetizadas con características desconocidas. Para optimizar su obtención, un estudio teórico se ha llevado a cabo para predecir la permeabilidad de membranas porosas con el desarrollo de un modelo basado en micrografías de corte transversal de membranas y los modelos de Darcy y Hagen-Poiseuille.

1

1. INTRODUCTION

This chapter aims to introduce a research on microalgae dewatering by membrane filtration. Membrane filtration is a field well known even if quite recent, but its application in microalgae biorefinery is not much explored yet. The intention of this work was to improve membrane knowledge and costs applied in microalgae biorefinery.

This chapter is addressed to the motivations, scope and objectives of this investigation. Last section of this chapter contextualizes the application field of this work.

1.1 Motivations

The motivation of this thesis was born with the interest of research on environmental issues, water treatments and sea products, interest born from previous studies and research experience.

The need to find a substitution to fuel is increasing year by year and microalgae biodiesel production is one of the possible ways to be considered in combination with other alternatives.

Membrane technology is attractive and used in many processes due to its versatility and precision.

1.2 Thesis scope

The scope of this thesis was to find better alternatives of separation in two of the many steps of the microalgae biorifining process. Cheaper, less energy demander and faster alternatives in the micoalgae dewatering step with membrane filtration and simpler one in the transesterification step.

1.3 Hypothesis

Key separation steps in microalgae biorefining, among others, are: (1) microalgae concentration by using static and dynamic filtration; (2) separation of FAME, methanol and glycerol from the transesterification process.

- Producing other products together with biodiesel can make the overall process economically viable.
    - A cost effective process to concentrate microalgae can be reached by combining properly several separation techniques including flocculation/sedimentation and membrane process.
    - Dynamic filtration, such as rotating or vibrating modules, enhances microalgae membrane concentration because of the reduction of fouling effects and concentration polarization.
    - Permeability, including fouling effects, can be modelled with morphological parameters, like porosity, tortuosity, *etc.*
- Regarding to the transesterification process:

- Performance of transesterification process can be improved by using an optimized membrane reactor.
- Catalyst inclusion in membrane reactor can significantly improve performance.

1.4 Objectives

The main objective of this thesis is to improve microalgae biorefining process by optimizing separation and membrane process within the overall process.

Specific objectives:

- To find proper combination of separation techniques in microalgae concentration.
- To study in depth microalgae concentration by using conventional and vibrating cross flow filtration.
  - Evaluation of different types of modules,
  - Evaluation of different membrane materials and characteristics,
- To study the viability of a catalytic membrane reactor for transesterification.
  - Identification of proper catalyst to include in the membrane reactor for the transesterification reaction,
  - Evaluation of different types of catalyst,
  - Development of a polymeric membrane reactor, characterization and testing.
- To develop a mathematical model for the prediction of membrane permeability.

1.5 Document description

A general introduction and a review of the current state of biodiesel production from microalgae are described in the present chapter (**Chapter 1**). This chapter is important to introduce the reader in the topic and to understand the interest on membrane thecnology for this application.

In **Chapter 2** the membrane synthesis with cheap and new materials for this application is presented, by the well known phase inversion process with immersion precipitation,. **Chapter 3** describes the dewatering process using a vibrating system and the differences observed between this vibrating system and the conventional cross flow filtration. Results will be compared with the same conditions, but at a pilot plant scale.

In the **Chapter 4** the transesterification reaction with heterogeneus catalyst is explored. **Chapter 5** is intented to model the work performed in the development of a tool for permeability calculation starting from the knowledge of membrane variables. Finally, general conclusions and future work of this thesis are presented.

Note that all chapters have been written as individual publications and can be read independently.

1.6 Background

The interest for microalgae lies in their potential utilization in several fields. First, studies were addressed to mariculture feed, fine chemicals and health food industries (omega 3 oil, chlorophyll, livestock feed), then the interest for this raw material started also in

pharmaceutical and nutraceutical industries, in agriculture as biofertilizer, as bioremediation of water pollution and, finally, as a power source to obtain different kinds of products as biomass to produce hydrogen, biomethane, bioethanol and biodiesel [1-7].

There are several advantages using microalgae as a feedstock instead of terrestrial plants; typical raw materials of biodiesel are rapeseed oil, canola oil, soybean oil, sunflower oil and palm oil. But, contrariwise of these, for microalgae there is not the necessity to encroach valuable crop and virgin land and it is not required to fertilize soils; algae can grow practically anywhere. Some algae can grow in saline water and they can be produced in laboratory. This is essential also because all parameters can be controlled, and, if marine algae are used, there is no need to carry important and often supplies of freshwater [4-14]. Advantage to use microalgae as raw material is also that they can be converted with a large number of different methods to obtain liquid fuel and gas, using biochemical or thermo-chemical processes. The former one will produce ethanol and biodiesel and the second one will produce oil and gas. Microalgae can be also directly combusted, even if it is not convenient because of high water content.

The process to produce biodiesel from microalgae consists in many steps, that can be summarized with four: cultivation, concentration, lipid extraction and, finally, transesterification + separation.

After the cultivation process a dewatering step is required. Common methods are: flocculation/sedimentation, dissolved air flotation (DAF), centrifugation and filtration processes. The flocculation/sedimentation process refers to the aggregation of microalgae in a suspension to form masses that subsequently can settle. It is done with different types of usual (aluminium sulphate, ferric chloride, ferric sulphate) and “unusual” (chitosan)

flocculants. This process reduces the need of energy intensive separation mechanisms like centrifugation. Even if flocculation is an economic method, the concentration obtained is low (<10% of solids content) [4]. This means that it is necessary further concentration using other methods. For this reason, it is commonly used as an initial dewatering step and centrifugation is the most combined method use with it. Centrifugation is the preferred one, but the shear forces during the process can disrupt cells and costs are high because it is energy intensive.

Alternatively a membrane microfiltration (MF) and ultra-filtration (UF) process can be performed, which are more suitable for fragile cells and small-scale production processes [1-7]. Filtration is the method that, still now, has proved to be competitive compared to all of them. But in this case it is appropriate doing a preliminary test. The reason is that the filtration efficiency is highly dependent on the size range of the species to be harvested. Studies are mainly addressed to MF and UF membranes, because of their size (in general higher than 4 micrometers and up to hundreds of micrometers, depending on the specie). This process allows the use of both polymeric and ceramic membranes. For the polymeric membranes several production methods can be used: stretched films, nucleation track, phase inversion, extrusion, casting solution, interfacial polymerization, and plasma polymerization. A most common method is the phase inversion one, because of its simplicity and versatility.

After membrane synthesis a step of membrane characterization should be carried out, to determine its characteristics. Many parameters can be studied, but the main important are: zeta potential, hydrophilicity/hydrophobicity, molecular weight cut-off (rejection), pore size, porosity and distribution.

The interaction between a charged membrane and a charged solution, which is pushed through the membrane pores with the application of a pressure or electric potential gradient,

causes some complex processes commonly called electrokinetic phenomena. Membranes, like most materials, acquire an electrical charge when they are left in contact with a polar medium. This leads to the formation of an "electrical double layer (EDL)" that restores the electro-neutrality in the solution. The same process appears around the solute molecules or particles. Among the parameters that characterize these EDL, one of the most relevant is the electrostatic potential, usually called zeta potential, ζ. The importance of zeta potential in describing and quantifying particle–surface interactions is increasingly recognised. A relevant example can be drawn from the strong dependence of protein fouling in microfiltration processes with the zeta potential of the surface and the charge of the protein. Recently it has been demonstrated that steady-state ultrafiltration flux increases with the square of the zeta potential of the particles [15].

For the evaluation of membrane surface hydrophilicity/hydrophobicity the contact angle is widely utilized owing to the simplicity of the method. Only small pieces of membrane are needed for the measurements that are fast to perform. The most common technique used for these measurements is the sessile drop method. Additionally, morphological, electrical and chemical surface changes associated to the addition of several additives or to the annealing at different temperatures are studied [16-18]. Studies regarding membrane characterization and modification are addressed to permeation flux and fouling phenomenon with special considerations on cut-off, constitutive materials and surface properties (charge, hydrophilicity) [14, 19-24].

To determine the porosity of a given material there are several methods. The main ones can be classified as indirect and direct methods. Among the direct methods, the most used are: apparent densities estimation, pycnometric methods and mercury intrusion. Indirect

methods allow the calculation of porosity only when a given geometry and/or size distribution of the pores is assumed. Some of the most frequently used indirect methods are: liquid permeability, permporometry, air-liquid or liquid-liquid porometry, microscopy methods (SEM: Scanning Electron Microscopy, TEM: Transmission Electron Microscopy, FESEM: Field Emission Scanning Electron Microscopy and AFM: Atomic Force Microscopy, *etc.*), gas adsorption-desorption and thermoporometry. This kind of evaluation is shown to be very useful [18, 25, 26], especially because sometimes manufacturer values deviate from measured ones. The best method to determine porosities depends on the material to be characterized and on how this method will be applied. A difficulty, which is common to all direct methods, is that these techniques can detect non-active pores, for example dead-end pores, or interstices not opened to flow. A proper knowledge of the pore size distribution (PSD) is of great interest to estimate the kind of particles these membranes should retain. Several complimentary methods could be employed to determine the PSD of porous membranes, including the microscopic observation methods (SEM or AFM), the bubble pressure method, usually known as gas–liquid displacement method, the mercury intrusion porosimetry, the permporometry, the gas adsorption–desorption method, *etc*. All these methods together cover a broad range in applicability, sensitivity, and information. However, some of them present specific disadvantages such as irreversible damage of the samples or long time consumption, which strongly limited their general application. Additionally, some of them, as occurs with mercury intrusion or gas adsorption–desorption techniques, need to assume additional features on the shape and structure of the pores in order to obtain porometric information, which makes the interpretation of their results more difficult and less reliable. Others as DSC thermoporometry are limited in the range of detectable pore sizes. Finally, thermoporometry, gas adsorption–desorption and mercury porosimetry and all the

microscopic techniques are unable to distinguish between pores contributing to the actual flow (active pores) and other pores/voids that do not control permeation.

Membranes can also be modified to improve their properties. With this objective, different methods can be used depending on the final aim. In general, membranes modifications are addressed to improve first of all fouling resistance, but also flux and selectivity, chemical resistance, to control pore size and to eliminate eventual defects. The most used modification method to improve fouling resistance is the surface coating. For the other goals modification methods studied still now are: annealing (heat and solvent treatment), solvent-exchange and chemical treatment (fluorination, cross-linking and pyrolysis) [27].

Algae are difficult to remove with conventional pre-treatment methods. MF and UF membranes are effective, but algal cells deposit on the membrane surface cause severe resistance to filtration. To find an efficient membrane technology for algae biomass concentration it is necessary to develop anti-fouling strategies. It is demonstrated that to have the minimum value of reversible fouling resistance the cross flow velocity should be controlled [23]. Lower values give higher fouling effects and higher values do not give significant differences.

Fouling and concentration polarization can be reduced, not only by modifying the membrane, but also using dynamic filtration instead of traditional static one. In fact, it is demonstrated that increasing shear rate makes it harder for algae to deposit on membrane; this means that a higher flux can be obtained with consequently reduction of concentration polarization and cake build-up [22-24]. To obtain this result without decreasing trans-membrane pressure a dynamic or shear-enhanced filtration can be used [28, 29]. Rotating disk and vibrating

systems have been studied. Three types of dynamic filtration have been studied in particular: with rotors between fixed membranes and rotating or vibrating membranes. The characteristics of these types of dynamic filtrations have been studied in various models produced by different manufacturers, with polymeric or ceramic membranes. Others studies in this field demonstrated that further improvement can be obtained by adding straight vanes of various height to rotating disks fixed in a dynamic filtration module. Studies show that this system yields higher permeate fluxes than conventional cross-flow filtration, but at the same time it is more expensive and complex, and it may consume more energy [30]. Dynamic modules performances, as well as static ones, can be improved also with in-depth analysis of pressure and flow distribution on the membranes, their share rate and others boundary conditions effects. Computational Fluid Dynamics is demonstrated to be a helpful tool to achieve these analyses [31].

After harvesting, biomass has to be processed further to produce feedstock (*i.e.* lipid fraction) for biofuels production [6]. This means that it needs an extracting phase. Methods to extract lipids can be various, like: expeller/oil press, osmotic shock, solvent extraction, supercritical fluid extraction (SFE) and ultrasound techniques [3-13]. Solvent extraction is the most used method for lipid extraction in biodiesel production still now. It is normally done directly from the lyophilized biomass, being a quick and efficient extraction method that slightly reduces the degradation. Several solvents can be used such as hexane, ethanol (96%), or hexane-ethanol (96%) mixture, being possible to obtain up to 98% quantitative extraction of purified fatty acids. Lipids obtained can be converted into biodiesel by using transesterification process.

Transesterification is a multiple step reaction, including three reversible steps in series, where triglycerides (TAGs animal fats or vegetables oils) are converted to diglycerides and then to monoglycerides, and, by replacing the glycerol with an alcohol in a chemical reaction, using an alkali/acid as catalyst, monoglycerides are then converted to fatty acid methyl esters (FAME), which corresponds to the biodiesel, and glycerol (by-product). Alcohols that can be used in the transesterification reaction are methanol, ethanol, propanol, butanol and amyl alcohol. Methanol and ethanol are used most frequently [13]. In general a catalyst is needed because of the low rate of the transesterification reaction due to the immiscibility of the two initial reactants, as oil and alcohol require vigorous stirring to promote good inter-phase contact. The vast majority of technologies used for transesterification reaction employed homogeneous catalyst in processes where both reaction and further separations steps create bottlenecks [32, 33]. Purification of biodiesel is one of the several expensive downstream steps required in the transesterification as well as separation of excess methanol, glycerol (by-product) and water coming from washing stage [34, 35]. An interesting alternative could be the substitution of the homogeneous catalyst with a heterogeneous one, in order to avoid the washing phase and simultaneously the soap formation. The remaining phases could be separated in continuous coupling the reaction with membrane filtration with a catalyzed membrane reactor.

The most studied parameter in membrane filtration technology is membrane permeability. This parameter depends from many variables and its study is particularly important when synthesized membranes with unknown characteristics are used. To simplify the related attainment in terms of time and costs a mathematical model can be an adequate tool for characterization.

UNIVERSITAT ROVIRA I VIRGILI
SEPARATION PROCESSES IN MICROALGAE BIOREFINING
Claudia Nurra

2

2. MEMBRANE MATERIALS FOR MICROALGAE DEWATERING[1]

In this chapter it is described the approach adopted to find the best material for microalgae dewatering by membrane filtration, in term of membrane cost, permeability, mechanical properties and biodegradability. For this reason commercial and synthesised membranes were tested and compared in a conventional cross-flow filtration system. Among the synthesised membranes polymers common in membrane industry as not common ones were studied. The performance results of different materials used and their characterizations (contact angle, Z potential, morphology, etc) are presented in this chapter and they permit to have a significant range for comparison and choice for a better option in this application.

[1] This chapter is partially based on the following publication and manuscript:

[1] Cheaper membrane materials for microalgae dewatering, C. Nurra, E. Franco, M. Maspoch, J. Salvadó and C. Torras; Journal of Material Science 49, 7031-7039, (2014).

[2] Membrane from sawdust of Pinus for microalgae filtration. T. Saucedo, C. Nurra, G. Gonzalez, L. Moñoz, C Torras, L. Ballinas, to be submitted.

2.1 Introduction

Environmental defence and depletion of fossil oil provisions lead to interests on biofuels production from microalgae [36]. In order to be cost-competitive with fossil based fuels, all the efforts to make feasible the production of biodiesel from microalgae are directed to the reduction of the investment cost and running cost that it entails [37-39]. Many studies are addressed to the investigation of microalgae cultivation process [40] and reactors design, but microalgae dewatering is still a major limiting factor for the economic point of view [41]. Consequently, a strategy to reduce its cost is being considered in this paper.

Since now, most used methods for dewatering are flocculation, flotation, filtration and centrifugation, in general combined [4]. Pros and cons are well described in other articles [42-44], and it is clear that improvements are still necessary. Membrane filtration is a promising technique in a large number of processes and in particular in this application [45-47]. Nevertheless, there is a necessity of technological development in this field to reduce process cost. Several approaches can be considered as dynamic filtration to reduce fouling [45], or membrane material optimization, which is the work being presented in this chapter. So, a comparison between performances of various membrane materials was carried-out in this research. Membrane performance is mainly assessed by its permeability that usually decreases significantly with time due to fouling and concentration polarization [14, 22, 24, 48, 49].

Ceramic membranes offer good performances in terms of flow, reproducibility and use, although they are more expensive than polymeric ones [50]. In order to find a membrane with the same or better performances as ceramic ones but cheaper, membrane synthesis, characterization and testing from different polymeric materials were investigated. A common

method to produce membranes is the phase inversion, which is the technique acquired in this work for membrane synthesis. In this method a polymer is dissolved to a non solvent and the solution is introduced in a coagulation bath. Here a mass transfer occurs: the solvent pass to the non solvent and conversely, giving way to the formation of the membrane.

According to several authors polyacrylonitrile (PAN) membranes are chemical stable and they show good performances and versatility in aqueous applications [51, 52], whereas polysulfone (PSf) membranes are the most commonly used and studied [53-56]. For this reason both were investigated. Furthermore, PSf was chemically modified to be more hydrophilic and to decrease fouling and concentration polarization effects with Pluronic®F127 blending, were chosen because of its antifouling [57], biodegradable and biocompatible characteristics.

As the aim of this investigation was to find cheapest way to process microalgae in a biorefinery concept, the attention was addressed not only to polymers commonly used for membrane production (PSf and PAN), but also three polymers not common in this field: PolyLactic Acid (PLA), GlycolModified Polyethylene Terephthalate (PETG) and Acrylonitrile Butadiene Styrene (ABS).

PLA is a polymer biodegradable coming from acid lactic. It is extracted from 100% renewable resources rich in amides (corn, sugar cane and beet) and its qualities are equivalents or, sometimes, betters than many plastics becoming from crude oil. In addition to be a biodegradable polymer it is also a biocompatible and bioabsorbable one, so it can be assimilated from a biologic system (*i.e*. human body). Therefore, it is a type of polymer introduced in membrane production especially in the biomedical applications [58, 59].

Mechanics characteristics, bioadsorption and degradation velocity of PLA can be controlled by modifying chemical composition, molecular weight and crystalline structure [60].

Studies about ABS membranes can be only found in gas permeation, in which it is reported to have good filtration and mechanical characteristics [61, 62].

PLA, PETG and ABS are generally used in the packaging industry. Although high technical materials need to be used in common membrane application, it is not necessary for this purpose, because large particles in aqueous media are to be concentrated, at low transmembrane pressures. To allow microalgae treatment process being feasible there is a necessity to decrease the costs and here is one of the key. These three polymers are extremely cheap compared to technical polymers normally used in membrane production. And if additionally it is possible to use an environmental friendly polymer the advantages duplicate.

The prices of raw materials change according to the market. Nevertheless, there are up to three order of magnitude differences in price between polymers. PSf has a cost of around 480 US$/kg (Sigma Aldrich), PAN 1,850 US$/kg (Sigma Aldrich), and not technical ones as PLA has a cost of 2.2 US$/kg [63], ABS 2.4 US$/kg (Plasticker) and PETG 1.1 US$/kg (Plasticker).

Even if it is still more expensive than ABS and PETG, PLA polymer has the opportunity to become even cheaper, since the continuous increase of crude oil price per barrel.

Despite all the efforts done so far in membrane research, the fouling problems are not completely solved yet. In this sense PLA membranes, thanks to its biodegradability, can be substituted with new ones more often without causing a big environmental impact.

Membrane production using economic materials could be a good alternative and if this solution is combined with material recuperation the advantages are multiplied, reducing dramatically the investment in raw materials for manufacturing. Membranes based on acetate cellulose, have been used since the beginning of this technology. Recent results on membrane production using cellulose chemical derivatives have been reported obtaining superior characteristics than commercial acetylated cellulose membranes [64, 65].

This work has been performed in collaboration with the Universidad Autónoma de Chihuahua. Chihuahua is the second state in timber production in Mexico and sawdust is the principal waste produced which is consecutively abandoned in garbage dumps. Cellulose is the most abundant biopolymer on the planet, occurring in large amounts in the biomass waste.

Sawdust is an enriched cellulose material that could be reused and valued by chemical modification, obtaining cellulose based materials. One of the possible applications is membrane synthesis, such as it has been reported for other biomass materials [66-68]. In this work, acetylated membranes have been obtained from sawdust of Pinus spp.

2.2 Membranes synthesis

2.2.1 Materials

Membranes and polymers

Commercial ceramic (Fig. 2.1), commercial polymeric and own produced polymeric membranes were investigated in this work. Previous studies showed that microfiltration is the best range for this microalgae specie [45, 50]. Therefore, ceramic membranes (ZrO_2/TiO_2)

with membrane cut-off equal to 1.4 µm were purchased from TAMI Industry and polymeric membranes of different cut-off (1.2, 3.0, 5.0 and 8.0 micrometers) were purchased from GE OSMONICS.

Fig. 2.1 Ceramic membrane.

For membrane synthesis PSf (Mw=35,000), PAN (Mw=150,000) and Pluronic® F127 were purchased from Sigma-Aldrich. N,N-dimethylformamide, DMF (99.9%, Multisolvent®), Dimethylacetamida, DMA (99.5%) and 1-Methyl-2-pyrrolidone, NMP (99.5%) were purchased from Scharlab. PLA 2002 D was kindly donated from AIMPLAS.

ABS copolymer Terluran® GP-22 from BASF was employed with a density of 1.04 g/cm3, processing temperatures between 220 and 260 ºC and a Tensile Strength at Yield of 45 MPa. PETG resin SKYGREEN K2012 manufactured by SK Chemicals with a density of 1.27 g/cm3, a Glass Transition Temperature of 80ºC and Tensile Strength at Yield of 50MPa.

For the synthesis of cellulose acetate (CA) membrane both immersion and evaporation precipitation methods were used in the phase inversion.

Dichloromethane, DCM (99.9%) purchased from Scharlab, was used as solvent for the evaporation method, whereas different solvent non-solvent combinations were used for the immersion precipitation one. Both extracted and commercial CA were used, the latter one (Mw=30,000) was purchased from Sigma-Aldrich. N,N-dimethylformamide, DMF (99.9%, Multisolvent®), Dimethylacetamida, DMA (99.5%) and 1-Methyl-2-pyrrolidone, NMP (99.5%) were purchased from Scharlab.

Dichloromethane was also used for CA attainment from pine sawdust.

2.2.2 Methods

Synthesized polymeric membranes were obtained by the phase inversion with immersion precipitation method (Fig. 2.2) in a coagulation bath of 100% demineralised water. This is a classic technique to prepare selective films, well known and described in the bibliography [69]. The polymer was dissolved in the solvent, by stirring for 24 hours at room temperature. Then the solution was deposited onto a glass plate using a casting knife. The gap thickness of the casting knife could be adjusted by using the incorporated micrometer.

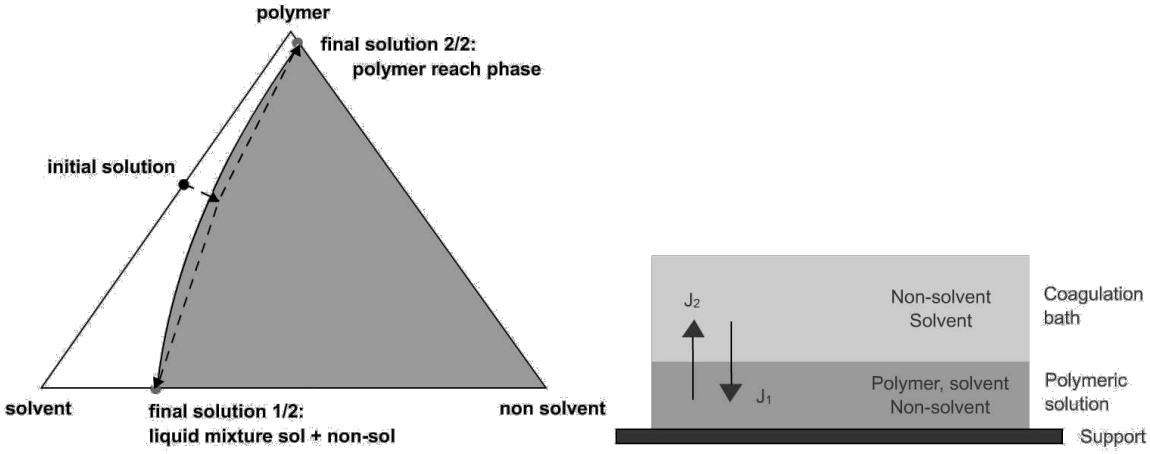

Fig. 2.2 Phase inversion method.

To allow proper comparison between the commercial and synthesised membranes, the last ones were produced with a similar thickness of 100 micrometers like commercial ones. In consequence, the casting knife was adjusted to 300, 250, 200, 200 and 150 micrometers for PLA, PSf, PAN, PETG and ABS membranes, respectively. The knife was pushed over the glass with an automatic film applicator (BYK-Gardner Automatic Film Applicator L, Fig. 2.3) at constant velocity rate of 110 mm/s.

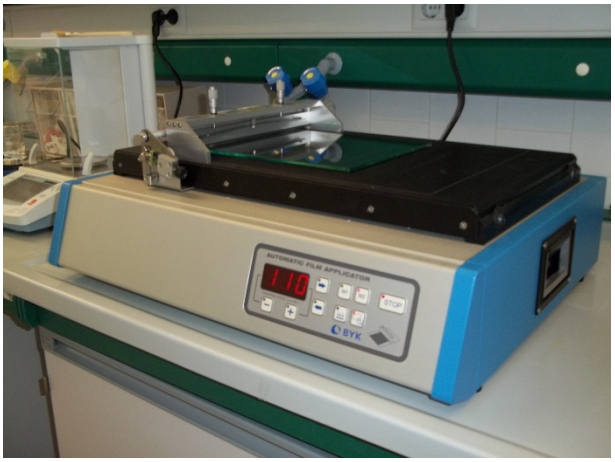

Fig. 2.3 Gardner Automatic film applicator.

Phase inversion occurred after immersing the polymeric solution (attached to the glass) in a precipitation bath. After synthesizing the membrane the final thickness was measured by the digimatic micrometer IP65 from Mitutoyo Corporation.

Polymeric membranes from different casting solutions with several polymers were synthesized. Below the different polymer-solvent systems are listed for the ternary groups studied: PSf-DMF, PAN-NMP, PLA-DMF, PETG-DMA and ABS-DMA. Demineralised water was always used as non solvent in the ternary systems. The polymer concentration was 10 wt % in all cases except for ABS that was 25 wt % to guarantee total microalgae rejection.

Tests were performed also with the additive Pluronic® F127 (3 wt %) in the solution of PSf-DMF. Only membranes with almost total rejection were used.

Cellulose acetate extraction from sawdust was carried out mixing 20 grams of sawdust with 500 ml of dichloromethane for 24 hours at room temperature by magnetic stirring at 300 rpm. This solution was later filtrated and the dichloromethane (DCM) was evaporated in a rotary evaporator (BUCHI, R-210) to recycle it. After DCM evaporation, CA, DCM and residual sawdust were weighed for mass balance calculations. Six experiments were repeated with this methodology. In the CA extractions about 5.5 ±0.2 grams were recuperated that it corresponded to the 27% of the initial pre-treated sawdust. Dichloromethane recuperation corresponded to the 52% of the initial amount used. The extracted CA was finally used for the membrane synthesis by phase inversion.

Both membranes from commercial and extracted CA were synthesised. Four different combination of polymeric solution were prepared, mixing the CA with DCM, DMF, 1,4-Dioxane and Acetone for 24 hours at room temperature with 400 rpm speed agitation.

Polymeric solution with DCM did not give membrane formation but many bubbles that converted into “pellets” with time. Therefore this combination was discarded for the

immersion precipitation method. Polymeric solution with acetone gave not homogeneous membranes, therefore, was also discarded for this method. Polymeric solution with DMF could not dissolved properly even with the addition of temperature (30ºC). The best solution was founded on the CA 1,4-Dioxane solution. Two percentages were tested for commercial and extracted cellulose (7% and 10% wt).

Membranes obtained were characterized in terms of their permeability by membrane filtration, structures by SEM, contact angle by OCA35 measurement system.

Before acetilation sawdust was previously pre-treated by four different treatments methods were compared: pulping (Sulphuric acid 10%, NaOH 1% for 15 minutes), pulping/bleaching (Sulfuric acid 10%, NaOH 1% NaHClO 1% for 4 hours), ethanosolv ($FeCl_3$ 1%, $AlCl_3$ 1% H_2SO_4 1%) and biopulping (Phaenocarete chrysosporium, 40 days). This pre-treatment was performed in the Universidad Autónoma de Chihuahua. Acetylation was attained using acetic anhydride and sulfuric acid as catalyst [68].

2.3 Membranes characterization

2.3.1 Contact angle

Contact angles were determined by sessile drop technique using the automatic video-based analysis system OCA 35 (Dataphysics) (Fig. 2.4). Measurements were carried-out dispensing 2 µL drops on the surface of the membranes, absorption was recorded and the measurement was taken at 31-32 seconds after the drop contacted the surface (time at which the steady-state angles were typically reached). More than six measurements were performed for each membrane.

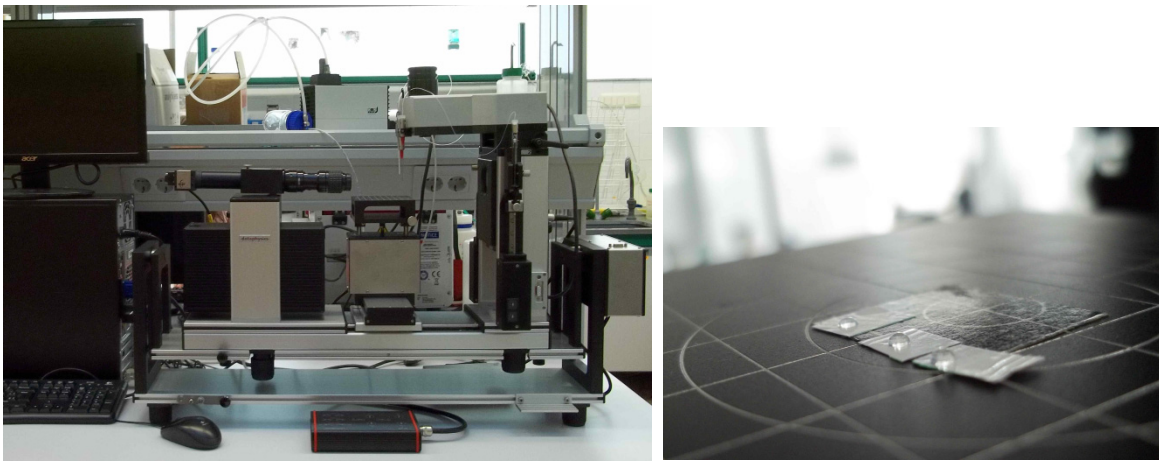

Fig. 2.4 Contact angle measurement system.

Contact angle measurements showed a hydrophilic behaviour for most of the membranes analyzed, except for the PSf and ABS synthesized ones (Table 2.1). Between all, the most hydrophilic membranes were the commercial ones. Between the synthesized membranes PAN, PLA and sawdust CA showed the most hydrophilic behaviour. PLA as well as sawdust CA membranes contact angles are reported for first time. Pluronic® F127 gave more hydrophilicity to the PSf membranes, which caused a permeability increase, as it is reported in the following sections.

	Membrane	Contact angle (degrees)
Commercial membranes	Ceramic	38 ± 3.1
	Polymeric	60 ± 1.0
Sinthesized membranes	Polysulfone	92 ± 3.0
	Polysulfone Pluronic® F127	81 ± 4.5
	Polyacrilonitrile	75 ± 2.5
	Polylactide	76 ± 2.4
	Acrylonitrile butadiene styrene	94 ± 2.8
	Sawdust cellulose acetate	70 ± 1.4

Table 2.1. Membrane contact angle measurement results.

2.3.2 Membrane morphological characterization

The morphology of the membranes was investigated by using the Scanning Electron Microscopy (SEM) and an Environmental Scanning Electron Microscopy (ESEM). The SEM used was a JEOL JSM-6400 Scanning Microscopy Series, with a working voltage of 15 kV. The ESEM used was a FEI Quanta 600, with a voltage between 15 and 20 kV and with low vacuum pressure, since the samples are not conductive and no sputtering was applied.

SEM micrographs of commercial ceramic membrane (Fig. 2.5 a, b) showed a thin selective layer (ca. 0.9 μm) as opposed to a thick non-selective one (ca. 2.5 mm). This structure guarantees a proper selectivity and higher strength. On the other hand PSf commercial membranes showed a symmetric structure (Fig. 2.5 c) really similar than other PSf membranes with different cut-off size.

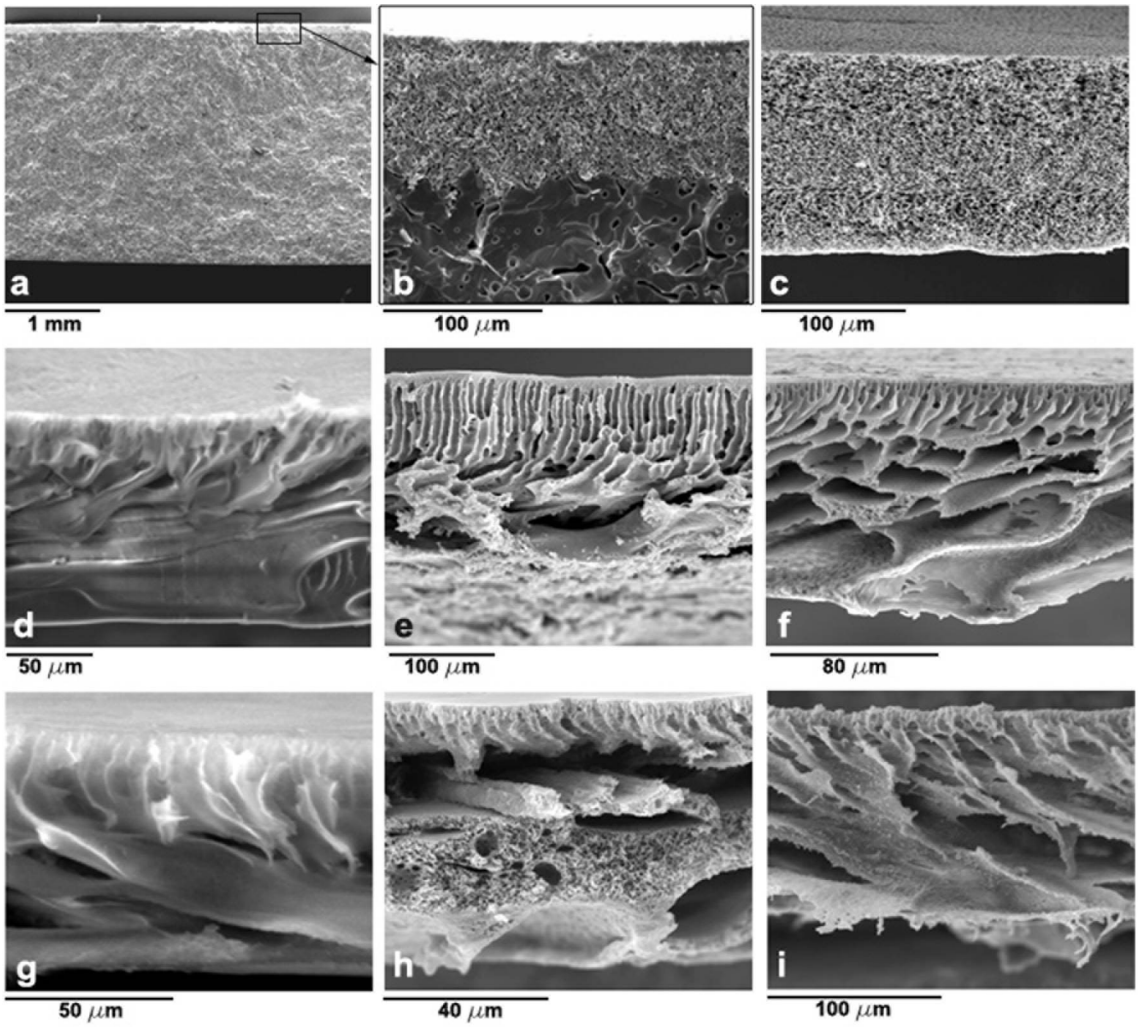

Fig. 2.5 SEM micrographs of membranes cross sections: a) Ceramic membrane; b) Ceramic membrane selective layer; c) Commercial PSf membrane; d) PAN-NMP membrane; e) PSf membrane; f) PSf-Pluronic® F127 membrane; g) PLA-DMF membrane; h) ABS-DMA membrane; i) PETG-DMA membrane.

PSf, PLA, ABS, PETG and PAN membranes (Fig. 2.5 d, e, f, g, h and i) showed similar structures, possessing long channels in the proximity of the selective layer and macro voids in the proximity of the micro-porous side. The achievement of similar structures was important for the comparison of the membranes permeabilities, as well as their thickness. PAN membrane (d) showed a smooth texture that, among other characteristics, could be used to explain its higher permeability, as explained next.

Furthermore, it can be observed that Pluronic® F127 is completely integrated to PSf membrane matrix. Moreover, this additive gives more homogeneity to the structure without the presence of a thin layer in the selective side (Fig. 2.5 e, f).

For the CA membranes it was observed that the lower percentage of the commercial ones gave not a homogeneous structure. Sawdust extracted CA at 7% wt gave good looking membranes and this was attested with SEM characterization (Fig. 2.6). Both commercial and extracted CA at 10% wt in the solution had good looking and really similar structures, presenting both macrovoids, as it can be observed from SEM micrographs (Fig. 2.7 and Fig. 2.8). The 7% wt sawdust extracted CA membrane showed a lower presence of macrovoids and a porous side structure more similar to a reticular than a porous surface (Fig. 2.6 b) than the 10% wt CA membrane (Fig. 2.7 b).

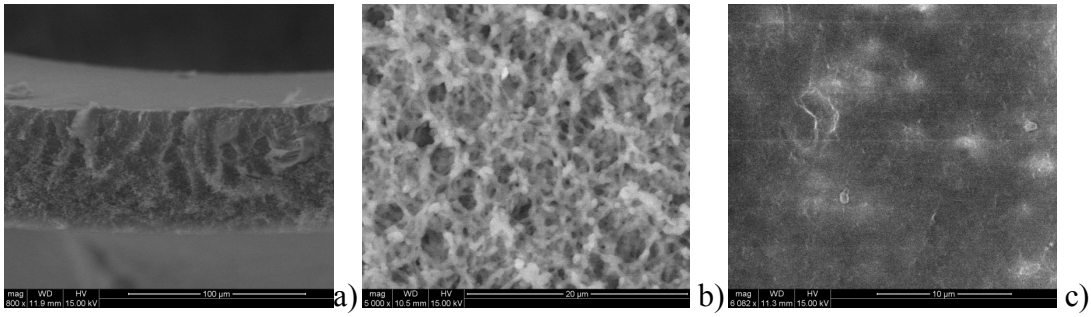

Fig. 2.6 Sawdust cellulose acetate membrane in 7% wt dioxane solution: a) cross section; b) porous surface; c) selective surface.

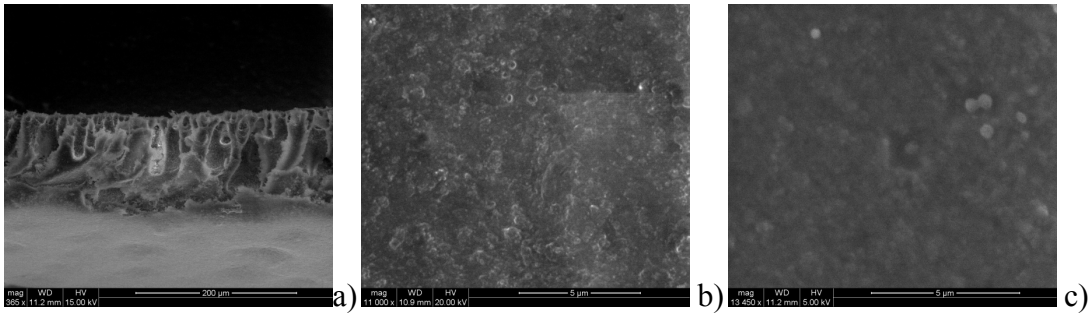

Fig. 2.7 Sawdust cellulose acetate membrane in 10% wt 1,4 dioxane solution: a) cross section; b) porous surface; c) selective surface.

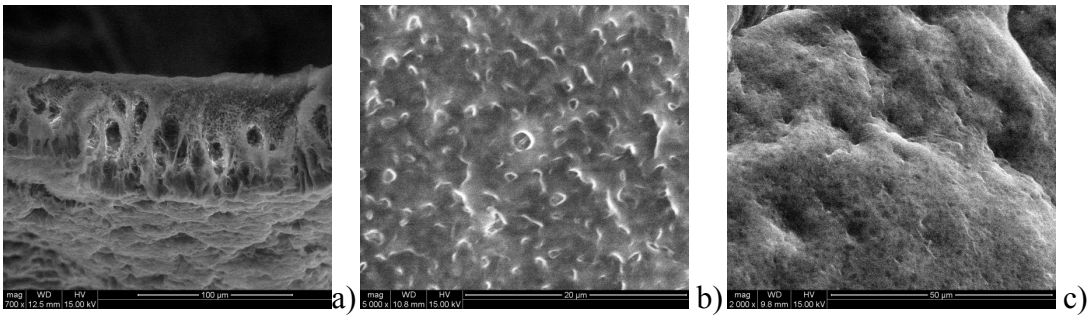

Fig. 2.8 Commercial cellulose acetate membrane in 10% wt 1,4 dioxane solution: a) cross section; b) porous surface; c) selective surface.

2.3.3 Membrane mechanical characterization

The mechanical properties from commercial and synthesised membranes were evaluated through uniaxial tensile tests following the procedure suggested by the ISO 527 standard. Because of the membrane dimensions, small test specimens were cut using an ISO 527 type 1BA tensile cutting die. The gage length and the width of narrow portion were 25 and 5 mm, respectively. The thickness of the membranes was measured using a coating thickness meter MEGA-CHECK 5F-ST to avoid damages on the specimen.

The samples were tested in a universal testing machine (Galdabini Sun 2500) equipped with a 1 kN load cell and data processing settings. The tests were performed at a crosshead rate of 1 mm/min and at room temperature (23 ± 2ºC). Young's modulus (E) and yield at break (σ_b) were obtained from the engineering stress versus strain curves, and the elastic deformation was measured using a video extensometer (Mintron OS-65D). When the curves showed a diffusive yielding, the Considère's criterion was applied [70].

Because of their biodegradability, mechanical properties of PLA membranes were evaluated and compared with commercial ones. Moreover, additional tensile tests were conducted on the PLA membranes after five hours of filtration. The mechanical parameters are listed in Table 2.2.

Membrane	E (MPa)	σ_y (Mpa)	σ_b (MPa)	ε_b (%)
Commercial polysulfone	0.88 ± 0.08	2.06 ± 0.04	3.45 ± 0.25	21.60 ± 5.90
PETG	2.35 ± 0.31	2.48 ± 0.03	2.89 ± 0.06	3.25 ± 0.59
PLA before filtration	2.69 ± 0.92	4.23 ± 0.26	5.51 ± 0.25	18.35 ± 4.53
PLA after filtration	1.76 ± 0.27	4.25 ± 0.24	4.53 ± 0.65	22.95 ± 4.63

Table 2.2. Mechanical parameters.

The engineering stress versus strain curves obtained from tensile tests of PLA and commercial membranes are shown in Fig. 2.9.

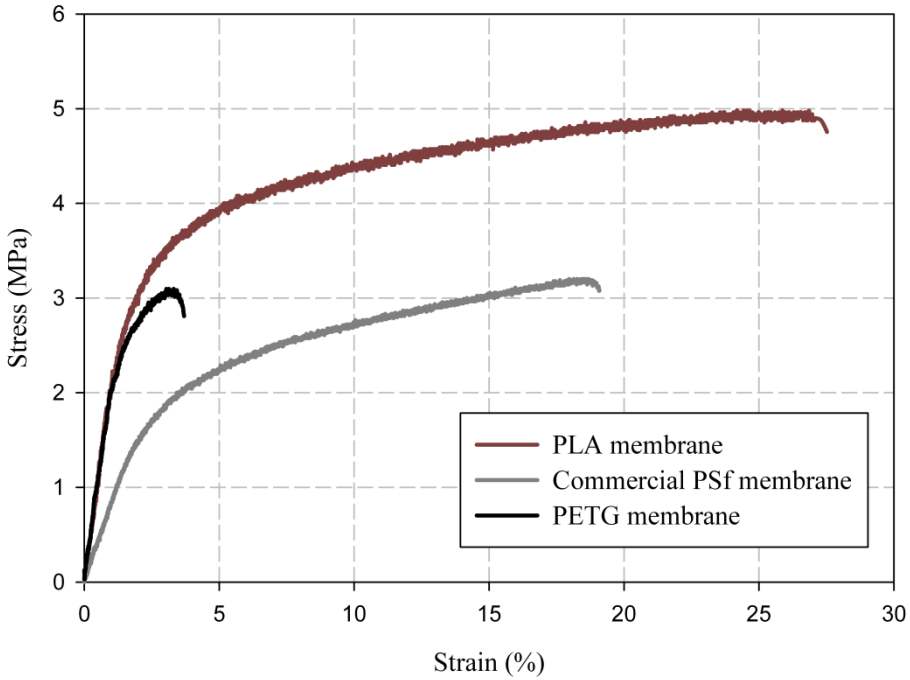

Fig. 2.9 Representative curves σ - ε of PLA, PETG and commercial PSf membranes.

The curves showed similar behaviour with a diffuse yielding and slight strain hardening, which indicates that the plastic region is not absolutely flat, before rupture. Physically, the specimens did not present traces of plastic deformation mechanisms like necking, shear bandings or whitening. Additionally, PETG membrane was also tested

showing a distinct mechanical response because it broke at low values of strain (approximately 3%, Table 4).

The mechanical parameters Young's modulus (E), yield strength (σ_y), tensile and elongation at break (σ_b and ε_b respectively) presented in Table 4 indicate the commercial membrane has values on Young's modulus and strength lower than that of PLA membrane.

Furthermore, the filtration process applied to the synthesized membrane affected some mechanical properties of the PLA because the stiffness and the strength were notoriously reduced without significant variations on ductility. The previous could be attributed to some physical damages on the membrane structure, probably caused by the water molecules during the filtration process.

2.4 Filtration experiments

2.4.1 Materials and biological biomass

Microalgae

Experiments were carried out with the microalga *Phaeodactylum tricornutum*Bohlin.

The strain used for the experiments was kindly provided by the Institut de Recerca i Technologia Agrolimentaries in Sant Carles de la Ràpita (Tarragona, Spain). Four litres cultures were grown in six litres round volumetric flasks with seawater (37 $g \cdot L^{-1}$ salinity) filtered through 0.22 μm, enriched with Walne's medium [71] and autoclaved. Cultures were kept at 22°C (±2), illuminated (16:8 light: dark cycle) with cool daylight fluorescents (Osram L30W/865), and aerated with air.

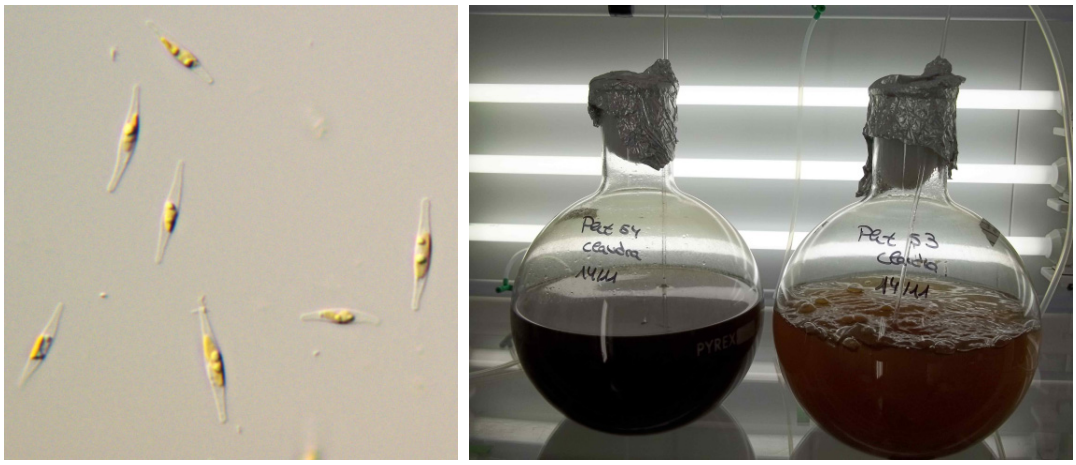

Fig. 2.10 *Phaeodactylum tricornutum.*

First studies showed that there was a great dependence of duration of the experiment and the microalgae concentration and especially the different kind of species [45]. For this reason, it was decided to repeat all experiments with constant microalgae concentration and only one species. For all experiments performed, cultures were harvested in a stationary phase and the concentration was measured with a microscope Carle Zeiss AxioScope A1 by hemocytometer and it resulted equal to $22.5 \pm 4.4 \cdot 10^6$ cell/ml (mean and standard deviation, as in the entire chapter). Cell concentrations were measured also for final retentate and for permeate in order to check membrane rejection.

2.4.2 Equipment

Experiments were carried-out using a setup containing two commercial tangential cross-flow membrane modules (Fig. 2.11 a, b), one for polymeric membranes (SEPA CFII, GE Osmonics) and another for ceramic ones (ISDRAM TAMI Industries). By using three-way valves, the module used could be chosen. Trans-membrane pressure (TMP) was set to 1 bar and controlled by using a TESCOM back-pressure. Broth temperature was also set to

21ºC and controlled by using a Huber, K6-cc-NR equipment. Recalculating flow rate was maintained at 55 ± 3 L/h in all experiments. Permeate was collected in a tank located on a scale that was connected to a computer in order to calculate the actual mass flow rate with one second frequency. This set-up is shown in Fig. 2.12.

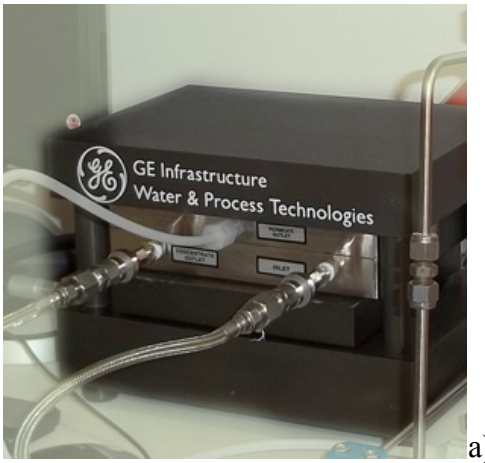

a)

b)

Fig. 2.11 Membrane modules: a) SEPA CFII, GE Osmonics; b) ISDRAM TAMI Industries.

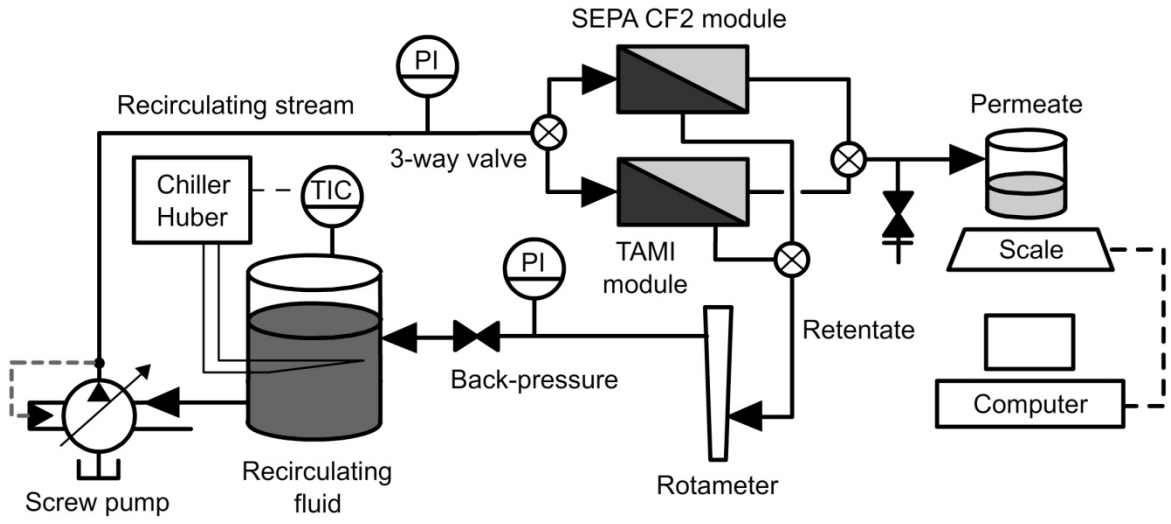

Fig. 2.12 Experimental set-up.

2.4.3 Membrane permeability

Membrane permeability values were obtained by measuring the mass flow rate collected in a tank on a scale and recorded by a computer. In order to measure the membrane irreversible fouling resistance and its recovery, water permeabilities were monitored before and after all experiments. Furthermore, the volumetric flux reduction (VFR) was calculated in order to evaluate the membrane fouling. The system was washed with water after each microalgal biomass permeability recording. Again, the water permeability was measured to determine the irreversible fouling resistance. Permeability values are reported at the steady state time, generally observed after two hours or more. Minimum three replicates were performed for each membrane.

2.4.3.1 Commercial membranes

Filtration performances of commercial ceramic and commercial polymeric membranes were studied.

Ceramic membranes showed a typical permeability curve fall (Fig. 2.14) with high permeability in water filtration (1275 ± 356 L/m^2/h/bar). It decreased two orders of magnitude when microalgae were filtrated (21 ± 3 L/m^2/h/bar) due to the membrane fouling and cake formation over its surface (Fig. 2.13).

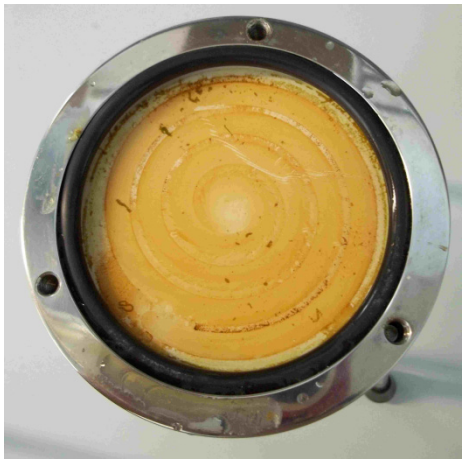

Fig. 2.13 Ceramic membrane with microalgae cake in its surface.

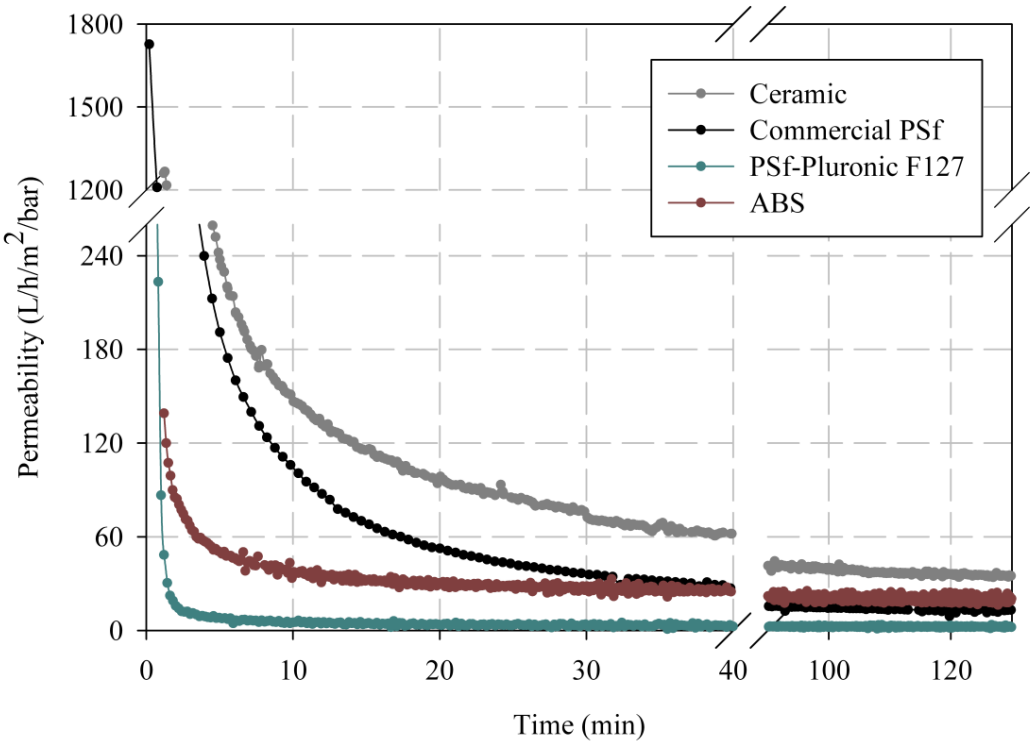

Fig. 2.14 Microalgae permeability falls of PSf-Pluronic®, ABS, ceramic and PSf commercial membranes.

Several commercial PSf membranes with different molecular weight cut-off were tested, starting from 1.2 µm (close to the ceramic one) till to 8.0 µm. Thus, the process performance could be assessed by considering the pore size as a variable.

Permeability studies performed with water before each microalgae experiment showed similar values for all of them (Table 2.3). Permeabilities obtained with PSf membranes resulted, in this case, higher than ceramic one. However, for ceramic and polymeric membranes microalgae permeability decreased of two orders of magnitude when microalgae were filtrated due to the membrane fouling and cake formation on their surface (Fig. 2.15).

Membrane	Membrane pore size (µm)	Water permeability ($L/h/m^2/bar$)	Permeability ($L/h/m^2/bar$)
Ceramic	1.4	1275 ± 356	21 ± 2.9
Polysulfone	1.2	4025 ± 126	10.5 ± 0.7
	3	4050 ± 140	10.0 ± 0.0
	5	4182 ± 212	11.5 ± 0.7
	8	4250 ± 71	14.7 ± 1.2

Table 2.3. Permeability results of commercial membranes.

The plateau (steady state) value was reached in all cases and a slight augmentation of permeability was observed with the increase of pore size (Table 2.3), getting closer to ceramic value (Fig. 2.14). In all cases, for ceramic and for PSf commercial membranes total rejection of microalgae was obtained. Their permeability falls were important with VFR values of 98% and 99% respectively.

Fig. 2.15 Polymeric membrane with microalgae cake in its surface.

2.4.3.2 Synthesized membranes

After finding the commercial polymeric membrane that better approached ceramic efficiency, it was investigated the possibility to use a material cheaper than PSf.

First tests were carried-out to reproduce PSf membrane performances. Several polymer concentrations were experimented (20%, 15%, 12% and 10%) till to obtain the maximum permeability within total rejection, with 10 wt %. Permeability results showed low values both with water and with microalgae (Table 2.4).

Membrane	Water permeability ($L/h/m^2/bar$)	Permeability ($L/h/m^2/bar$)
Polysulfone	5 ± 2.1	2 ± 2.0
Polysulfone -Pluronic® F127	80 ± 28.3	11 ± 0.7
Polyacrilonitrile	400 ± 60.8	22 ± 0.6
Acrylonitrile butadiene styrene	260 ± 173	19 ± 1.9
Polylactic acid	7 ± 0.0	5± 1.4
Sawdust cellulose acetate	21 ± 4	5 ± 0.0

Table 2.4. Permeability results of synthesized membranes.

Commercial membranes usually contain some additive to improve their performances. For this reason, Pluronic® F127 was added to the ternary solution and, even if the addition was modest (3 wt %) the increment of permeability values were important. Water permeability was one order of magnitude higher than PSf membranes (Table 2.4) and when microalgae were filtrated permeabilities increased till to reach commercial ones, with 11 ± 0.7 L/h/m^2/bar (Fig. 2.17). Its VFR one of the best resulting equal to 86%. Rejection higher than 99% were obtained with both membranes.

Another well-known polymer in membrane technology is PAN, which was chosen for its good characteristics (specially hydrofilicity) and for the possibility to be turned biodegradable [72]. It achieved, without any additive, high permeability values in water filtration and the same permeability that ceramic one when microalgae were filtrated (see Table 2.4). PAN has higher costs than PSf, but lower than ceramic, its rejection was almost total and its permeability fall resulted slighter than both of them (VFR of 95%), so it resulted a good candidate for this application with *Phaeodactylum tricornutum* microalgae. This membrane should be preserved wet because of its morphology change in dry condition (Fig. 2.16).

Fig. 2.16 PAN membranes a) wet membrane b) dry membrane.

To further decrease microalgae concentration costs other three polymers, not common in water filtration, were studied: ABS, PETG and PLA; plus the extracted sawdust CA.

For these polymers preliminary experiments were carried out to screen the appropriate parameters and to determine the experimental conditions (including different kinds of suitable solvents: 1.4 dioxane, tetrahydrofuran, dichloromethane, NMP, DMF and DMA; temperature addition, till to 80º when possible, and change of polymer weight percentages). Among the solvents tested the one that showed the better results for PLA polymer was the DMF, on the other hand for PETG and ABS was the DMA. They showed a white colour which suggested that they were porous, confirmed by SEM micrographs, see below.

PETG homogeneous membranes were difficult to synthesize and they showed poor mechanical properties. More polymer weight percentage did not allow the pellets to dissolve in the solution and less than 10 wt% did not allow a homogeneous membrane formation. Furthermore, PETG membranes synthesis was performed after only 4 hours of PETG dissolution in DMA, because after 24 hours the solution became too viscous and no homogeneous membrane were attained. Nevertheless, some membranes were obtained and even with the poor mechanical properties filtration was possible. With rejections higher than 93%, this membrane reached a permeability of 23 L/h/m^2/bar, with a VFR of 97%. This result deserves more investigation on the production of these membranes.

PLA membrane gave similar permeability efficiency as the PSf one with values equal to 5 ± 1.4 L/h/m^2/bar and rejection higher than 97%. On the other hand, it showed better efficiency in term of VFR (of only 29%) and mechanical properties (as discussed previously).

Extracted CA membrane gave a better result than that of PLA for the water permeability, with values of 21 ± 4 L/h/m^2/bar, but the same performance than it with a microalgae permeability of 5 ± 0 L/h/m^2/bar. It showed a good VFR of about 76%.

ABS membranes gave the most interesting results. Even if with water the permeability was lower than that ceramic one, with microalgae it increased till to 19 ± 1.9 L/h/m^2/bar, value really close to the higher ones obtained with PAN and ceramic membranes (Fig. 2.17). Its VFR was also appreciable and equal to 93% and total retention was given. Those values could be probably improved, as well as the permeability, with surface modification using for example some additive, as Pluronic® F127, or other techniques, like surface-coating [73].

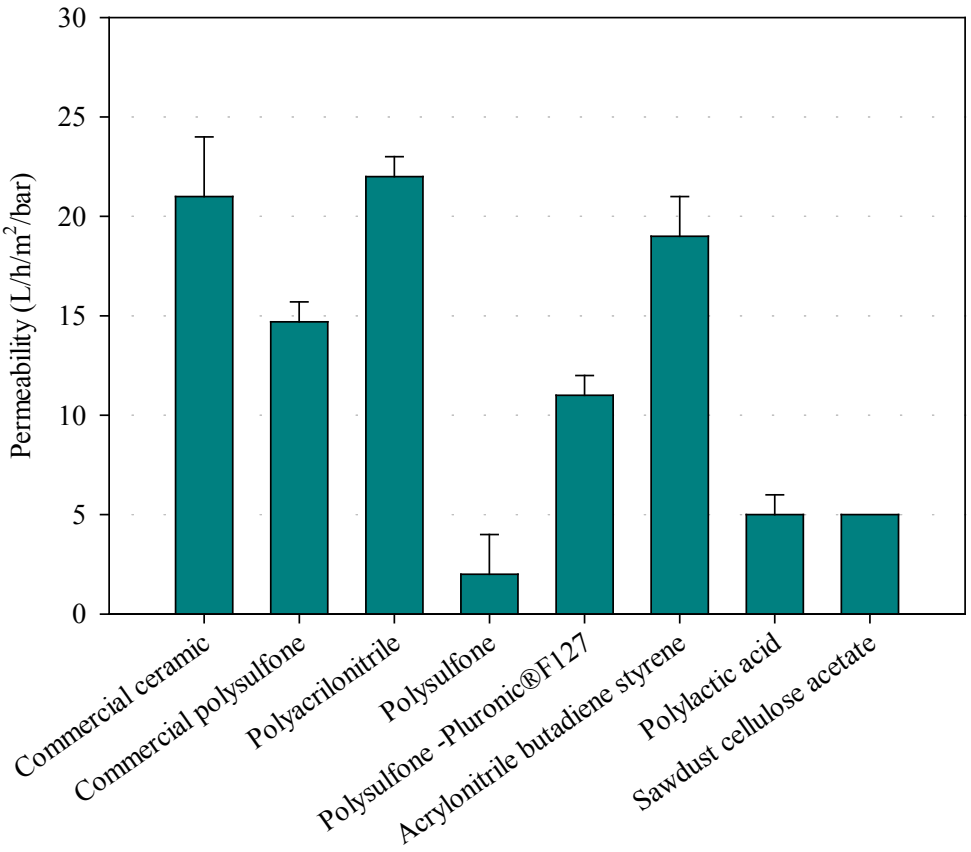

Fig. 2.17 Permeability comparison of all membranes studied.

2.5 Conclusions

To summarize, a screening of various membrane materials to concentrate microalgae has been performed in this study. Best reference permeability values were found in ceramic and PAN membranes. Pluronic® F127 was found to be a proper additive in PSf blended membranes to increase permeability. Regarding the new tested and cheaper materials, PLA membranes gave better permeability results and mechanical properties than those of PSf synthesized membranes. Moreover, the new synthesized membranes are good candidates in term of costs and they have lower VFR. Best results were obtained with the ABS membrane with values close to ceramic and PAN membranes. The results of this study show the potentiality of introducing cheap materials (not common in membrane technology) in microalgae dewatering. Further experiments should be performed to assess whether they can be used alone or blended. In addition, other membrane applications could be use these kinds of materials.

UNIVERSITAT ROVIRA I VIRGILI
SEPARATION PROCESSES IN MICROALGAE BIOREFINING
Claudia Nurra

3

3. MICROALGAE DEWATERING BY VIBRATING MEMBRANE FILTRATION[2]

This chapter is devoted to the study of the performances of membrane filtration for microalgae dewatering process. Conventional cross-flow filtration was compared with vibrating one in laboratory set-up and at pilot plant scale. Finally, a test with coupled sedimentation plus vibrating filtration was carried out for the same microalgae culture.

3.1 Introduction

The interest for microalgae lies in their potential utilization in several fields. Firstly, studies were addressed to mariculture feed, fine chemicals and health food industries (omega 3 oil, chlorophyll, livestock feed). Secondly, the interest for this raw material started also in pharmaceutical and nutraceutical industries, in agriculture as biofertilizer, as bioremediation of water pollution and, thirdly, as a power source to obtain different kinds of products as biomass to produce hydrogen, biomethane, bioethanol and biodiesel [74-77]. Nowadays, to allow the process being economically feasible, all microalgae metabolic products should be

[2]This chapter is partially based on the following publications:

[1] C. Nurra, E. Clavero, J. Salvadó, C. Torras, Bioresource Technology, 157 (2014) 247−253.

[2] C. Nurra, C. Torras, E. Clavero, S.Rios, M.Rey, E.Lorente, X. Farriol, J. Salvadó, Bioresource Technology, 163 (2014) 136−142.

extracted as final usable products to take advantage of all their properties within a biorefinery concept [36].

There are several advantages using microalgae as a feedstock instead of terrestrial plants; several vegetable oils are used as typical raw materials of biodiesel. But, an advantage over these is that, for microalgae there is neither need to encroach valuable crop and virgin land nor it is necessary to fertilize soils. Algae can grow practically anywhere, where there is enough light. Algae can grow in fresh or saline water and can be produced in the laboratory.

This is essential also because all parameters can be controlled, and, if marine algae are used, there is no need to carry large quantities and frequent supplies of fresh water [78, 79]. Another advantage for using microalgae as raw material is also that they can be converted with a large number of different processes to obtain liquid fuel and gas, by using biochemical or thermo-chemical processes. The former will produce ethanol and biodiesel; the latter will mainly produce oil and gas. Microalgae can also be directly combusted, even if it is not convenient because of high water content.

The process to produce biodiesel from microalgae consists of four main steps: cultivation, concentration, lipid extraction and, finally, transesterification. After the cultivation process a dewatering step is required. Common methods are: flocculation/sedimentation [80], dissolved air flotation (DAF), centrifugation and filtration processes [81]. Novel methods are also being investigated such as using magnetic nanoparticles [44]. The flocculation/sedimentation process refers to the aggregation of microalgae in suspension to form masses that can subsequently settle. Its efficiency is increased by using several flocculants. This process reduces the need of energy intensive separation mechanisms like centrifugation. Even if flocculation is an economic method, the

concentration obtained is low (<10% of solids content) [78]. This means that further concentration is necessary by using other methods. For those reasons, it is commonly used as an initial dewatering step and centrifugation is the most combined method use with it. Centrifugation is the preferred one, but the shear forces during the process can disrupt cells and costs are high because of energy intensive.

Alternatively, a membrane microfiltration (MF) and ultra-filtration (UF) process can be performed, which are more suitable for fragile cells and small-scale production processes [22]. For microalgae harvesting, studies are mainly addressed to MF and UF membranes, this is because of their cut-off size (in general higher than 4 micrometers and up to hundreds of μm, depending on the species), but they involved mostly cross-flow filtration processes.

It was demonstrated that algal filtration causes noticeable fouling and too large cake resistance [82]. Membrane performance is mainly assessed by its permeability that decreases significantly with time due to these above mentioned phenomena. Dynamic filtration has been proved to be a successful method in several processes since high shear rates can reduce fouling resistance [83]. In particular, vibratory shear enhanced process (VSEP) has been studied in drinking water purification, pervaporation, baker's yeast microfiltration and skim milk ultrafiltration, landfill leachates, *etc*. [84]. In fact, it was demonstrated that increasing the shear rate makes it harder for algae to deposit on membrane; this means that a higher flux can be obtained with the consequent reduction of concentration polarization and of cake build-up [22]. To obtain this result without decreasing trans-membrane pressure a dynamic or shear-enhanced filtration can be used. Three types of dynamic filtration have been studied so far: 1) with rotors between fixed membranes and 2) rotating or 3) vibrating membranes [85]. The characteristics of these types of dynamic filtrations have been studied in various models

produced by different manufacturers, with polymeric or ceramic membranes [50]. Others studies in this field demonstrated that further improvement can be obtained adding straight vanes of various height to rotating disks fixed in a dynamic filtration module [85]. Studies showed that this system yields higher permeate fluxes than those of conventional cross-flow filtration [86], but at the same time it is more expensive and complex, and it consumes more energy.

A step of membrane characterization should be considered, also to determine or to confirm commercial membranes characteristics. Many parameters can be studied, but the most important are: zeta potential, hydrophilicity/hydrophobicity, molecular weight cut-off size (rejection), pore size, porosity and pore size distribution [87, 88]. Studies regarding membrane characterization and modification are addressed to the permeation flux and fouling phenomenon with special considerations on cut-off, constitutive materials and surface properties (charge, hydrophilicity).

In this work, a comparison between the performances of vibrating and conventional cross-flow filtration systems has been made from culture growth both in laboratory and at pilot plant. Several experiments with different membranes have resulted in an understanding which membrane material and cut-off size could be the best for this application.

3.2 Dewatering strategies

3.2.1 Membranes and microalgae biomass

3.2.1.1 Microalgae

Experiments were carried-out with two types of microalgae strains: *Phaedoactylum tricornutum* Bohlin (Fig. 3.1a) fusiform cells with an approximate length of 40 μm and width

of 4 μm, and *Nannochloropsis gaditana* Lubián (Fig. 3.1b) spherical cells and an approximate diameter of 3-4 μm. These strains have long been used in aquaculture and as they are very diverse in size and shape they offer two different particle characteristics that are interesting to compare in filtration. Algal strains were kindly provided by the Institut de Recerca i Technologia Agrolimentaries in Sant Carles de la Ràpita (Tarragona, Spain).

Algae were grown in 300 L polyethylene bags with seawater (37 $g \cdot L^{-1}$ salinity) filtered through 25, 10, 5 and 1 μm pore size filters (polyKLEAN, MICRO-KLEAN, 3M/ Cuno), UV sterilized and enriched with commercial fertilizer (0.3 $mL \cdot L^{-1}$ of Codafol 14.6.5, Sustainable Agro Solutions S.A., Lleida, Spain). Cultures were kept at 25°C (±2), aerated and illuminated (16:8 light: dark cycle) with daylight fluorescents which gave an irradiance of 200 μmol $photon \cdot m^{-2} \cdot s^{-1}$ at the bag surface. In all experiments recollection was performed at the stationary phase, which was reached by all cultures after a period of about 10 days. Before each experiment the concentration of the culture was measured and this resulted in about 21 ± $2.7 \cdot 10^6$ cells/mL for *Nannochloropsis gaditana* and approximately 21 ± $1.8 \cdot 10^6$ cells/mL for *Phaeodactylum tricornutum.* These concentrations were measured with a microscope Carle Zeiss AxioScope A1 by hemocytometer.

(a)
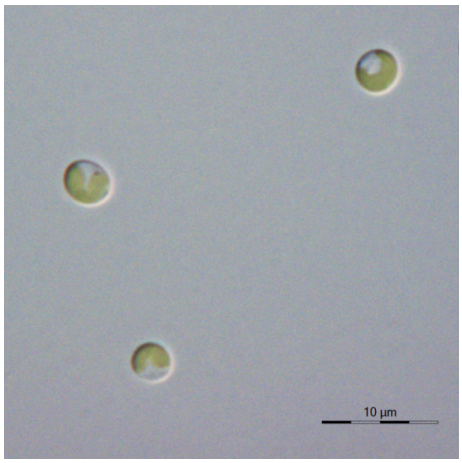

(b)

Fig. 3.1 Images of the microalgae species used: (a) *Phaeodactylum tricornutum*; (b) *Nannocloropsis gaditana*.

3.2.1.2 Membranes

Commercial polymeric membranes were used and their properties are listed in Table 3.1. Their filtration area was 0.0155 m^2 for conventional cross-flow filtration module, with a rectangular shape, and 0.0446 m^2 for a dynamic one, with a circular shape. Membranes of several materials and with lower pore size than those of microalgae were chosen.

Membranes commercial name	**Membrane producers**	**Material**	**Molecular weight cut-off**
Ultrafiltration			
PES 5	Sepro	Polyethersulfone	7,000 da
PVDF 50	Synder	Kynar PVDF	50,000 da
PAN 50	Sepro	Polyacrylanitrile	50,000 da
PES 20	Sepro	Polyethersulfone	200,000 da
Microfiltration			
PVDF 200	Sepro	Kynar PVDF	250,000 da
PAN 400	Sepro	Polyacrylanitrile	400,000 da
PES MF	Sepro	Polyethersulfone	0.2 μm

Table 3.1. Membranes used during microalgae filtration process.

3.2.1.3 Sedimentation

Sedimentation experiments were carried out with *Nannochloropsis gaditana* strain (Fig. 3.2) in four cylindrical bags of 300 L. Flocculation was induced by modifying the pH with a NaOH solution (2 N) from 9.54 ± 0.07 to 10.00 ± 0.05. In order to homogenize the solution agitation in the bags was produced by the same aeration system used for culture respiration. After mixing the solution pH measurement was followed by settling time and settled culture

harvesting for the vibrating filtration. Filtration performed with the PES 5 ultrafiltration membrane, chosen because its performances obtained (section 3.2.4.2).

Fig. 3.2 *Nannochloropsis gaditana* culture.

3.2.2 Methods

3.2.2.1 Membrane morphological characterization

The morphology of the membranes was studied by using SEM (JEOL JSM-6400 Scanning Microscopy Series, with a working voltage of 15 kV) to obtain cross-section or surface micrographs of the membranes. Samples were wetted into ethanol and immersed into a liquid nitrogen bath to freeze them, which allowed the membranes to be broken preserving the internal porous structure. After that, samples were covered with a gold layer with sputtering process in order to make them conductive [25].

3.2.2.2 Membrane electrokinetic potential

The membranes surface charge was calculated from the zeta potential measure as a function of pH over the range 2–10 with a 1 mM KCl electrolyte solution by SurPASS Surface Potential Analyzer (Anton Paar, Fig. 3.3). The membranes were immersed in the back-ground electrolyte before the measurement. For each experiment, two samples of 20

mm x 10 mm were attached on the sample holders with a double side adhesive tape. Operating pressure range varied between 0 and 250 mbar at room temperature with an adjustable gap cell height of about 100 µm. Solution pH was adjusted by the addition of HCl or NaOH. Experiments were performed in triplicate with virgin samples for each.

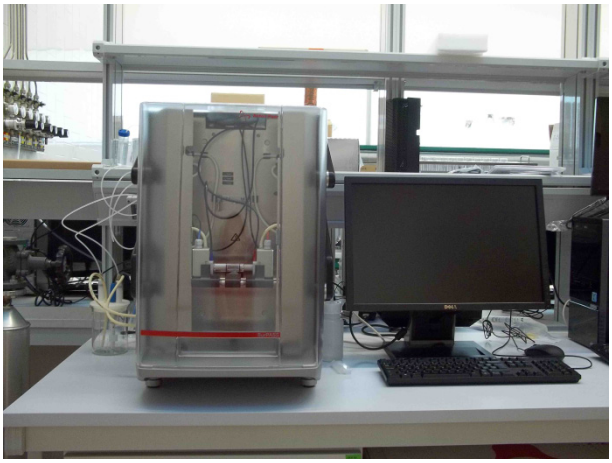

Fig. 3.3 SurPASS Z potential analyzer.

3.2.2.3 Membrane contact angle

Membrane contact angles were measured by sessile drop technique using the automatic video-based analysis system OCA 35 (Dataphysics). Contact angles were determined from the steady-state angles, which were typically observed to reach at around 30 seconds after the drop contacted the membrane surface. No less than six measurements were performed for each membrane with 2 µL drops dispensed.

3.2.2.4 Membrane permeability

In the filtration experiments, water flux was firstly measured to determine the initial permeability. Subsequently microalgal biomass was filtered and the filtration permeability

was recorded. After this, the system was washed with water. Again, the water permeability was measured to determine the irreversible fouling resistance.

3.2.3 Equipment

In the conventional cross-flow filtration experimental set-up, microalgae culture flowed from a temperature controlled recirculation tank (refrigerated with a Huber, K6-cc-NR cooled) towards a membrane cell system (SEPA CFII, GE Osmonics). A screw pump was used in order to minimize the damage inflicted on the microalgae cells. After the membrane separation unit, the retentate was turned back to the recirculation tank. In between, a volumetric flow meter and a compact back pressure regulator were placed at the outlet of the membrane cell system in order to regulate transmembrane pressure. Permeate was conducted to a permeation tank, located over a load cell in order to determine permeate mass flow rate. The load cell was connected to a computer in order to calculate the actual mass flow rate at one second frequency.

Transmembrane pressure was fixed at 3.5 bars and recirculating flow rate at 50 L/h. Dynamic microalgae concentration was performed with a Vibratory Shear Enhanced Processing (VSEP, serie L, New Logic Research, Inc.) commercial set-up (Fig. 3.4). Description of this equipment can be found elsewhere [89].

Fig. 3.4 VSEP, serie L, New Logic.

The two experimental conditions were vibrating speed equal to 3/4 inches (depending on the membrane these parameters changed between 545 ± 45 L/h, 55.7 ± 0.1 Hz and 0.42 ± 0.08 kW) and transmembrane pressure of 3.5 bars.

Experiments with the VSEP system were carried out with volumes of 50 L of biomass cultured, while experiments carried out with conventional cross-flow filtration were performed with volumes of 3L.

The VSEP operational energy demand was measured by FLUKE 1735 three-phase power logger analyst. Measurements were taken during the operation of the system with and without the pump and vibrating motor operation, in order to see the energy demand of each component.

3.2.4 Results and discussions

3.2.4.1 Membrane characterization

Contact angle

Experimental results are summarized in Table 3.2. They show that most of the membranes had a hydrophobic behaviour with contact angles values greater than 80º and a maximum value was obtained for PES-20, equal to 89.4º ± 1.1. Only PAN-50 membrane exhibited a hydrophilic behaviour with a contact angle equal to 55.1º ± 0.5. This is a desired result in the case of water filtration. As shown in Table 3.4, this property gave the highest permeability result with water and the lowest one with microalgae filtration. One reason for this result could be that solution charge influences membrane performances more than hydrophilicity for this application, as showed in the zeta potential study.

Membranes	**Contact angle (º)**
Ultrafiltration	
PES-5/Tyvek	86.9 ± 1.1
PAN-50	55.1 ± 0.5
PVDF-50	83.4 ± 1.5
PES 20	89.4 ± 1.1
Microfiltration	
PVDF 200	81.1 ± 1.8
PAN 400	80.5 ± 1.5
PES MF	88.6 ± 1.1

Table 3.2. Membranes contact angles.

Zeta potential (ζ)

All microfiltration (MF) membranes showed negative zeta potentials in the entire pH range (Fig. 3.5), this means that they had no isoelectric point (Table 3.3). For these membranes, cake formation is not favoured since there is no bulk solution pH value, which would make repulsive forces to be zero. Even if in the experimental pH range they had different values, no influence had been observed in the permeability with microalgae, probably due to the most important pore size influence than charge effect.

On the other hand, for three of the four ultrafiltration (UF) membranes an isoelectric point showed values close to pH 4. Only the PAN 50 membrane had no isoelectric point at all, as the other polyacrilonitrile membrane, PAN 400. This is a typical behaviour observed for this material attributed to the specific adsorption of electrolyte anions onto its surface [90]. Fig. 3.5 shows pH dependence of the zeta potential ζ determined from streaming potential measurement of all membranes, which characteristically decreases by pH increasing. If the zeta potential is known over the entire pH range it is possible to decide a proper pH value when operating in order to improve performance, by reducing fouling or diminishing cake formation caused by charge effects.

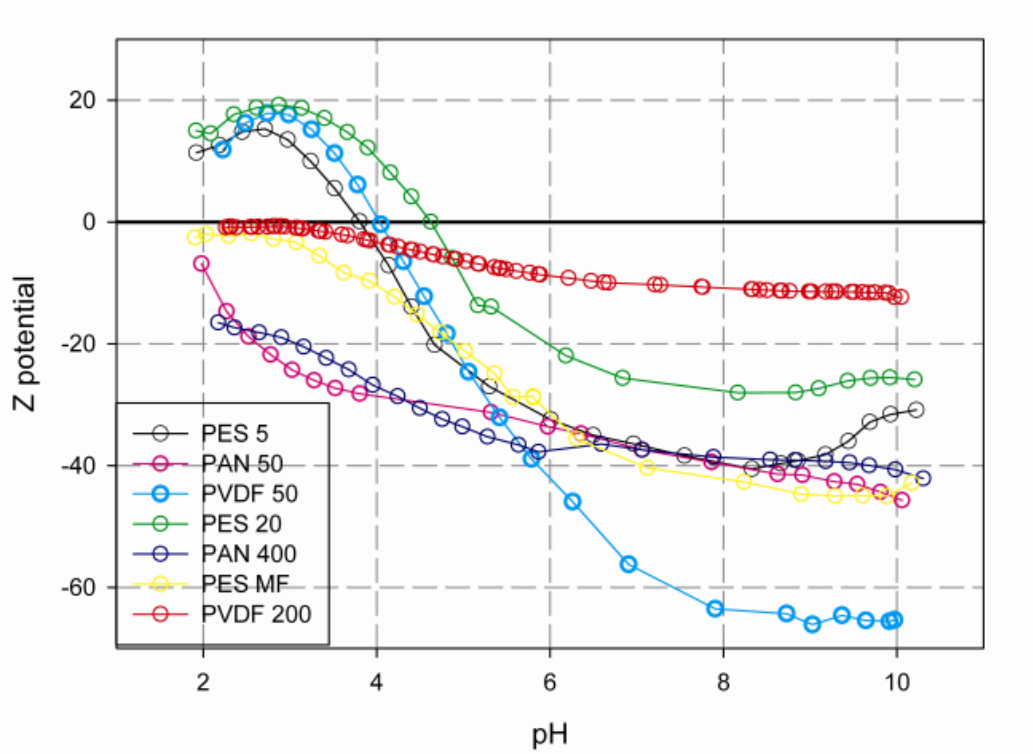

Fig. 3.5 Membrane Z potential along the entire pH range.

It is interesting to observe the curves trend of same materials. In theory this should be the same for the same membrane but, for PES 5 and PES 20 membranes a tendency has been observed of a slight shift to lower zeta potential values. PAN 50 and PAN 400 showed almost the same trend. On the other hand, an important difference between PVDF 50 and PVDF 200 curves trend has been observed. Even if they are made of the same material (according to the fabricant specifications) the PVDF 50 showed the larger zeta potential divergence during pH difference from acid to basic values and the PVDF 200 showed the flattest of all curves. These results showed that probably several materials are present in the membrane surface, for this reason a preliminary study is essential.

As the microalgae pH was around 7.42 ± 0.45 for *Phaeodactylum tricornutum* and 7.27 ± 0.40 for *Nannochloropsis gaditana* the value of zeta potential at pH 7 was reported in

order to see which membrane would attract positive feed constituents more strongly than others. As it is shown Table 3.3 and Fig. 3.5, PAN 50 membrane is the one having the closest zeta potential to the isoelectric point and it is the one having the lowest microalgae permeability too.

Membranes	**Isoelectric point (pH)**	**Zeta potential at pH 7**
Ultrafiltration		
PES-5/Tyvek	3.70 ± 0.13	-37 ± 6
PAN-50	none	-29 ± 7
PVDF-50	3.99 ± 0.09	-65 ± 12
PES 20	4.81 ± 0.23	-30 ± 9
Microfiltration		
PVDF 200	none	-10 ± 2
PAN 400	none	-38 ± 4
PES MF	none	-52 ± 11

Table 3.3. Membranes isoelectric points and zeta potential at pH = 7.

On the other hand, the more negative value in this pH range is given by the PVDF 50 membrane. This comparison shows how important the zeta potential evaluation is especially when the membrane cut-offs are the same. This behaviour should be taken into account for the fouling of the membranes, because a reduction of interactions is required for process optimisation. This is possible only knowing the zeta potential in all pH range.

Morphology. Scanning electron microscopy images

Analysis by SEM provided visual characterization of the cross section morphology of the commercial membrane (Fig. 3.6). The SEM images revealed that thickness varied between 50 and 100 micrometers. All of them possess the same structure with large macrovoids that allow them to achieve such high water permeability values due to the less hydraulic resistance.

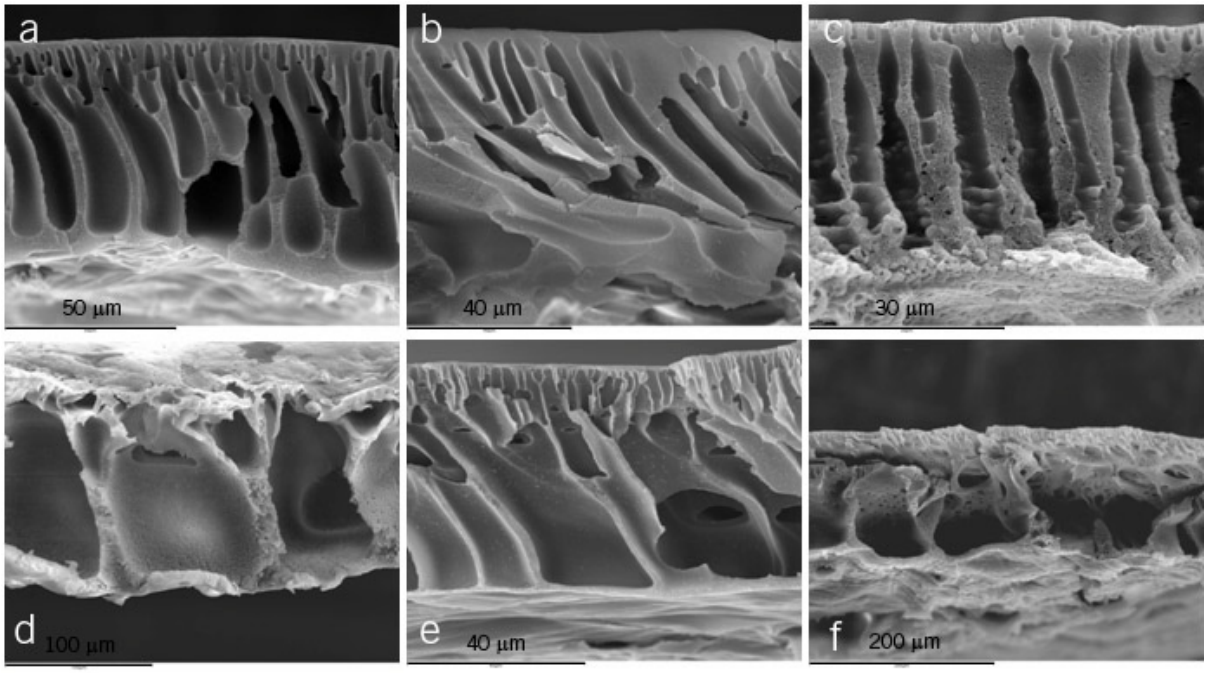

Fig. 3.6 Cross-section membrane scanning electron microscopy micrographs: (a) PES 5; (b) PES 20; (c) PVDF 50; (d) PVDF 200; (e) PAN 400; (f) PES MF.

3.2.4.2 Filtrations experiments

Nannochloropsis gaditana

Dynamic filtration

Permeability tests with water previous to microalgae filtrations showed higher values for microfiltration membranes than those for ultrafiltration ones, as expected. The one having

higher permeability is the polyethersulfone membrane (PES MF) with cut-off equal to 0.2 micrometres (Table 3.4).

Membranes	**Water permeability ($L/h/m^2/bar$)**	**µalgae permeability ($L/h/m^2/bar$)**
Ultrafiltration		
PES 5	65 ± 8	49 ± 6
PVDF 50	271 ± 24	43 ± 5
PAN 50	363 ± 34	30 ± 0
PES 20	170 ± 18	36 ± 4
Microfiltration		
PVDF 200	230 ± 26	33 ± 1
PAN 400	587 ± 154	34 ± 4
PES MF	698 ± 123	31 ± 4

Table 3.4. Water and microalgae permeabilities.

This could be deductible from the cut-off, but experiments showed that the material was a crucial parameter for the choice of the most adequate membrane as well. As can be seen from Table 3.4, in the case of PVFD 50 and PAN 50, even if the membrane cut-off was the same, permeability changed considerably, both in the case of water and microalgae filtration, but in an opposite manner. For water permeability PAN 50 has the highest value that confirmed its hydrophilic behaviour showed by the contact angle measurement, and for microalgae permeability it has the lowest value that confirms its high tendency to particles aggregation showed by the zeta potential measurement.

With water permeability results it could be expected that the bigger cut-off (PES MF) could be the best one for microalgae filtration. But, experiments showed that the high water permeability was not a guarantee of high microalgae permeability (Fig. 3.7).

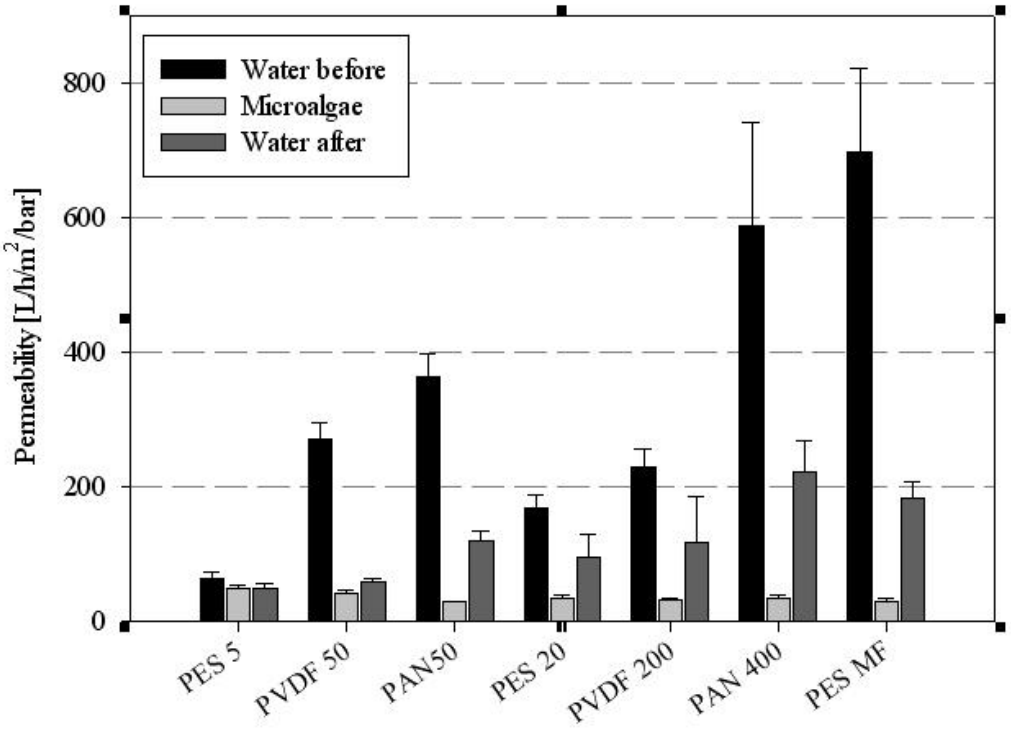

Fig. 3.7 Membrane permeabilites. Water and microalgae permeability for several membranes in dynamic filtration with *Nannochloropsis gaditana*.

Membrane with higher value was not the PES MF (Table 3.4). Therefore, it was not the most suitable for this application. On the contrary, PES 5 had the highest value and it was the one with the lowest permeability value. The reason behind this behaviour is the fouling reduction due to the pore size decrease, as is also observed by [22]. Although microfiltration membranes are useful for microalgae rejection, they are not the most appropriate in term of fouling reduction.

Besides membrane material and pore size, another key parameter that permitted the evaluation of membrane properties was the membrane regeneration. It was observed that the high water permeability did not offer any clues about how permeability performance could be

with microalgae. And it is demonstrated that the same can be noticed about the water permeability after microalgae filtration. This means that it was also relevant to check after the experiment if the membrane was regenerated, as the permeability fall is related to the membrane reversible fouling.

Membrane that recovered the initial water permeability in a better way after washing was the PES 5 one. For this membrane, permeability value decreased to the 77% against the 22% of the PVDF 50 membrane. This means that after several hours of the experiment the membrane got dirty mostly on its surface and almost no pore blocking occurred. This is an advantage for its possible cleaning and reuse. Once cleaned with water it recovered almost all its filtration potentiality as at the beginning.

For the membrane selection it is necessary to analyse all parameters togheter. From this point of view, even if PVDF 50 and PES 5 had close permeability values, the membrane that gave the best results was PES 5. Even if the virgin membrane water permeability was lower than that of PVDF 50 it remained almost the same as the microalgae permeability, that was also of a higher value compared to the other membranes.

Comparison between laboratory scale and pilot plant scale

A comparative study between cultured biomass from laboratory (300 litres bags) and cultured biomass from a pilot plant (9000 litres outdoor photobioreactors) was performed (Fig. 3.9). This study showed in both cases a drop in values from ultrafiltration to microfiltration due to fouling reduction (Fig. 3.8), as explained in the previous paragraph.

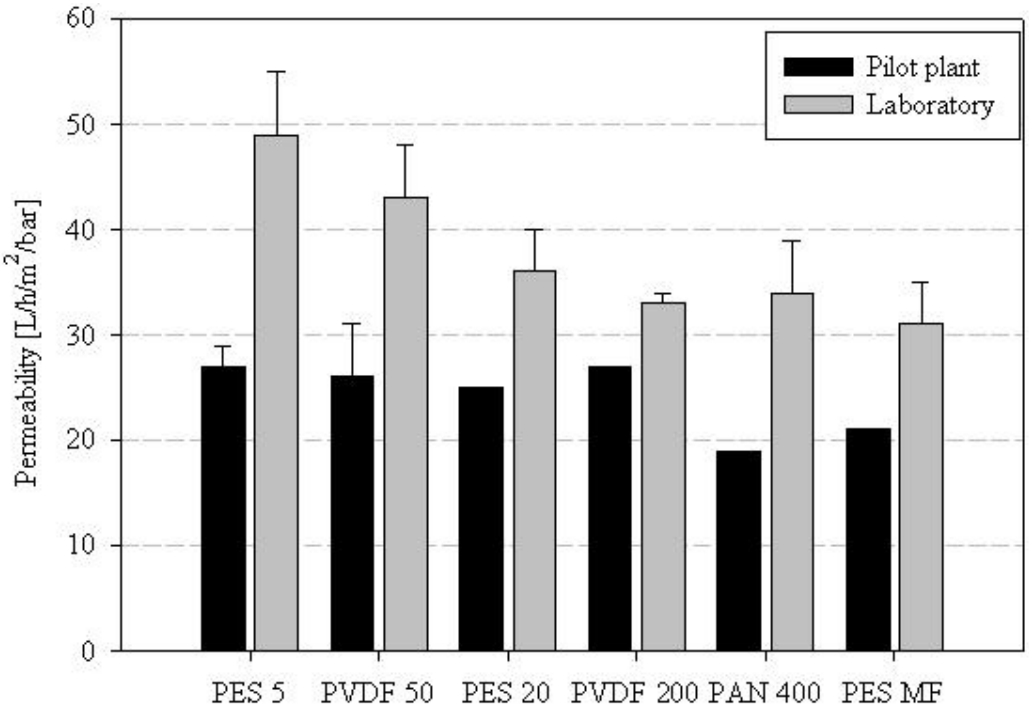

Fig. 3.8 Comparison between results obtained at lab scale from 300 L photobioreactor cultured biomass and at pilot scale from 8500 L photobioreactor cultured biomass with Nannochloropsis gaditana.

Permeability values were from 30% to a maximum of 40% lower in the case of pilot plant scale than laboratory ones. This can be explained by the higher cells concentration in the culture of about 54±10 x 10^6cells/mL and the open system conditions (possible contamination, etc).

Ultrafiltration membranes are still considered to be the best for this application, in particular the PES 5 one.

Fig. 3.9 Pilot plant installation.

Conventional tangential cross-flow filtration

Dynamic filtration system performances were compared with conventional membrane filtration in order to confirm that the method is the best one as hypothesized and reported.

For dynamic filtrations, the steady state in all cases was achieved in less than 30 minutes, within the interesting case of PES 5 membrane that reached it almost immediately (Fig. 3.10) and, which confirms the low presence of fouling. On the other hand, it was the slowest to achieve the steady state with conventional filtration (Fig. 3.10).

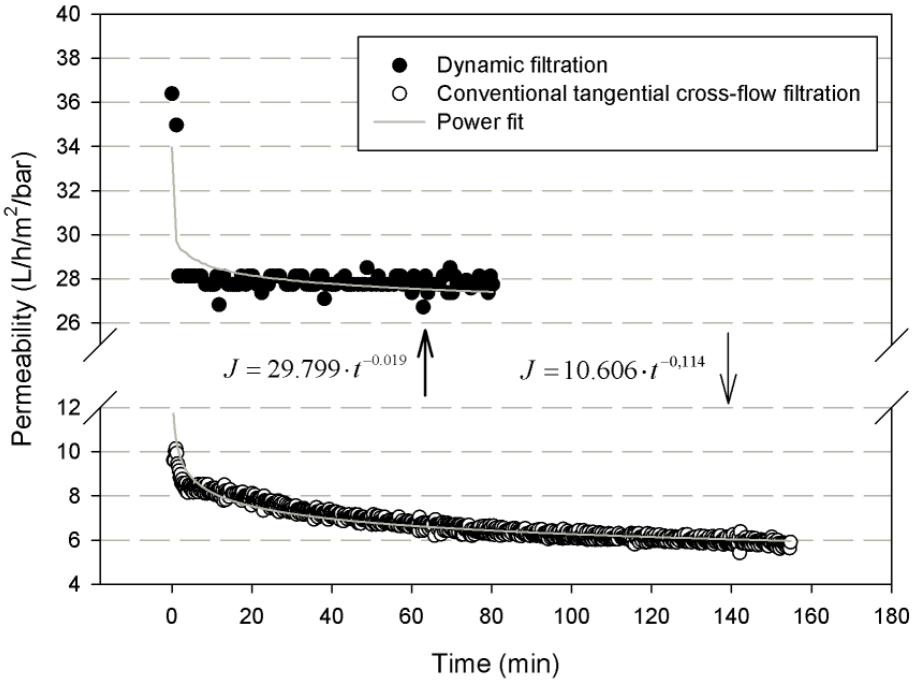

Fig. 3.10 Permeability profiles with time for PES5 membrane with dynamic and conventional filtration.

It was observed for all permeability profiles in conventional filtration that already after the first 5 minutes of work the permeability was really lower than the lowest permeability with dynamic system (examples in Fig. 3.11). In only 30 minutes a value was achieved of about 10 L/h/m^2/bar that was less than the half compared with vibrating filtration.

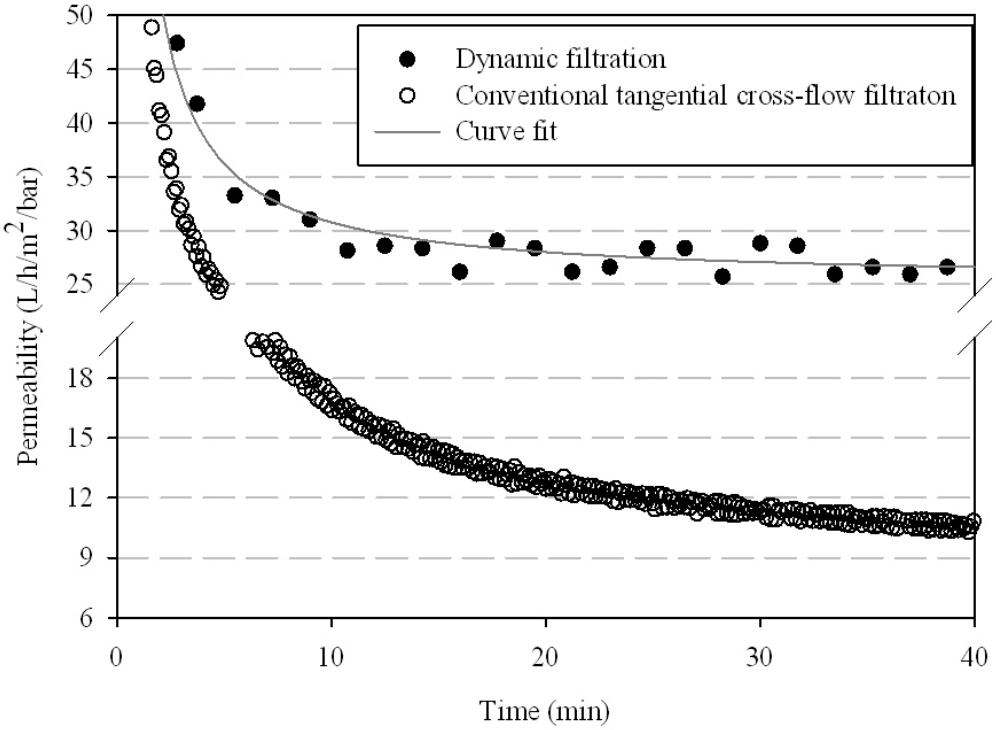

Fig. 3.11 Permeability profiles with time of PVDF-50 membrane with a) dynamic filtration, b) conventional filtration.

Phaeodactylum tricornutum.

Dynamic filtration experiments with *Phaeodactylum tricornutum* species showed that a specific study has to be performed for each species, because in this case permeability results showed the opposite tendency to *Nannochloropsis gaditana*. With *Phaeodactylum tricornutum* species, permeability values were always higher than 40 L/h/m^2/bar and they increased with the increment of the pore size. The highest permeability was given by PES MF membrane (Fig. 3.12) and total retention was obtained.

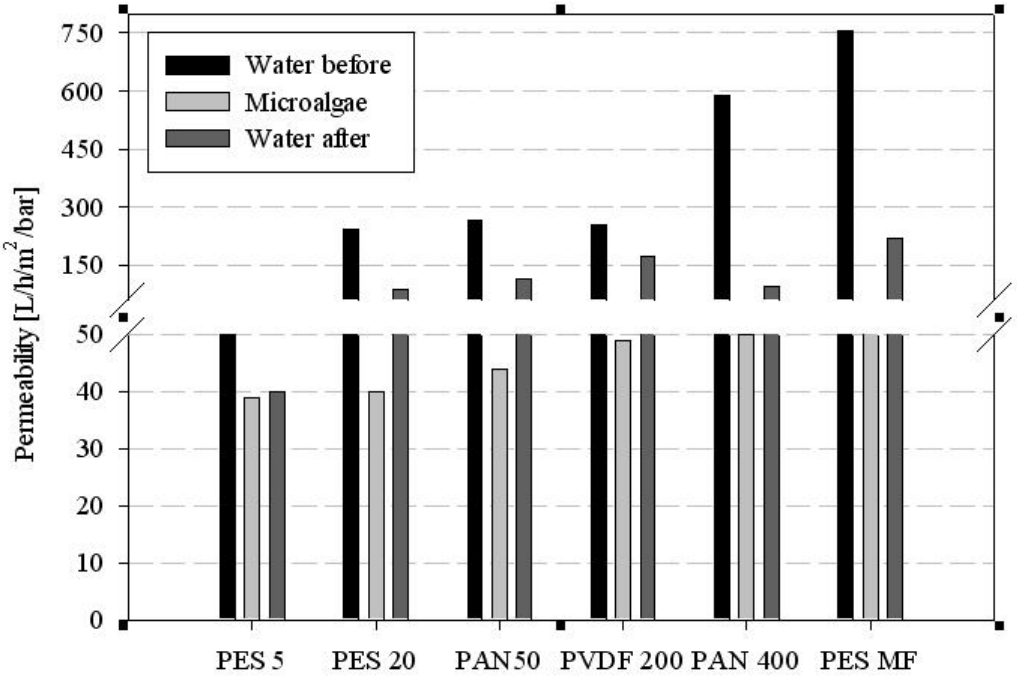

Fig. 3.12 Water and microalgae permeability for several membranes in dynamic filtration with Phaeodactylum tricornutum.

These results are probably due to the differences in microalgae morphology. As *Nannochloropsis gaditana* is spherical and smaller, it has more chances to penetrate in the pores of the membranes than *Phaeodactylum tricornutum,* which is fusiform and bigger. This occurred in particular in the case of MF membranes causing more pore blocking and fouling. On the other hand, the same tendencies as *Nannochloropsis gaditana* were obtained regarding the regeneration of the membrane with a permeability value equal to the 80% of the virgin PES 5 membrane.

3.2.4.3 Coupled sedimentation plus dynamic filtration

Microalgae sedimentation was successfully obtained (Fig. 3.13 a, b) after about 45 minutes from the NaOH solution addition. A change of pH from 9.62 ± 0.12 to a pH of 9.94 ± 0.04 was observed. Absorbance analysis showed a clarified/settled factor of 0.1 and a clarified top cylinder/clarified bottom cylinder of 1. This means that total sedimentation was achieved with 99% of culture contained in the settled phase. The total volume of culture to harvest was reduced from 1200 L to 25 L, obtaining a concentration factor of 17.


a)

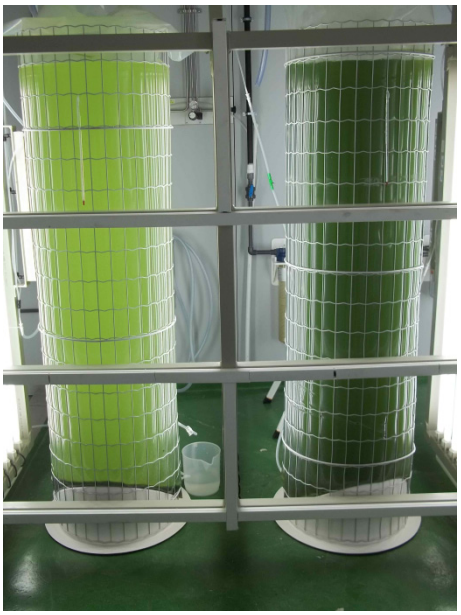
b)

Fig. 3.13 a) Settled culture at the bottom of the bag; b) settled culture in the bag at the left and not settled one in the bag at the right.

Settled microalgae (25 L) were harvested and finally filtrated by vibrating membrane system with the best membrane previously founded for this strain (PES 5). After about 6 hours the volume was reduced to about ten times, to 2.4 liters, obtaining, like this a sludgy retentate (Fig. 3.14 a), obtaining a concentration factor of for this stage of about 7. This gave a total concentration factor of sedimentation plus filtration system of about 125. Total rejection was

obtained already visible with nacked eyes (Fig. 3.14 b) and confirmed later by absorbance analysis with a total absence of microalgae in the permeate.

Fig. 3.14 Dewatering products: a) sludgy microalgae retentate at the end of the process; b) final retentate and clear permeate.

Membrane permeability obtained with settled culture was about 20 L/h/m^2/bar (Fig. 3.15). This value is sensibly lower than the one measured with not settled culture, but the time gained with previous sedimentation compense the total harvesting time needed to achieve this final culture concentration.

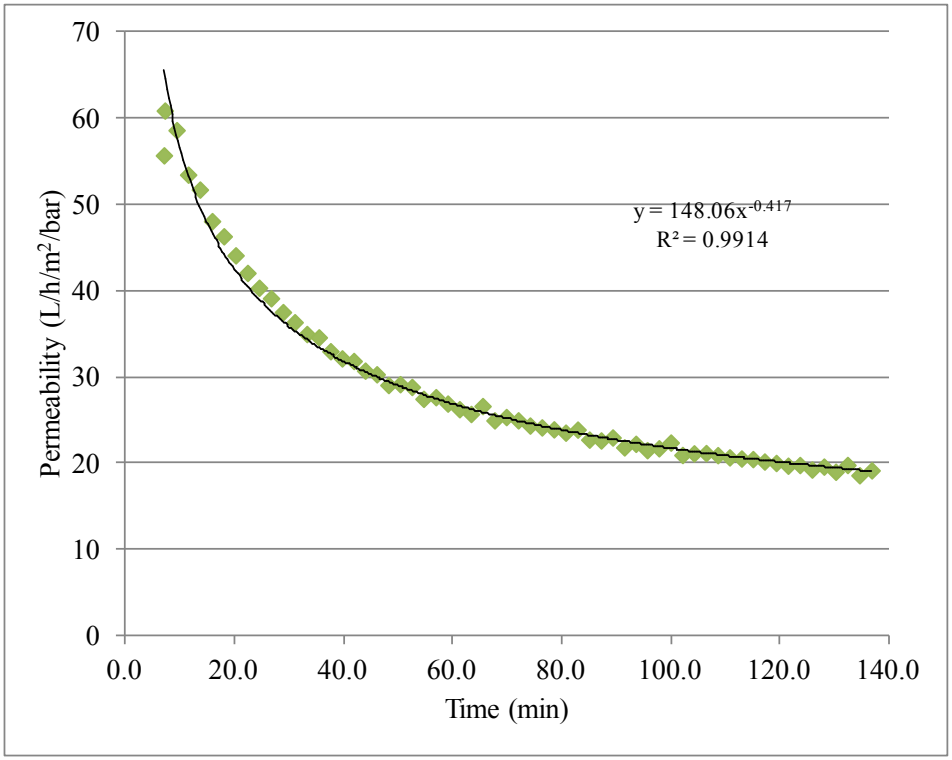

Fig. 3.15 Permeability fall of sedimented culture.

Energy demand

Energy demand of the system was measured and correspond to 0.8 A when pump and vibrating motor are turned off to 4.5 A when only vibrating motor is off and 4.9 A corresponding to the total system operation. This means that the energy required by the vibrating system is only the 8% of the total. This extra energy demand required by the filtration respect to the conventional system is noticeably compensated by the performance growth of this process.

3.3 Conclusions

In this research dynamic MF was the most adequate for *Phaeodactylum tricornutum* filtration, when permeabilities reached approximately 50 L/h/m^2/bar; UF resulted the best for *Nannochloropsis gaditana* filtration with permeabilities around 30-50 L/h/m^2/bar.

Vibrating membrane filtration was demonstrated to largely improve conventional tangential cross-flow membrane filtration in microalgae dewatering. Permeate flow rates were at least doubled in dynamic filtration compared to the conventional one (around 10 L/h/m^2/bar). In some case, the improvement almost implies the elimination of fouling.

This progress is directly related on the process cost, since it allows incrementing the production yield, or reducing substantially the membrane area needed.

Further progresses were obtained settling the culture with pH induced flocculation before filtration in terms of time, costs and final concentration.

UNIVERSITAT ROVIRA I VIRGILI
SEPARATION PROCESSES IN MICROALGAE BIOREFINING
Claudia Nurra

4

4.CATALYTIC MEMBRANE REACTOR FOR TRANSESTERIFICATION

In this chapter an alternative to conventional process in sunflower oil transesterification is explored. The investigation started with the substitution of the generally used homogeneous catalyst with a heterogeneous one and continued with the coupling of the process with membrane filtration. The study was addressed to the manufacturing and characterization of a catalytic membrane reactor (CMR) to produce and isolate FAME from oil in a coupled process (transesterification + separation).

4.1 Introduction

Biodiesel is receiving increasing consideration in the last decades because of the petroleum scarcity and environmental issues. Transesterification of bio oil with methanol is the most common process used for biodiesel production. This process is generally carried out by using homogeneous catalyst (usually alkali-catalyst) in a stirred vessel reactor, it provides fast reaction rates than heterogeneous ones [91]. Due to the low cost of raw materials sodium and potassium hydroxides are usually used as alkali homogeneous catalyst. They are the most economic because the process is carried out under low temperature and pressure environment and the conversion is high with any intermediate steps [92]. However, this production method

implies several by-products, as soap and water, generated due to the need of a washing step for catalyst removal [93], that entails the necessity of more energy and investment. For this reason, a substitution of the homogeneous catalyst with a solid heterogeneous catalyst (SHC) could be an appropriate solution, allowing an easier separation of the catalyst (for example by filtration), that permits a catalyst reuse for further reactions, and no water need. In addition solid heterogeneous catalyst can simultaneously catalyze the transesterification and esterification reactions that can avoid the pre-esterification step [92].

SrO can be used for many catalytic reactions [91], it has strong basic sites and is insoluble in methanol, vegetable oils and fatty acid methyl ester. Amberlyst®15 is a promising catalyst because of its good activity at moderate temperature and durability [94]. Zeolites have been demonstrated a good catalyst in the transesterification of triglycerides for biodiesel production [95].

Among the different alcohol materials that can be used in transesterification process, methanol is especially used because of its lower cost and its physical and chemical advantages.

In biodiesel production it is necessary to remove residual triglyceride and glycerol from the FAME. One method is to drive the reaction as close to complete conversion, however this is an equilibrium reaction and for this reason there are limits to this approach. Other approaches employ multiple water washing steps, which can give rise to a waste treatment problem in the wastewater stream [96]. FAME, methanol and glycerol can be separated by settling in a step that follows the batch transesterification reaction. Membrane reactor can be an excellent tool for transesterification process [97-101], in order to separate these products in a continuous process. The combination of the two solutions mentioned gave a catalytic membrane reactor (CMR) with solid heterogeneous catalyst inclusion. This system

can improve performance because of the low rate of the reaction in conventional process, due to catalyst low use efficiency, not need of catalyst recovery, etc. In the CMR the large droplets of oils are not able to cross the membrane to the contrary of methyl esters and methanol. This permits to remove the products from the reactor overcoming the equilibrium limitations. Moreover methanol and catalyst can be reused in further reactions. Membrane reactor for biodiesel attainment have been investigated recently [96, 97] but homogeneous catalyst issues follow. For this reason this work wanted to identify an appropriate SHC for transesterification, its immobilization in the CMR, and finally the evaluation of the catalytic performance.

4.2 Experimental

4.2.1 Materials

For the transesterification reactions commercial common regional sunflower oil from Borges Company was used, because of its similar characteristics to microalgae oil. Methanol (99.9%, was purchased from Scharlau). Commercial biodiesel was kindly provided by Stocks del Valles, S.A.

Heterogeneous catalysts in both acid and/or base forms were studied. Two catalysts were selected from literature zeolite-based catalyst (MFI 90: commercial zeolite from Sud-Chemie, with a Si/Al ratio = 90), acid catalyst (Amberlyst®15, hydrogen form Sigma-Aldrich), and base catalyst (Strontium Oxide, technical grade, Alfa Aesar).

For GC analysis N-Heptane (>99%, VWR), methyl heptadecanoate (standard for GC, Sigma-Aldrich) and F.A.M.E. MIX, C8-C24 (Sigma-Aldrich) were purchased.

Commercial polysulfone membranes of 8, 5, 3, 1.2 and 0.2 μm were tested (purchased respectively from GE Osmonic and New Logic). For the catalyst immobilization PSf (Mw = 35,000 purchased from Sigma Aldrich) membrane were synthesized. Solvents used: DCM (99.99%), 1,4-Dioxane (99%), THF(99.8%) and DMF (99.9%, Multisolvent®), DMA (99.5%) and NMP (99.5%) were purchased from Scharlab. 100% purified water was used in the coagulation bath.

4.2.2 Methods

For the transesterification reactions, process properties were reproduced as found in literature for other applications (Table 4.1).

Property		
Catalyst	Amberlyst®15[a]	Strontium Oxide[b]
Catalyst loading	3%	3%
Temperature	65	65
Oil to alcohol ratio	12:1*	12:1
Time of conversion	2 hours	30 minutes

* 6:1 in literature
[a] Applied Catalysis A: General 295 (2005) 97 – 105
[b] Catalysis communication 8 (2007) 1107 – 1111

Table 4.1.Variables values from literature in distinct applications.

Oil and methanol were weighted and placed to be pre-heated on a heating oil bath over a hot plate in a round bottom flask equipped with a magnetic stirrer and thermometer.The catalyst was added to the flask.

Three configurations were studied for the reaction: (i) conventional one with the catalyst in the round bottom flask (Fig. 4.1 a), followed by a separate standard phases partition; (ii) reaction with the catalyst in the round bottom flask in which phases separation is performed by continuous filtration with a commercial membrane (0.2 μm); and, finally, (iii) reaction in a synthesized catalytic membrane (Fig. 4.1 b).

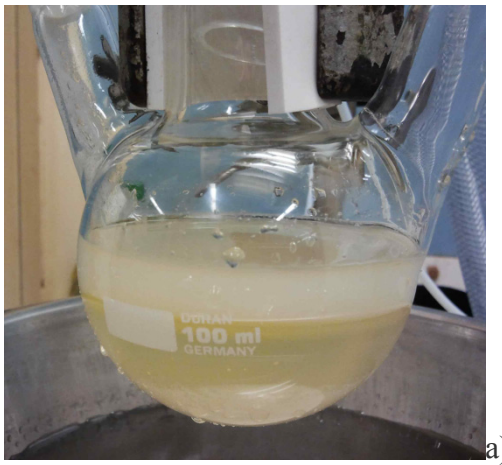

a)
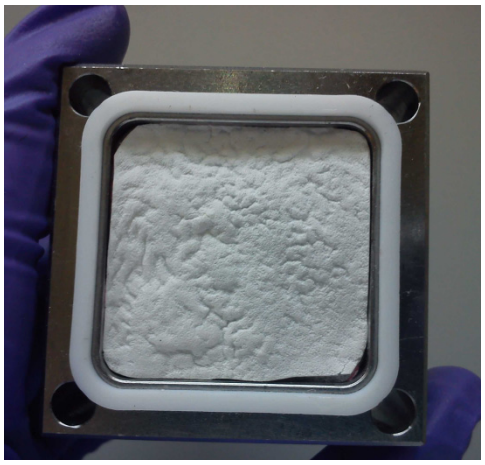
b)

Fig. 4.1 Configurations studied: a) SrO in batch b) SrO on the membrane matrix inside the module.

Transesterification reaction conditions were fixed in all cases to: temperature of 65ºC, oil to alcohol ratio 12:1, flow of 3 ml/min with a trans-membrane pressure between 1 and 4 bar.

Reactions were stopped at the corresponding reaction times by cooling the flasks and halting agitation. As glycerol was formed during the transesterification reaction, three phases are spontaneously separated (Fig. 4.2.). The top phase contained the esters formed (FAME), while the excess methanol was dragged to the glycerol phase in the middle phase of the flask and the catalyst to its bottom. In the case when the SrO is immobilized within the membrane there is no catalyst in the liquid phase (two phases).

Fig. 4.2 Transesterification reaction products (FAME, glycerol, SrO catalyst).

Separation of FAME, methanol and glycerol from the transesterification by membrane filtration was one of the objectives of this study and corresponds to the second configuration mentioned before. Molecular size of each component is as follow: triglycerides 5 x 0.6 nm, FAME 2.5 x 0.3 nm, glycerol 0.6 nm and methanol 0.4 nm. The membrane should reject oil and allow the permeance of reaction products, specially the FAME. To test the separation, filtration experiments of all products separately with the membrane without catalyst have been performed. To limit the variables, at this stage, only commercial polymeric membranes have been considered. The minimum oil droplet size is 12 µm, for this reason, it has been decided to start from a membrane pore size of 8 µm. Commercial polysulfone membranes with 8, 5, 3, 1.2 and 0.2 µm were tested.

For the last configuration studied (iii), membranes were synthesized by the phase inversion with immersion precipitation method (technique well known and described in previous chapters) of a polymeric solution 10% wt PSf in DMF, prepared by magnetic stirring for 24 hours at room temperature. Then the solution was deposited onto a glass plate using a casting knife. The knife was pushed over the glass thanks with an automatic film applicator (BYK-Gardner Automatic Film Applicator L, Fig. 2.3) at constant velocity rate of 110 mm/s and the glass plate was immersed into a coagulation bath to form the membrane. Membranes were characterized by ESEM (FEI Quanta 600), with a voltage between 15 and 20 kV and with low vacuum pressure, since the samples were not conductive and no sputtering was applied.

Catalysts immobilization on or in a membrane surface/matrix was studied. First of all, it was investigated the feasibility of catalyst immobilization and later the possible interaction between the polymer solution and the catalyst. For this reason, comparison before and after immobilization were done of: the membrane and catalyst morphologies and the reaction activity. SrO was immobilized with two different procedures. The first one consisted in the dispersion of the catalyst on the surface of the polymeric solution after casting it over the glass plate with the knife and before immersing it into the coagulation bath. The second procedure lied in mixing the catalyst with the polymer and the solvent during the polymeric solution preparation. Amberlyst®15 was also immobilized into a PSf membrane obtained by the phase inversion method. Amberlyst®15 was dispersed on the surface of the membrane, in an area equal to the membrane size of the micro module (6 cm^2). The catalyst was dispersed after that the polymeric solution was put on the glass plate and before immersing it into the precipitation bath.

Moreover, the interaction between the catalyst and the only solvent present in the polymeric solution was investigated in order to observe if the morphologic modification of the catalyst was caused by the solvent or by the polymeric solution preparation. For this reason SrO and DMF were put in contact by magnetic stirring for 24 hours (as the polymeric solution).

Triglycerides and fatty acid fatty acid methyl esters (FAME) were characterized trough GC analysis, with HP-INNOWax column 19091N-113, 30 m, 0.32 mm, 0.25 μm from Agilent Technologies in a 7890A Agilent Technologies chromatograph, and determined according to the European standard test EN 14103 method. Triglycerides content was obtained by GC analysis where wt% = (triglycerides area in the initial sample – triglycerides area in the actual sample) / triglycerides area in the initial sample.

The addition of a third solvent to the initial solution was studied in order to avoid critic phase separation between oil and methanol due to their immiscibility. Solvents tested were: acetone, chloroform, diethyl ether, ethanol, heptane, methyl ethyl ketone, propanol and toluene, Fig. 4.3) in different oil:chloroform:methanol ratios (1:1:12, 1:6:12, 1:9:12, 1:12:12).

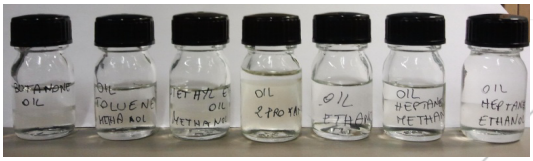

SOLVENT MISCIBILITY TABLE

Solvent	Polarity Index	Refractive Index @20°C	UV(nm) Cutoff @1AU	Boiling Point(°C)	Viscosity (cPoise)	Solubility in water (%w/w)
Acetic Acid	6.2	1.372	230	118	1.26	100
Acetone	5.1	1.359	330	56	0.32	100
Acetonitrile	5.8	1.344	190	82	0.37	100
Benzene	2.7	1.501	280	80	0.65	0.18
n-Butanol	4.0	1.394	254	125	0.73	0.43
Butyl Acetate	3.9	1.399	215	118	2.98	7.81
Carbon Tetrachloride	1.6	1.466	263	77	0.97	0.08
Chloroform	4.1	1.446	245	61	0.57	0.815
Cyclohexane	0.2	1.426	200	81	1.00	0.01
1,2-Dichloroethane[1]	3.5	1.444	225	84	0.79	0.81
Dichloromethane[2]	3.1	1.424	235	41	0.44	1.6
Dimethylformamide	6.4	1.431	268	155	0.92	100
Dimethyl Sulfoxide[3]	7.2	1.478	268	189	2.00	100
Dioxane	4.8	1.422	215	101	1.54	100
Ethanol	5.2	1.360	210	78	1.20	100
Ethyl Acetate	4.4	1.372	260	77	0.45	8.7
Di-Ethyl Ether	2.8	1.353	220	35	0.32	6.89
Heptane	0.0	1.387	200	98	0.39	0.0003
Hexane	0.0	1.375	200	69	0.33	0.001
Methanol	5.1	1.329	205	65	0.60	100
Methyl-t-Butyl Ether[4]	2.5	1.369	210	55	0.27	4.8
Methyl Ethyl Ketone[5]	4.7	1.379	329	80	0.45	24
Pentane	0.0	1.358	200	36	0.23	0.004
n-Propanol	4.0	1.384	210	97	2.27	100
Iso-Propanol[6]	3.9	1.377	210	82	2.30	100
Di-Iso-Propyl Ether	2.2	1.368	220	68	0.37	
Tetrahydrofuran	4.0	1.407	215	65	0.55	100
Toluene	2.4	1.496	285	111	0.59	0.051
Tichloroethylene	1.0	1.477	273	87	0.57	0.11
Water	9.0	1.333	200	100	1.00	100
Xylene	2.5	1.500	290	139	0.61	0.018

Xylene, Water, Tichloroethylene, Toluene, Tetrahydrofuran, Di-Iso-Propyl Ether, Iso-Propanol, n-Propanol, Pentane, Methyl Ethyl Ketone, Methyl-t-Butyl Ether, Methanol, Hexane, Heptane, Di-Ethyl Ether, Ethyl Acetate, Ethanol, Dioxane, Dimethyl Sulfoxide, Dimethylformamide, Dichloromethane, 1,2-Dichloroethane, Cyclohexane, Chloroform, Carbon Tetrachloride, Butyl Acetate, n-Butanol, Benzene, Acetonitrile, Acetone, Acetic Acid

Immiscible

Miscible

Immiscible means that in some proportions two phases will be produced

Synonym Table
[1] Ethylene Chloride
[2] Methylene Chloride
[3] Methyl Sulfoxide
[4] tert-Butyl Methyl Ether
[5] 2-Butanone
[6] 2-Propanol

Fig. 4.3 Solvent miscibility.

4.2.3 Equipment

The set-up used in this study varied depending on the configuration used (detailed in the previous section 4.2.2). The three configurations used a round bottom flask, equipped with a magnetic stirrer and condenser and placed on a glycerol bath over a hot plate.

In the latter two configurations the reaction products (methanol, FAME, oil and glycerol) were continuously filtrated in a membrane micro-module system working with tangential cross flow filtration. The system pumped the products from the top layer and gave back those products to the vessel after filtration. This system enhanced the contact between the reactants their selves and with the membrane surface and the catalyst. Membrane area was equal to 6 cm^2; a SFT Series II Digital Pump and a back pressure (TESCOM Corporation) (Fig. 4.4). The micro-module was immersed in a heated bath at 70ºC.

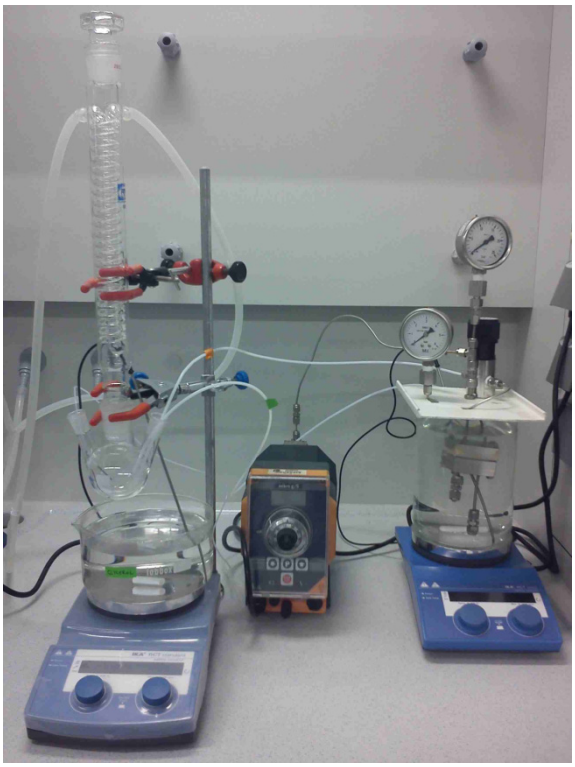

Fig. 4.4 Experimental set-up.

4.3 Results

4.3.1 Membrane pore size distribution study

The cut-off size of the membrane used in the CMR should be according to the separation needs. Triglycerides should be rejected by the membrane and methyl esters have to cross the membrane. Therefore, several membranes with different cut-off sizes were tested. Despite the minimum droplet size and triglycerides molecular size, complete oil rejection was observed with only the 0.2 µm membrane of all the ones tested (Table 4.2). Glycerol was rejected with all applied membranes, whereas FAME and methanol permeate. This permitted to separate triglycerides and glycerol from methanol and FAME in continuous, as desired without the necessity of a following settling phases separation.

		Ability to cross the membrane			
Type of membrane	**Pore size (micrometers)**	**Triglycerides**	**FAME**	**Glycerol**	**Methanol**
Commercial polysulfone	8.0	Yes	Yes	No	Yes
	5.0	Yes	Yes	No	Yes
	3.0	Yes	Yes	No	Yes
	1.2	Yes	Yes	No	Yes
	0.2	No	Yes	No	Yes

Table 4.2. Membrane rejections.

4.3.2 Oil-methanol immiscibility

Of all solvents tested to resolve the oil-methanol immiscibility issue only chloroform could make the three components solution miscible with a volumetric ratio oil:methanol:chloroform of 1:12:6.

A transesterification reaction in batch was performed in order to see if this solvent affects its performance. The same conversion as the reaction without chloroform was successfully obtained.

A last test has been performed for chloroform in order to see its compatibility with the process and especially with membrane filtration. But, as chloroform dissolved the polymeric membranes used, it was not possible to combine it with this configuration.

4.3.3 Identification for catalyst in transesterification

A preliminary study showed that zeolite-based catalyst had no conversion in the transesterification process of sunflower oil. For this reason, studies were focused on Amberlyst®15 and Strontium Oxide (SrO).

Transesterification reactions with Amberlyst®15 and SrO achieved a lower conversion than literature, probably due to the different applications. For Amberlyst®15 the time of conversion was more than 8 hours and low conversions were achieved (5 wt%) (Fig. 4.5). Higher percentage of methyl stereate was obtained instead of methyl linoleate and cis-9-oleic methyl ester.

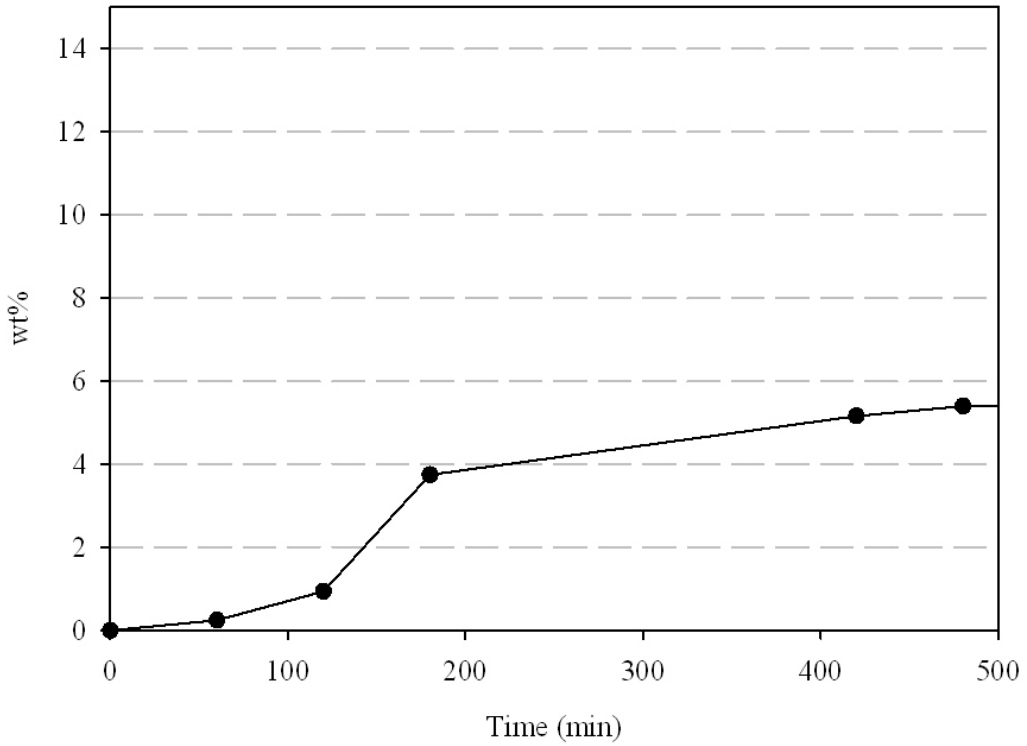

Fig. 4.5 FAME yield of sunflower oil biodiesel in Amberlyst®15 reaction during time (wt% according to EN14103 method).

For Strontium Oxide higher conversion was obtained, 64 ±2 wt %, was after 180 minutes of experiment (Fig. 4.6), with a peak of 73 ±3 wt % after 30 minutes. The reaction needed a period of about 4 hours before getting stable to this percentage, as it can be seen also from the FAME and triglycerides content evolution (Fig. 4.7).

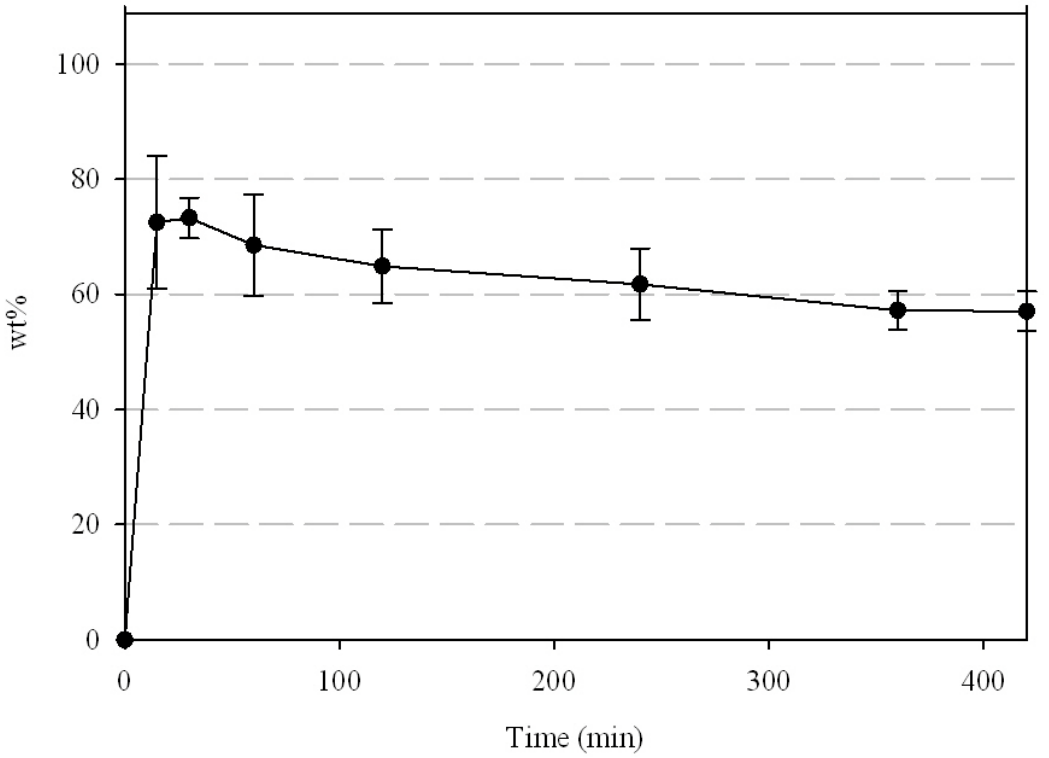

Fig. 4.6 FAME yield of SrO transesterification reaction during time (wt% according to EN14103 method).

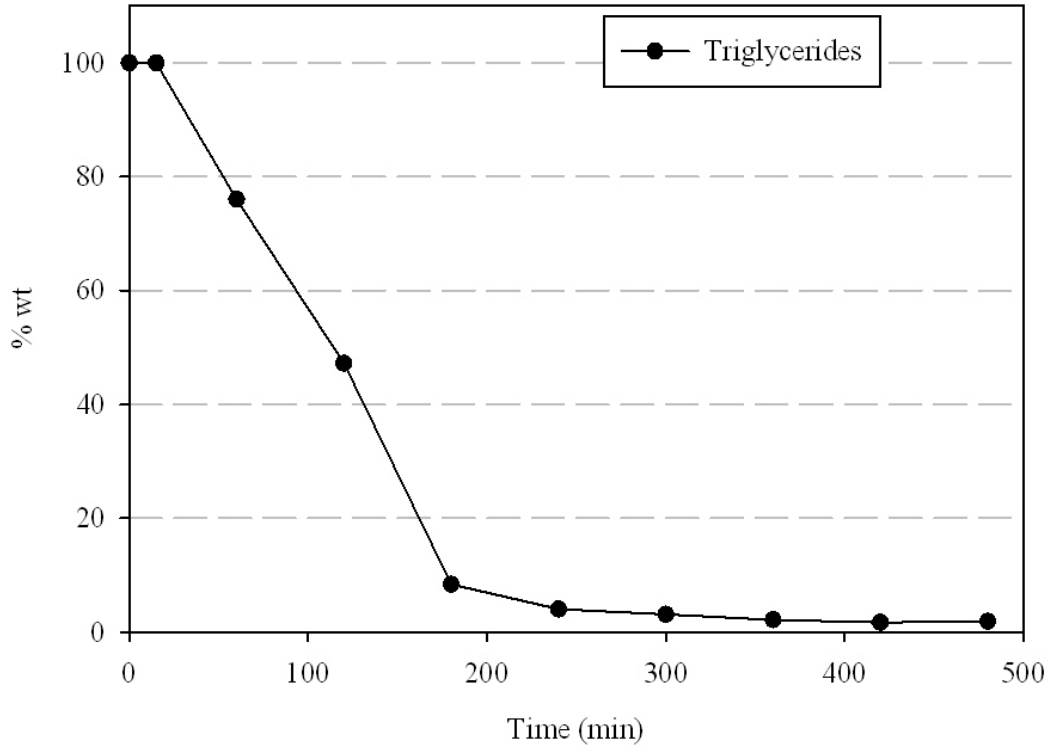

Fig. 4.7 Evolution of triglycerides content in SrO reaction during time. Where wt% = (triglycerides area in the initial sample – triglycerides area in the actual sample) / triglycerides area in the initial sample.

Because of its yield conversion, Strontium Oxide was chosen as best catalyst for this application and the biodiesel composition was measured and compared to literature (Table 4.3). These percentages were obtained starting from 180 minutes from the beginning of the reaction (Fig. 4.8). Ester (C14-C24) content was obtained by GC analysis were wt% = (esters total areas – ester area) / esters total areas.

	Typical composition of sunflower oil biodiesel		Experimental values
Methyl Palmitate	16:0	6 % wt	1 % wt
Methyl Stearate	18:0	3-5 % wt	3-4 % wt
Cis-9-oleic methyl ester	18:1	17-22 % wt	34-36 % wt
Methyl Linoleate	18:2	67-74 % wt	56-60 % wt

Table 4.3. Methyl esters composition in sunflower oil biodiesel.

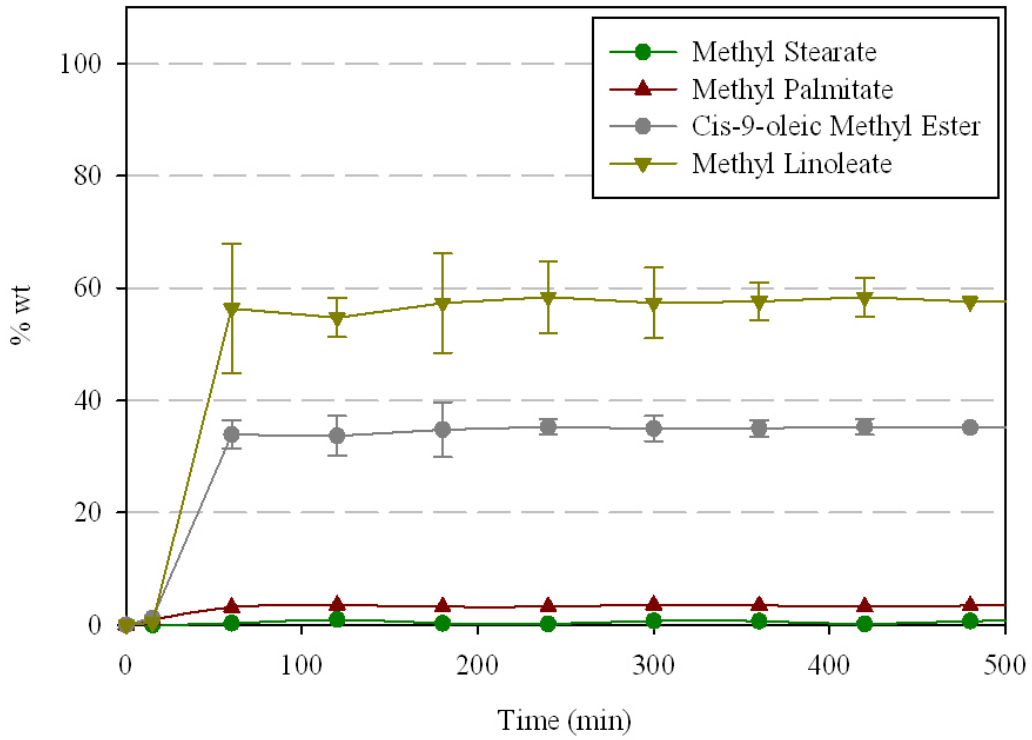

Fig. 4.8 Evolution of esters content in SrO reaction as a function of time.

4.3.4 Membrane catalyst immobilization

As the method used to synthesis the CRM was the immersion precipitation one, an interaction between the solvent and the catalyst was expected to possibly occur. Thus, to study this phenomenon, the catalysts were dispersed in several solvents used to obtain the catalytic membranes. The morphology of the catalysts was investigated before and after the soaking as described in the methodology section.

4.3.4.1 SrO interaction with solvents

Some interaction was observed between the SrO catalyst and the solvents (DMF, DCM, 1,4-Dioxane, NMP, THF and DMA). Fig. 4a shows the catalyst particles before immersing them in solvents. Different morphological changes in the particles were observed with different solvents. SrO was affected by DMF (Fig. 4.10 a) forming as "thorns" (Fig. 4.10 b) that are the parts that probably became that "rice shapes" afterwards during the membrane synthesis.

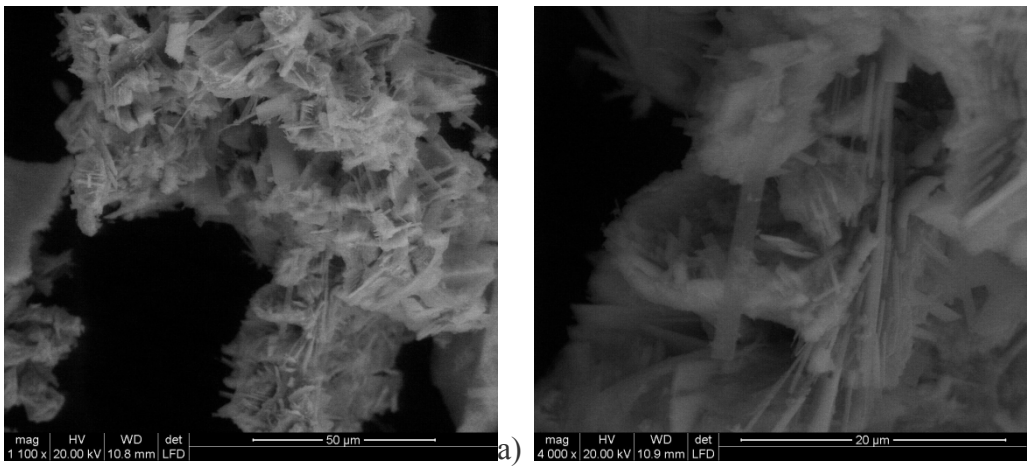

a) b)

Fig. 4.9 SrO interaction with DMF.

DMA gave a similar result as DMF, with a modification of the morphology and a formation of thorns, but thinners than in the previous case (Fig. 4.10e). Finally, no significant changes were observed with the other solvents.

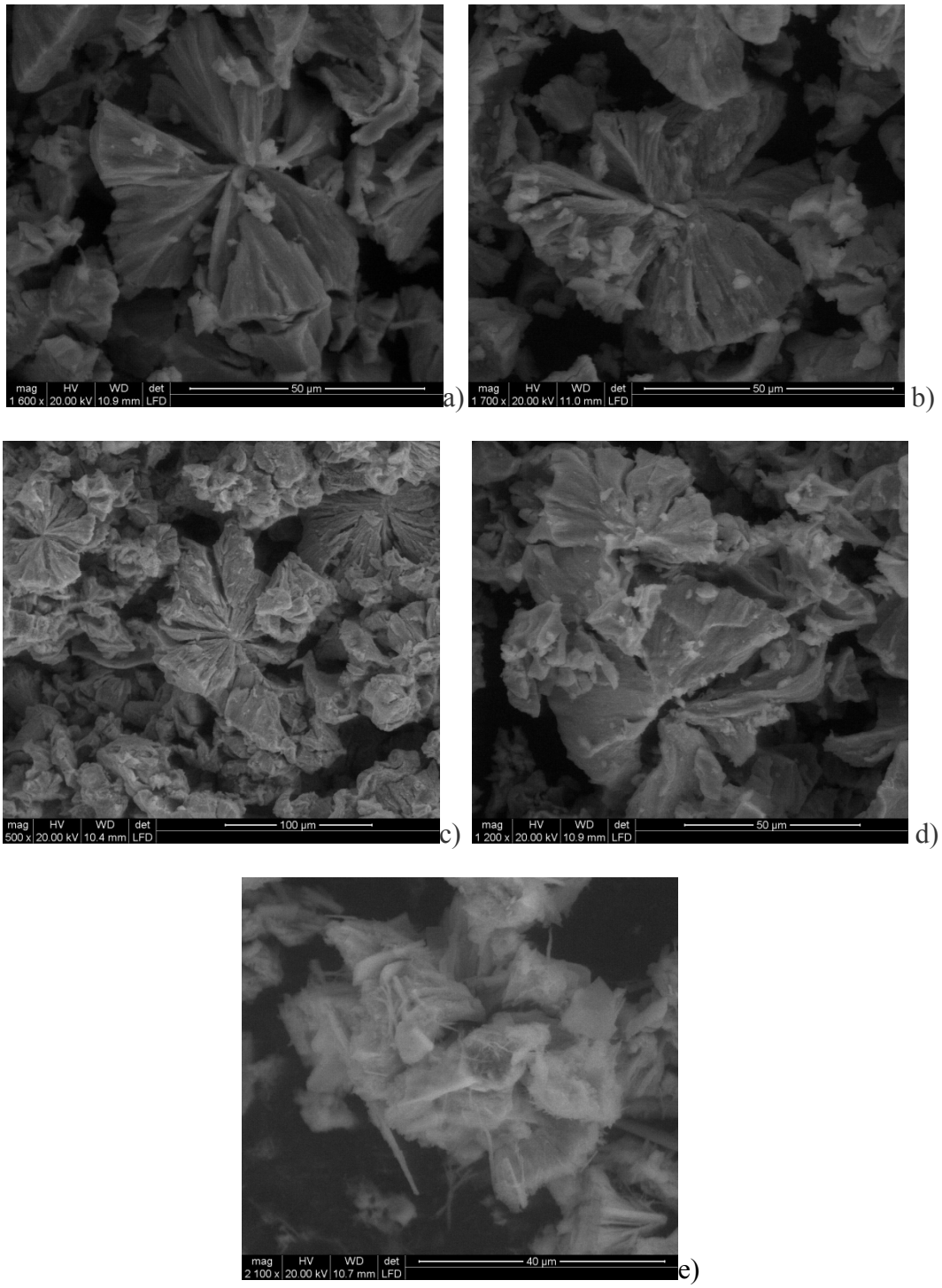

Fig. 4.10 SEM micrographs of SrO interaction with several solvents: a) DCM; b) 1,4-Dioxane; c) NMP; d) THF; e) DMA.

In all cases the reticular structure showed by membranes with catalyst in the polymeric solution is absent. It is probably due to a particular interaction between the polymer solution and the catalyst.

4.3.4.2 Amberlyst®15 immobilization

Amberlyst®15 immobilization on the surface of the synthesized PSf membranes was successful and quite homogeneous (Fig. 4.11).

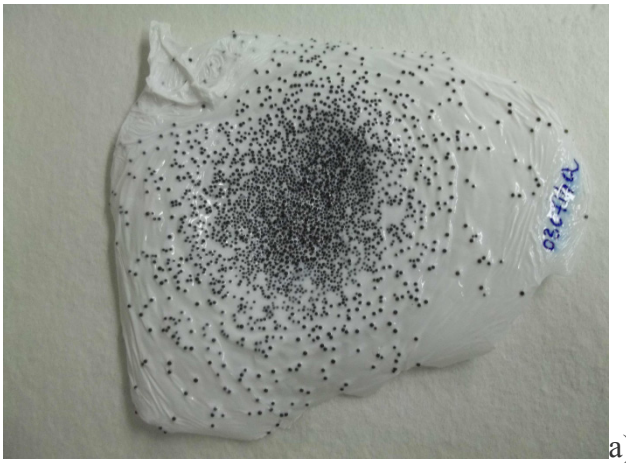
a)

b)

Fig. 4.11 a) Amberlyst®15 immobilized membrane after formation, b) Amberlyst®15 membrane in membrane reactor size.

Amberlyst® 15 was observed with magnifying glass before and after immobilization. Some particles immobilized showed cracks on their glassy surface, probably due to mechanical shocks during membrane formation (Fig. 4.12b).

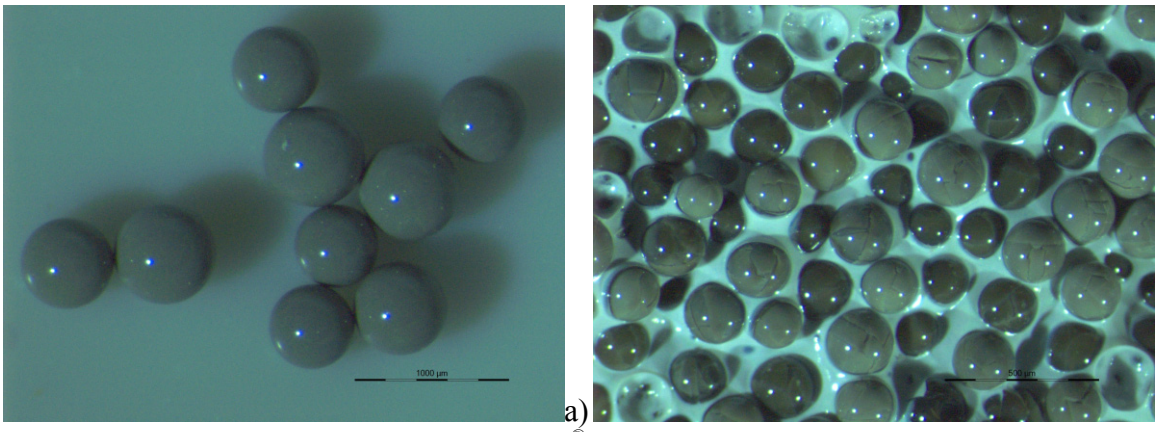

a) b)

Fig. 4.12 Magnifying glass image of Amberlyst® 15: a) without treatment, b) immobilized on a PSf membrane.

4.3.4.3 SrO immobilization

SrO was successfully immobilized with the two different procedures used (section 4.2.2). In the first case, a decomposition of the catalyst was observed. The catalyst is converted from an "agglomerate particle" with a size around 500 µm (Fig. 4.13a) to two different shapes particles: one of 50 µm with "flower shape" and the other of about 1 micron with "rice shape" (Fig. 4.13 b,c,d).

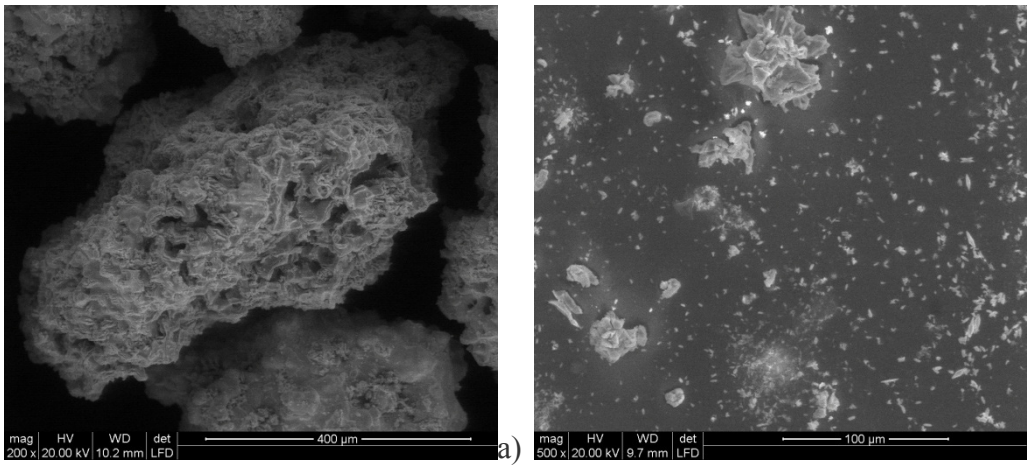

a) b)

c)
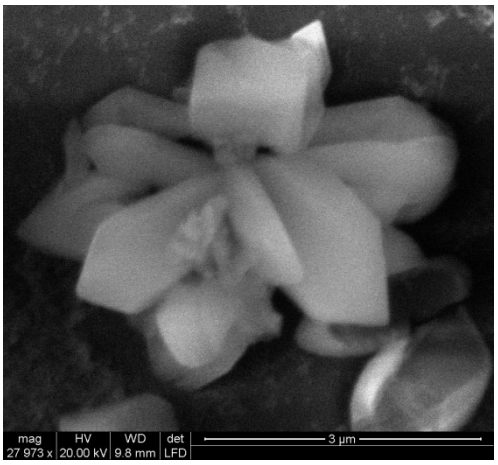

d)

Fig. 4.13 SEM micrographs of: a) Virgin SrO; b,c,d) SrO on the surface of PSf membrane at different magnifications.

Moreover the membrane took a wrinkled look (Fig. 4.14) as confirming some interaction between catalyst and polymer formation.

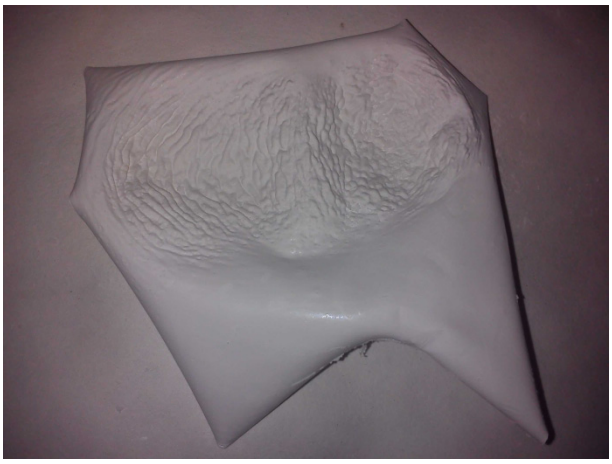

Fig. 4.14 SrO membrane with catalyst on the surface.

The second procedure, apart from giving the two particles shapes as the previous case (flower and rice, Fig. 4.15 a,b,c), it formed inside the membrane a reticular structure (Fig. 4.15 c and d).

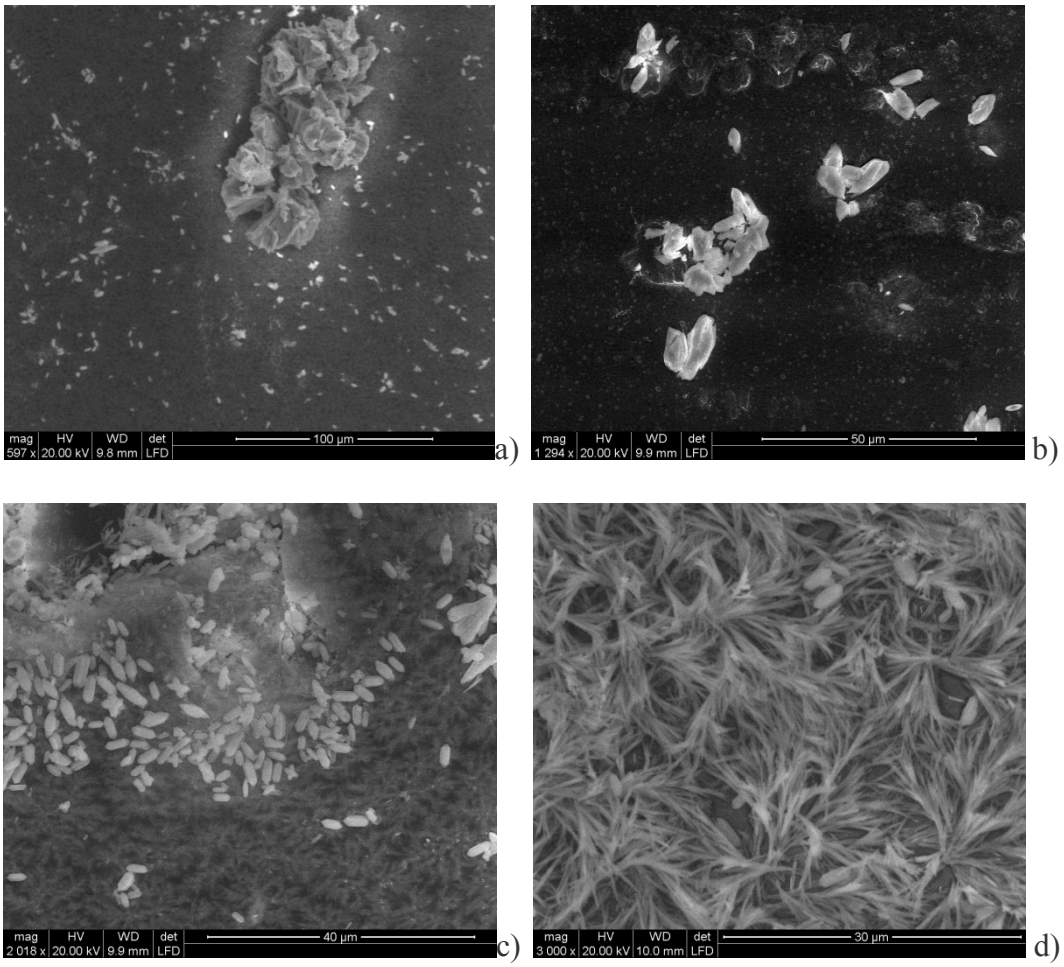

Fig. 4.15 SEM micrographs of SrO membranes with catalyst in the polymeric solution: a) SrO flower shape, b) SrO rice shape, c) SrO reticular structure inside the membrane, d) SrO reticular structure out of themembrane.

4.3.5 Membrane reactor

4.3.5.1 Commercial membrane

To test the catalytic membrane reactor, SrO catalyst was firstly considered due to the higher conversion that offered when tested in batch with the sunflower oil.

A first filtration test was carried out with the 0.2 µm commercial membrane (PESMF, purchased from NewLogic), in order to see if time and yield of conversion were the same as without filtration system. Even if reaction and filtration started at the same time, methanol started to flow in the permeate outlet after 5 minutes of operation, due to the membrane

hydration time needed. Methanol plus FAME both together started to flow in the permeate outlet after 37 minutes, due to FAME formation. The time of conversion was slower than the transesterification reaction in vessel without filtration and the peak was obtained after about 50 minutes instead 20 minutes. The yield of conversion in the filtration case was of about 20% lower (Fig. 4.6 and Fig. 4.16) than without filtration. This is probably due to the loss of temperature in the connection system between the flask and the membrane module reactor.

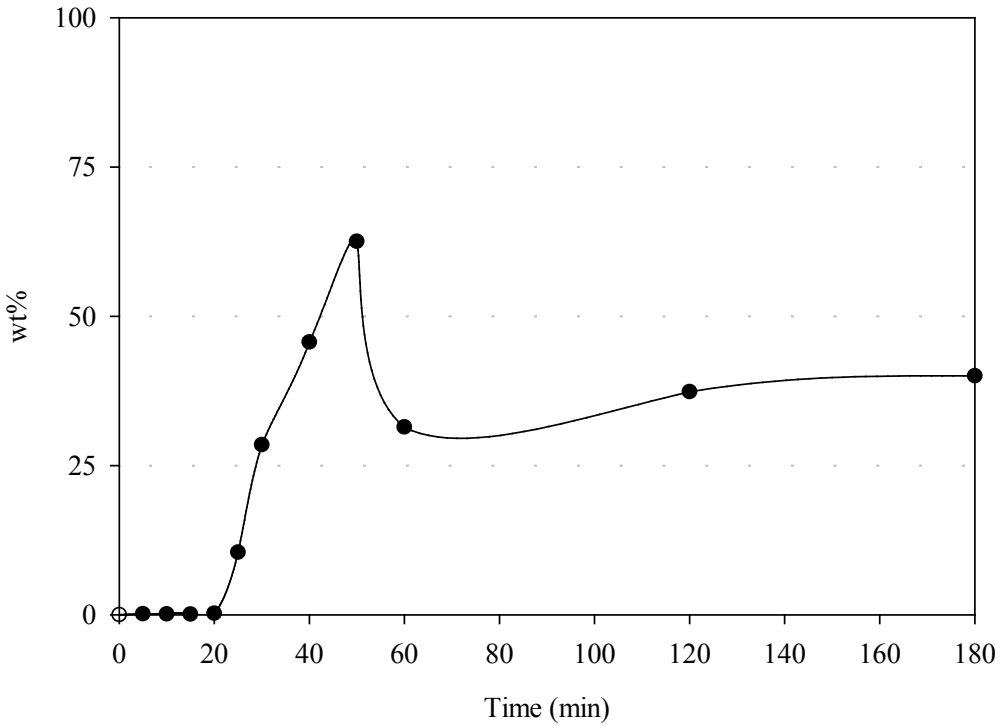

Fig. 4.16 FAME yield with SrO catalyst.

4.3.5.2 Synthesized membranes

CMRs were synthesized (polymeric membranes with catalyst immobilized). Two configurations were tested: with the catalyst fixed on the surface and on the whole matrix of the membranes. Of the two configurations the only showing conversion was the one with catalyst inside the matrix of the membrane. The yield conversions obtained were low due to the small contact area membrane surface (about 3 cm^2) and consequently the limited

percentage of catalyst applicable in this area. Another factor that also could influence in the values obtained was the loss of temperature in the system. Nevertheless the production of methyl esters was clear indicating that an optimized CMR could offer adequate performances. The methyl esters obtained in the experiments carried out were methyl palmitate, cis-9-oleic methyl ester, methyl linoleate.

4.4 Conclusions

In this work, the potentiality of using a catalytic membrane reactor for performing transesterification reactor was investigated and confirmed.

The adequate membrane cut-off (0.2 μm) was chosen for the separation of isolated transesterification products. A possible cut-off between 1.2 and 0.2 μm could be taken into consideration for future investigations. The best SHC for this application was founded in SrO with interesting yield of conversion in the batch reaction of about 60% and about 40% for the batch plus commercial membrane filtration. Chloroform solvent helped the oil-methanol mixture to be miscible, but even if it did not effect in the reaction conversion, it dissolved polymeric membranes. Its application could be more suitable with other kind of membranes, as, for example, ceramic ones. The immobilisation of the catalyst on the membrane was successful for both catalysts and also the filtration of joined transesterification products. Thanks to heterogeneous base-transesterification there are no percentage yield losses due to triglyceride saponification. Catalytic activity was detected in continuous experiments, where the catalyst was immobilized in the membrane.

Future works will focus on the optimization of the CMR configuration in order to achieve proper conversion results as well as adequate compounds separation.

UNIVERSITAT ROVIRA I VIRGILI
SEPARATION PROCESSES IN MICROALGAE BIOREFINING
Claudia Nurra

5

5. AN APPROACH FOR MEMBRANE PERMEABILITY PREDICTION[3]

One of the challenges in membrane technology is the opportunity to predict permeability in porous membranes for liquid applications in an easy and cheap way. This was the aim of this work. To achieve this objective, several techniques can be considered. In this prediction, the morphological approach from two-dimensional scanning electron micrographs was used. Firstly, numerical membrane morphological parameters from micrographs using the QUANTS tool are determined, which uses a texture recognition methodology. Secondly, the data is fit in Darcy's and Hagen-Poiseuille models to calculate permeations. QUANTS results were also compared with ones obtained from mercury porosimeter, as another classic and well-known methodology. Each parameter of the Darcy and Hagen-Poiseuille model was analysed and particularly, the tortuosity influence was evaluated.

[3]This chapter is based on the following to be submitted article:

C. Nurra, L. Pitol-Filho, R. Carraud, S. Pertuz, D. Puig, M.A. García, J. Salvadó and C. Torras, Towards de prediction of porous membrane permeability from morphological data, to be submitted.

Comparison between experimentally measured permeations and calculated ones was performed. Finally, an even easier approach was proposed to predict flow rate by knowing only the membrane surface mean pore size. The method is based on cross-section pore size interpolation by using function fits from the surface mean pore sizes. Results showed a reasonable agreement between measured and computed results, allowing the consideration of this Darcy and Hagen-Poiseuille model as a valid approach to predict membrane permeability.

5.1 Introduction

In the field of membrane synthesis and characterization, modelling plays an important role in order to optimize the membrane process. Therefore, full numerical correspondences between membrane properties and process performance need to be achieved. One of the challenging tasks are to be able to predict the membrane flux from the membrane morphology. With this information, operating parameters such as fluid viscosity or temperature have to be also considered.

One of the most used and accepted model for predicting membrane flux in pressure-driven processes and with porous membranes, where the convection is the predominant mechanism, is the general Darcy's law [102], which describes the flow of a fluid through a porous material. Applied to membranes, it states that flux is proportional to the transmembrane pressure over the thickness of the membrane through a constant of permeation. Several approaches can be considered to define the permeation constant. A main classic model dealing with laminar flow, the morphology of the membrane and the viscosity of the fluid is known as the Hagen-Poiseuille model [103]. This model, described in depth in

the experimental section, considers the porosity of the membrane, the mean pore size, the tortuosity and the fluid viscosity.

Thus, to predict the membrane flux, fluid viscosity, membrane thickness, porosity, tortuosity and mean pore size should be determined (transmembrane pressure is usually fixed, so it is already known). Viscosity is often known or it can be easily measured. Thickness can be easily measured with a micrometer or also determined by microscopy. There are several methods to measure porosity and mean pore size such as microscopy, gas penetration or mercury porosimetry [88, 104]. Finally, tortuosity is probably the most difficult parameter to determine. Mercury porosimetry performs estimation, as well as it can be performed by analyzing membrane porous structure by microscopy.

Tortuosity

Evaluation of the structural properties is important to design a physical/chemical process using a catalyst or a membrane, since both porosity and tortuosity contribute to the effective diffusivity of the transported species, as described by the equation 1 [105].

$$[Eq\ 1] \quad D_{eff} = D_{AB} \frac{\varepsilon}{\tau^2}$$

In equation 1 it is assumed that the effective diffusivity (D_{eff}) is the product of the molecular diffusivity (D_{AB}) to the ratio between the spaces available for transport (porosity, represented by ε) and the tortuosity (τ^2). If there is a medium with porosity and tortuosity equal to 1, the

effective diffusivity is equal to the molecular diffusivity. The tortuosity comprises in its value the deviation that the porous media have from a sequence of regular and straight pores.

A form to evaluate tortuosity is the corrugated pore structure model (CSPM) that considers a porous media as a sequence of cylindrical pore segments of a constant length and distributed diameter [106]. Such model, however, have adjustable parameters that should be obtained by applying the relation to materials of known tortuosity. Same assumptions of CSPM model (length and diameter) were used previously by Pinto [107] to obtain an expression for tortuosity from data of mercury porosimetry for the diffusion of gases.

Other approaches have been used to calculate totuosity. Fractal analysis was used to evaluate tortuosity of particles of red pepper [108] and soil [109]. Tortuosity of soil, expressed in terms of effective percolation and straight percolation lengths, is also obtained by adjusting hydraulic conductivity to relative saturation of soil [110]. By applying the relation between effective and molecular diffusivities, tortuosity was determined analysing the permeation of protons through polymer/silicate gels [111].

In the case of membranes, however, molecular diffusivity is not so easily determined, owing to the facilitated transport. Commercial membranes were analyzed through transmission electronic microscopy and tortuosity was correlated to the average angle of incidence of pores to the membrane surface [112]. Tortuosity of functionalized silica obtained by Monte Carlo pore network was lower than that obtained by applying the CSPM model to the same material [113], and authors could not evaluate which method gave better results. However, for engineering applications and using common sense, in some cases it is better to have a relationship that underestimates properties than another that overestimates them. In this case, the CSPM would be more adequate to predict effective diffusivity. Also

nuclear magnetic resonance (NMR) was used to measure tortuosity by comparing effective and molecular diffusivities of n-heptane through coked pellets of alumina [114].

However, there is still missing a method able to predict tortuosity from microscopic images of a membrane. Scanning electron microscopy (SEM) images may be used to evaluate structural properties of several materials, including membranes [115]. In the present paper, the same technique is extended in order to calculate tortuosity as an association of segment pores of distributed diameters by using the equation derived by Pinto [107].

5.2 Experimental

5.2.1 Materials

Membranes

Four types of polymeric commercial membranes from GE Osmonics were acquired and used. They corresponded to microfiltration membranes produced from polysulfone with different pore sizes: 1.2, 3.0, 5.0 and 8.0 micrometers. These membranes were selected because they belong to the same range of filtration, with different pore sizes but with the same pore structure and without macrovoids.

5.2.2 Methods

To model the permeability of the membranes several tests were performed. First of all, water permeability experiments were carried-out to measure the flux of the membranes

(details in section 5.3). Second, experimental morphological determinations to validate the model were achieved. Regarding the morphological study, two types of approaches were considered: mercury porosimetry and scanning electron microscopy. With the results obtained, the permeability model was discussed.

5.2.2.1 Mercury porosimetry

Intrusion mercury porosimetry is one of the classical methods to determine membrane porosity and it also measures tortuosity [116]. It was chosen along with scanning electron microscopy to quantify membrane porosity by the two different techniques. The equipment used was a Quantachrome Poremaster 60 apparatus. Porosity and tortuosity of the membranes were measured at low and high pressure (up to 4137 bar) to acquire a complete size range from 0.0036 to 950 micrometers.

5.2.2.2 Microscopy

The morphology of the membranes was investigated by using the Scanning Electron Microscopy (SEM) and an Environmental Scanning Electron Microscopy (ESEM). The SEM used was a JEOL JSM-6400 Scanning Microscopy Series, with a working voltage of 15 kV [16]. The ESEM used was a FEI Quanta 600, with a voltage between 15 and 20 kV and with low vacuum pressure, since the samples were not conductive and no sputtering was applied.

The micrographs obtained were further interpreted with specific computational software in order to obtain the main numerical membrane morphological parameters: pore number and

pore size distribution, membrane asymmetry and membrane regularity. The software used was QUANTS [117].

5.2.2.3 The permeability model

As described in the introduction, Darcy's equation (equation 2) is a key model for describing membrane permeability. Flux (J, $m^3 \cdot s^{-1}$) is calculated from the transmembrane pressure (ΔP, Pa), the membrane thickness (m), the area (A, m^2) and the permeation constant (P, $m^3 \cdot s \cdot kg^{-1}$).

$$[Eq\ 2]\quad J = P \times \frac{\Delta P}{l} \times A$$

The permeation constant can be established morphologically following the Hagen-Poiseuille principle as shown in equation 3, where n is the pore number (m^{-2}), r is the pore radius (m), η ($kg \cdot m^{-1} \cdot s^{-1}$) is the dynamic viscosity and τ is the tortuosity (non-dimensional).

$$[Eq\ 3]\quad P = \frac{n \times \pi \times r^4}{8 \times \eta \times \tau}$$

Important properties in the mass transfer through a porous media are porosity and tortuosity. In the case of tortuosity, the diffusion is more difficult when the pore geometry is irregular. On the other hand, diffusion mechanism is not the same for transient and steady-state operations. In the transient state, each component tends to distribute itself homogeneously for the whole solid matrix, even reaching pores blocked at any extremity.

Once system reaches steady state, there is a preferential diffusion through the sections where a concentration gradient exists, which corresponds to the driving force for diffusion. So transport does not occur in blocked pores, where the chemical potential has already reached the equilibrium value. In order to make calculations simpler, it was decided to determine tortuosity for the steady state, with a model that considers a porous media as an association of pores with different diameters [107], as in equation 4.

$$[Eq\ 4] \quad \tau^2 = \sum_{i=1}^{p} \frac{V_i^p}{d_i^4} \frac{\sum_{i=1}^{p} V_i^p}{\left(\sum_{i=1}^{p} \frac{V_i^p}{d_i^2} \right)^2}$$

In equation 4, d_i (m) is the diameter of pores in a membrane, and the V_ip (m^3) values represent their volumes. By considering the pores either as spheres or as cylinders of length equal to diameter, equation 4 reduces to equation 5.

$$[Eq\ 5] \quad \tau^2 = \sum_{i=1}^{p} \frac{n_i}{d_i} \frac{\sum_{i=1}^{p} n_i d_i^3}{\left(\sum_{i=1}^{p} n_i d_i \right)^2}$$

In equation 5, the number of pores for each diameter is expressed by n_i. By using such approach, the tortuosity may be calculated from SEM images of membranes.

Computational language

In this work and to perform all the calculations needed, Matlab version 2011b scripts were used.

5.3 Equipment

Membrane water permeability was experimental measured for all the membranes. Experiments were carried-out with a setup (Fig. 5.1) containing a commercial tangential cross-flow polymeric membrane module (SEPA CFII, GE Osmonics). Trans-membrane pressure (TMP) was set and controlled by using a TESCOM back-pressure. Water temperature was also set to 21 ºC and controlled by using a Huber, K6-cc-NR equipment. Recirculating flow rate was maintained at 55 ± 3 $L \cdot h^{-1}$ in all experiments. Permeate was collected in a tank located over a scale that was connected to a computer in order to calculate the actual mass-flow rate in a one second frequency.

Permeability was measured after determining the flow rate at three different TMP: 1.3, 2.4 and 3.7 bar. The transmembrane pressure corresponded to the mean between the pressures at the module inlet and at the module outlet (retentate), which were measured with a manometer. For each membrane, measures at each TMP were performed per triplicate.

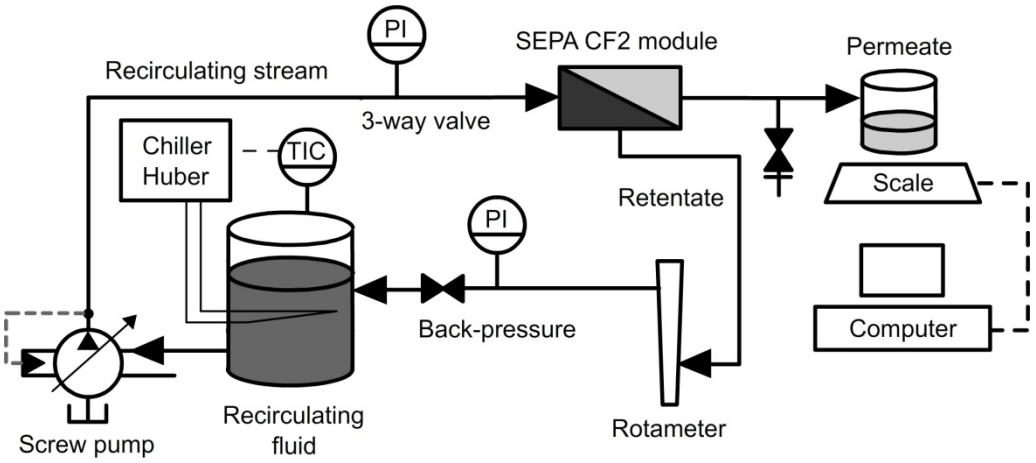

Fig. 5.1 Scheme of the experimental set-up used for permeability measurements.

5.4 Results and discussion

5.4.1 Influence of the model variables in P (permeation constant)

P (permeation constant) is defined by equation 3 and it depends on four parameters: porosity, mean pore size, tortuosity and fluid viscosity. Checking the influence of each one may assess the decision of how precise each one needs to be determined. Similarly, it may help assessing if the error carried-out in the calculation of the P is significant from each parameter uncertainty.

A first calculation was considering a variation of 10% of each one of the variables and checking the variation of P. A base case was defined by fixing a mean pore size (pore radius) of 0.5 micrometer, a tortuosity of 1.1, a porosity of $1 \cdot 10^{11}$ m^{-2} and a fluid viscosity of 0.001 $kg \cdot m^{-1} \cdot s^{-1}$. With these values, P = $2.23 \cdot 10^{12}$ $m^3 \cdot s \cdot kg^{-1}$. All these values can be considered as a typical one in a microfiltration process. In this case, the 10% variation in the mean pore size implies a variation in 146% P. The 10 % variation in porosity implies a variation in 110% P. The variations of the viscosity and the tortuosity imply a variation in

91% P each one. Thus, the pore size is the variable that has dominant influence, followed by all others with a same one.

But not all variables have the same probability to perform such variations. Viscosity can change during operation mainly due to temperature or concentrations changes. In steady state, both variables are kept constant in time, but small oscillations might occur. A variation of 1 ºC in temperature makes viscosity change in a 2 % (at 35 ºC). For morphological properties and considering the membranes used in this work, the differences in these parameters comparing the 1.2 and 8 micrometers membranes are 116 % for tortuosity, 139 % for porosity and 115 % for mean pore size. Therefore, porosity may change two times larger than the tortuosity or mean pore size.

Considering the mentioned facts, porosity and mean pore size are the major sensible variables, while tortuosity is less dominant.

5.4.2 Model validation. Agreement between measured and calculated permeabilities

Water permeabilities of the four membranes were measured by measuring the flow rate at three different transmembrane pressures. Tap water was used and therefore it was expected fouling to occur from a determined TMP. Fig. 5.2 shows the measured flow rates for all membranes as well as the curve fittings. It can be observed that the fit correlates to a logarithmic curve as expected due to fouling from 1 bar and that the linear behaviour is lost for all membranes at TMP = 1.2 bar (critical flux). The membranes permeabilities measured were 4124 ± 91, 4415 ± 244, 4745 ± 275 and 4854 ± 57 L/h/m^2/bar for the 1.2, 3.0, 5.0 and

8.0 micrometer membrane, respectively. It can be observed that the permeability of these membranes do not change at the same ratio that the theoretical mean pore size given by the manufacturer does.

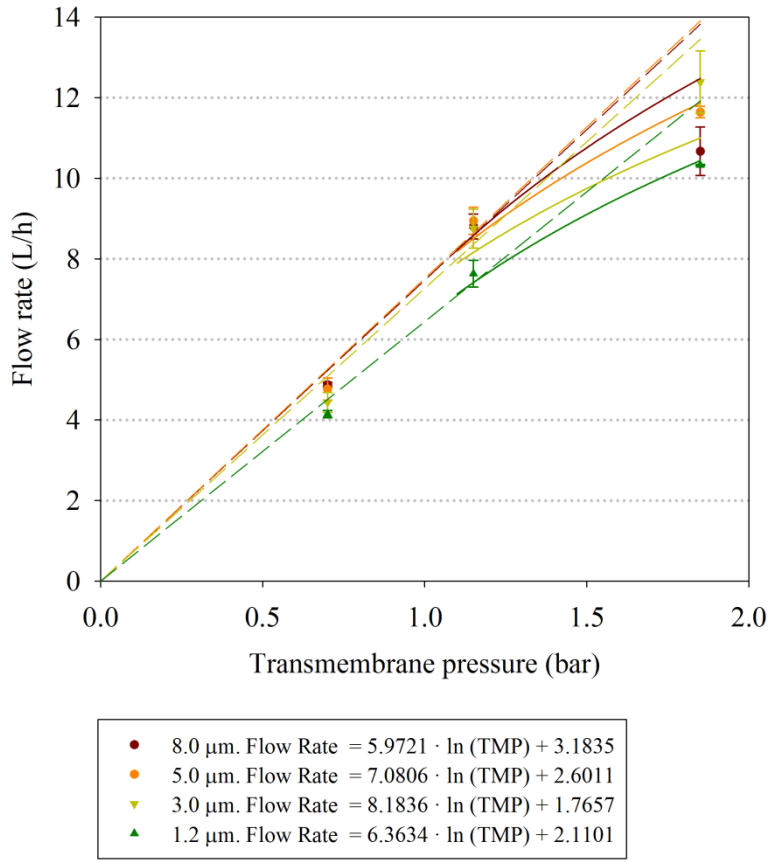

Fig. 5.2 Water permeabilites measured for all the membranes tested, including curve fitting.

On the other side, samples used were examined by SEM. Fig. 5.3 shows the cross-section of the membranes, where the porous structure can be examined. In these types of membranes, it can be noticed that no macrovoids exists and that the structure is quite regular and high symmetric.

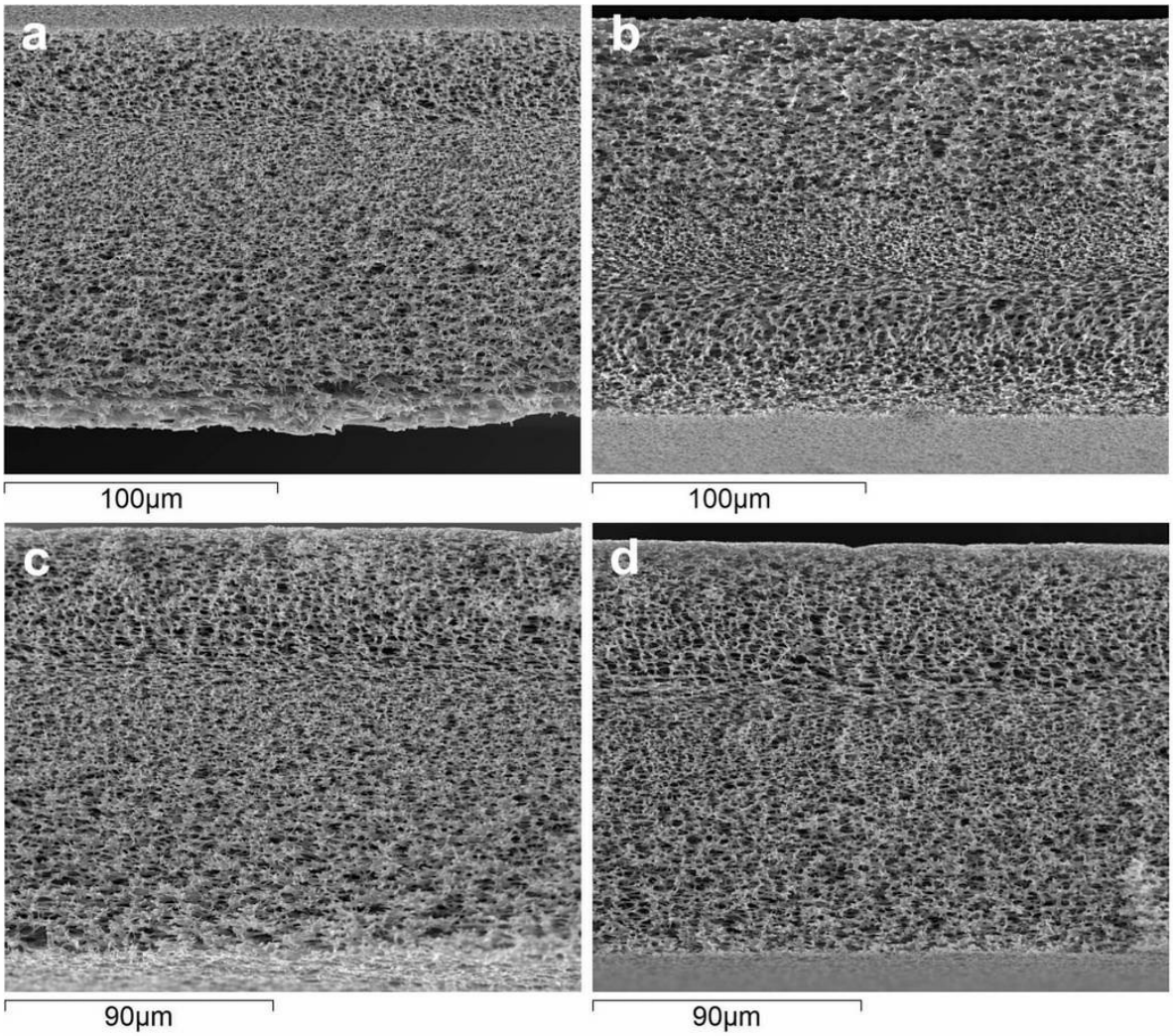

Fig. 5.3 Cross-section micrographs obtained by SEM of the membranes used. (a) 1.2 µm, (b) 3.0 µm, (c) 5.0 µm and (d) 8.0 µm.

The micrographs obtained were further processed with QUANTS software in order to obtain the numerical properties of the membranes. Table 5.1 shows the results. It can be observed that a progressive increment of the calculated mean pore size is achieved with the increment of the membrane mean pore size (the one given by the manufacturer). Nevertheless, there is not a fine agreement between the two values due to different reasons: techniques are different (often, manufacturer values are determined from the membrane performance) and QUANTS have limitations with the smallest pores that are not properly

reflected in the macrograph due to resolution. Regarding porosity, it can be concluded that it is practically constant for the four membranes. When calculated as number of pores over area, there is a smooth tendency that shows that as the membrane pore size increases, the porosity decreases. Regarding asymmetry, it can be noticed that there is not any clear correlation with the membrane pore size and that in all cases, values are low (as it is expected). Tortuosity was calculated following equation 5 from results obtained by QUANTS. Results show a tendency for tortuosity to increase with membrane nominal pore size.

Membrane	GE 1.2 µm	GE 3.0 µm	GE 5.0 µm	GE 8.0 µm
Area (μm^2)	27216.9	25067.5	26299.8	25826.9
Mean pore size (µm)	3.01	3.31	3.38	3.59
Number of pores	3156	2479	2455	2156
Porosity (pores / m^2)	0.1160	0.0989	0.0933	0.0835
Porosity (%)	82.75	85.00	83.61	84.65
Relative asymmetry (%)	20.081	9.638	17.588	13.202
Absolute asymmetry	86.123	40.689	70.903	53.229
Tortuosity	1.5180	1.7302	1.6465	1.7643

Table 5.1: Numerical morphological membrane properties obtained by QUANTS software.

In order to compare methods and to have a second input regarding morphology quantification, membranes were also analyzed with mercury porosimeter. With this equipment, porosity, mean pore size and tortuosity can be determined. Regarding porosity, it can be noticed that the method tends to be over predicted, since for the case of the 1.2 µm

membrane, the value obtained is 100 % and it is not possible, since the membrane contains polymer. Nevertheless, the trend is the same as the one obtained from QUANTS (in number / area) and the values are quite similar between the terms calculated with the same units. The maximum difference is achieved with the 1.2 μm membrane (21 %), while the minimum is achieved with the 8.0 μm membrane (3 %). Considering tortuosity, the tendency of the results obtained by mercury porosimetry is the same than the one obtained from QUANTS, but values in this case show moderate differences between 36 – 55 %.

Regarding pore size, the difference is notorious with a difference factor of approximately two. The main explanation is that the SEM technique has the limitation of resolution. At a magnification that the whole membrane is observed, the smallest pores have not enough resolution to be distinguished and thus, they are not detected. The consequence is that the method tends to overestimate the mean pore size.

Membrane	GE 1.2 μm	GE 3.0 μm	GE 5.0 μm	GE 8.0 μm
Porosity (%)	100.00	98.43	89.92	87.40
Mean pore size (μm)	1.381	1.435	1.634	1.657
Tortuosity	1.0996	1.1177	1.2132	1.2423

Table 5.2. Numerical morphological membrane properties obtained by mercury porosimetry.

Finally, with all the above results and as Table 5.3 shows, the measured permeability could be compared from the calculated one, following the Darcy's and the Hagen-Poiseuille models (equation 2 and 3, respectively) and considering intrusion mercury porosimetry as well as SEM + QUANTS approach. Thus, for both methods, parameters used were those

obtained from each respective technique except for pore number, which in both cases values used were those obtained from QUANTS, since mercury porosimetry does not calculate it.

The difference between the measured permeability and the calculated one are of the same order of magnitude for both methods, but inversely: while for the SEM + QUANTS method is around 6, for the mercury porosimeter is around 0.13. Thus, it can be concluded the measured permeability is inside an interval provided by the two techniques used to measure membrane morphology.

Membrane	GE 1.2 µm	GE 3.0 µm	GE 5.0 µm	GE 8.0 µm
Measured permeability ($m^2 \cdot s / kg$)	$1.331 \cdot 10^{-8}$	$1.301 \cdot 10^{-8}$	$1.210 \cdot 10^{-8}$	$1.131 \cdot 10^{-8}$
SEM + QUANTS				
Calc. permeability ($m^2 \cdot s / kg$)	$2.660 \cdot 10^{-9}$	$1.549 \cdot 10^{-9}$	$2.331 \cdot 10^{-9}$	$1.832 \cdot 10^{-9}$
Ratio	5.0	8.4	5.2	6.2
Mercury Porosimetry				
Calc. permeability ($m^2 \cdot s / kg$)	$1.056 \cdot 10^{-11}$	$1.032 \cdot 10^{-11}$	$1.512 \cdot 10^{-11}$	$1.392 \cdot 10^{-11}$
Ratio	0.162	0.150	0.109	0.109

Table 5.3. Comparison between measured permeability and calculated ones from SEM + QUANTS technique and mercury porosimetry one, using Darcy's and Hagen-Poiseuille laws.

An interesting consideration is whether the deviation is important, or how much should change the measured morphological parameters to agree with the calculated values. An individual variable study has been performed to check its contribution. Considering SEM + QUANTS technique, regarding thickness and keeping constant the other variables, it should be a mean of 41 % for the actual value. For tortuosity it should be 17 %. Regarding

the pore size, its value should be increased in a 56 %. Finally, regarding porosity, its value should be multiplied by a factor of 6.2. From these results, the variation of the pore size and/or porosity is the most likely to be adjusted because of the resolution limitation commented above and because changes in the other variables seem dramatic (variation of thickness is too large and tortuosity minimum). Therefore, if a factor is considered for the SEM + QUANTS technique to compensate the smallest pore that are not detected, a very good agreement would be obtained between the measured and calculated permeability.

5.4.3 A simplification of the membrane porous structure

From the analysis of the membranes cross-section micrographs obtained by SEM, it was investigated the possibility of modelling their porous structure by adjusting simple fits. A main advantage would be that by knowing the mean pore size of the two sides of a membrane, the cross-section porous structure could be predicted. Additionally, excepting a range of microfiltration membranes, for all other cases the mean pore size of the selective side of the membrane is much smaller than the mean pore size of the non-selective side. Thus and for these cases, the approach of considering the mean pore size of the selective surface equal to zero could be reliable. Therefore, only by determining the mean pore size of the non-selective side the entire membrane morphology could be predicted.

To study this hypothesis, the mean pore sizes of the membranes used in previous sections (Fig. 5.3) were determined. Afterwards, with a programmed Matlab function (Annex 1), artificial cross-section porous structures were created from the following input: mean pore size of the two membrane sides, membrane thickness and type of fit. By visual observation of

typical SEM membrane cross-section micrographs if was concluded that linear and power curves would best fit. Then, artificial cross-section figures were interpreted and the results obtained were compared with the ones obtained with the real cross-section micrographs. Interpretation was performed in this case with ImageJ software (by using two filters: edge detection and image binarization). Table 5.4 shows the results and comparison.

	Mean pore size (μm)			**Number of pores**		
	Real	**Artificial L**	**Artificial P**	**Real**	**Artificial L**	**Artificial P**
GE 1.2 μm	3.01	2.799	3.305	3156	1617	1104
GE 3.0 μm	3.31	2.986	3.605	2479	1187	780
GE 5.0 μm	3.38	3.034	3.816	2455	1514	899
GE 8.0 μm	3.59	3.265	4.405	2156	1251	635

Table 5.4. Mean pore size and number of pores results comparison between those obtained from SEM cross-section micrograph and generated cross-section figure from membrane surface pore sizes of GE Osmonics microfiltration membranes. Notes: Real means values obtained by QUANTS from the real cross-section SEM micrographs. Artificial L means results from artificial images created by using a linear fit. Artificial P means results from artificial images created by using a power fit.

Results show a good agreement between real and artificial images in terms of pore size. Real values are between the ones obtained by linear and power fit. Regarding the number of pores, real image resulted in larger number. A reason for that could be the presence of residual pores in real micrographs. In all cases, the pore size changes proportionally to the membrane cut-off size, but not the number of pores to the influence of membrane thickness which differs in each case.

A final test was performed with a representative ultrafiltration/nanofiltration membrane, where selective surface side has pores that can be assumed to have a mean size of zero, compared with the non-selective side. Fig. 5.4 shows the cross-section micrograph of the

real membrane, the porous surface one as well as generated images from the interpretation. It can be observed then in overall, power fit correlates better than linear one. This visual observation is confirmed by the numerical results shown in Table 5.5. Table 5.5 shows numerical results obtained from QUANTS software from the SEM cross-section micrograph and the same results obtained with ImageJ after analysing the images generated from the mean pore size of the two membrane surfaces (0 and 0.327 micrometers). The mean pore size of the membrane porous surface was determined with ImageJ from the surface SEM micrograph.

	Mean pore size (μm)			**Number of pores**		
	Real	**Artificial L**	**Artificial P**	**Real**	**Artificial L**	**Artificial P**
Ultrafiltration mem.	0.852	0.164	0.526	3039	38066	3733

Table 5.5. Mean pore size and number of pores results comparison between those obtained from SEM cross-section micrograph and generated cross-section figure from membrane surface pore sizes of an ultrafiltration membrane. Notes: Real means values obtained by QUANTS from the real cross-section SEM micrographs. Artificial L means results from artificial images created by using a linear fit. Artificial P means results from artificial images created by using a power fit.

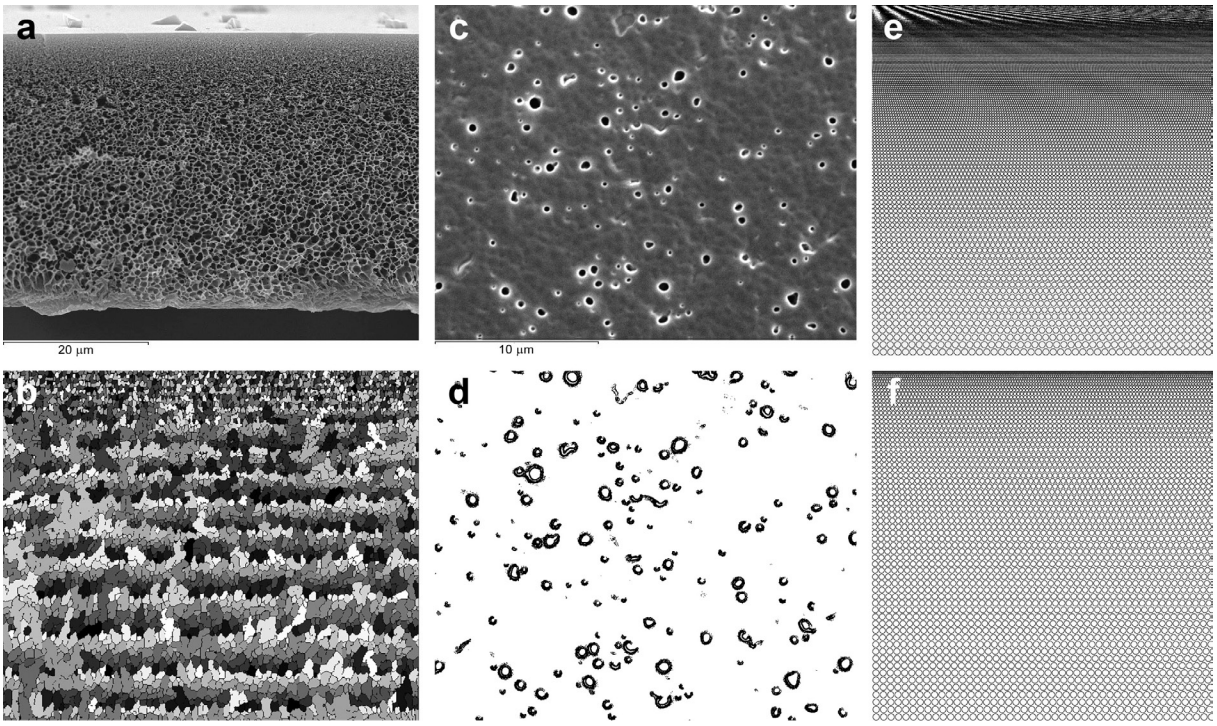

Fig. 5.4 Interpretation of an ultrafiltration membrane. A) Original SEM cross-section micrograph, B) Artificial cross-section micrograph from QUANTS interpretation of the original SEM cross-section micrograph, C) Original SEM porous surface micrograph, D) Pores detected and quantified by ImageJ from original SEM porous surface micrograph, E) Artificial cross-section micrograph, linear fit, F) Artificial cross-section micrograph, power fit.

5.5 Conclusions

This study framework concerns about the challenge of predicting porous membrane permeation, where transmembrane pressure is the driven force, from simple and cheap membrane morphological characterization. SEM membrane micrographs are easy and cheap to obtain and they provide valuable qualitative information about membrane morphology. In previous studies we introduced a tool to obtain the numerical membranes morphological properties from SEM micrographs. In this study, work performed to use the morphological data to predict membrane flow from already known models and its validation is presented.

Darcy's and Hagen-Poiseuille models were considered to use membrane morphological data obtained from SEM micrographs. The influence of each parameter from the models was evaluated, concluding that porosity and mean pore size are the most sensitive variables, while tortuosity is the less one. Membrane permeations were experimentally measured and calculated from the mentioned model. Acceptable agreement was found, which lets conclude the reliable possibility to use the mentioned techniques to predict membrane flow.

Mercury porosimetry was also used as alternative method to compare results. Results confirmed the reasonable agreement as well as let to detect the lacks of all methods.

Finally, a further simplified method was proposed to even make the membrane flow prediction easier and less time consuming just from analysing non-selective porous membrane surface sides. Results showed that although uncertainty may increase, results are enough close to those obtained from whole membrane analysis to allow the method being considered as approach to predict permeation.

In summary, results presented in the work show a reliable, cheap and easy method to predict porous membrane permeation with water from its morphological study.

UNIVERSITAT ROVIRA I VIRGILI
SEPARATION PROCESSES IN MICROALGAE BIOREFINING
Claudia Nurra

GENERAL CONCLUSIONS

The work presented in this thesis deals with membrane separation processes that can be integrated in microalgae biorefining. The number of stages that this application includes are large, and an actual main challenge is to decrease the overall cost. In several of these stages, membrane processes can be considered offering the possibility to lower cost and improve performance. In particular, main attention has been paid in microalgae dewatering and also in the transesterification step (where microalgae oil is converted in biodiesel). Main efforts have been devoted to the first one to develop new cheaper membrane materials as well as to improve process performance. In the second issue, more basic research has been performed introducing the possibility of use catalytic membrane reactors for transesterification. The results obtained from this work provide a number of advances in this field, which are summarized in the following conclusions.

In particular, it has been demonstrated that membranes for microalgae dewatering can be synthesized and used from polymers generally not used in membrane industry, but in others applications, as for example packaging. Packaging polymers used to prepare membrane for microalgae dewatering (with low TMP and no chemicals attack) have adequate mechanical properties. They results, comparing with typically used ones, cheaper and with good performances. Membrane polymers for this application can be also obtained from residual waste, as forestry sawdust. Finally microalgae dewatering permeability can be improved by membrane modification with hydrophilic additives, as Pluronic® F127.

Permeability performances are improved with the use of a vibrating filtration system, that for *Nannochloropsis gaditana* achieve its maximum with the use of the PES5 ultrafiltration membrane while for *Phaeodactilum tricornutum* this it is achieved using PESMF microfiltration membrane. It was showed that vibrating technique considerably reduces fouling phenomena during microalgae membrane filtration compared with conventional filtration and that the energy input required by the system is clearly compensated by the total process cost reduction due to the performance increment. This technique is successfully operated at a pilot plant scale and the energy demand required for the vibration is low (8%) respect of the total pumping/general system.

Regarding the catalytic membrane reactor it has been showed that heterogeneous catalysts are able to give reasonable performances compared to homogeneous ones in transesterification reaction. In particular, SrO gives good yield conversion in sunflower oil transesterification. This catalyst can be easily immobilized in polymeric membranes during their preparation and the solvents used for it can affect morphologically the catalyst, but not its activity.Catalytic membrane reactors offer reactivity for sunflower oil transesterification reaction.

Porous membrane permeation can be predicted from its morphological characterization in an easy and cheap way. Membrane morphological data can be extracted from microscopy and image interpretation. Then, permeation can be calculated by using these data with Darcy's and Hagen-Poiseuille models. Several techniques can be used to obtain membrane morphological data: microscopy, mercury porosimeter, physisorption , etc. Each

one has its own limitations, which provides no exact results. Regarding the mentioned models, membrane porosity and mean pore size are the most sensible variables, while tortuosity is the less one. In UF and NF only determining the pore size of non selective membrane surface and membrane thickness it is possible to predict its permeability. So it is a cheap, easy and quick method to get the prediction.

UNIVERSITAT ROVIRA I VIRGILI
SEPARATION PROCESSES IN MICROALGAE BIOREFINING
Claudia Nurra

CONCLUSIONES GENERALES (SPANISH VERSION)

El trabajo presentado en esta tesis se ocupa de los procesos de separación por membranas que se pueden integrar en la biorefineria de microalgas. El número de etapas que pueden incluir esta aplicación es considerable, y un principal desafío es disminuir el coste global. Los procesos de membrana pueden ser considerados en varias de estas etapas ofreciendo la posibilidad de mejorar el coste y rendimiento. En particular, se ha prestado principal atención en la deshidratación de microalgas y también en la etapa de transesterificación (donde el aceite se convierte en biodiesel). Los principales esfuerzos se han dedicado a la primera de las dos para desarrollar nuevos materiales de membrana más baratos, así como para mejorar el rendimiento del proceso. En la segunda, más investigación se ha realizado para la introducción de uso de reactores de membrana catalíticos de transesterificación. Los resultados obtenidos de este trabajo ofrecen una serie de avances en este campo, que se resumen en las siguientes conclusiones.

En particular, se ha demostrado que las membranas para la deshidratación de microalgas pueden ser sintetizadas y utilizadas a partir de polímeros generalmente no utilizados en la industria de la membrana, pero en otras aplicaciones como por ejemplo en el industria de los envases. Los polímeros de embalaje utilizados para preparar las membranas para la deshidratación de microalgas (operación con baja TMP y sin ataque por parte de productos químicos) tienen propiedades mecánicas adecuadas. Los resultados mostraron que estos polímeros, comparados con los utilizados normalmente, son más baratos y con buenos rendimientos. Polímeros de membrana para esta aplicación también se pueden obtener a partir de desechos residuales, como el aserrín forestal. Finalmente la permeabilidad de estas

membrana para la deshidratación microalgas se puede mejorar mediante su modificación con aditivos hidrófilos, como el Pluronic®F127.

Los rendimientos de permeabilidad se mejoran con el uso de un sistema de filtración vibratoria, que en la filtración de *Nannochloropsis gaditana* alcanza su máximo con el uso de la membrana de ultrafiltración PES5, mientras que para la *Phaeodactilum tricornutum* esto se consigue utilizando membrana de microfiltración PESMF, de entre un amplio rango de membranas probadas. Se mostró que la técnica de vibración reduce considerablemente los fenómenos de ensuciamiento de la membrana durante la filtración de microalgas en comparación con la filtración convencional y que la energía requerida por el sistema está claramente compensada por la reducción total de costes de proceso debido al incremento del rendimiento. Esta técnica se utiliza con éxito en una escala de planta piloto y la demanda de energía necesaria para la vibración es un 8%del bombeo/sistema general.

En cuanto al reactor de membrana catalítico se ha demostrado que los catalizadores heterogéneos son capaces de dar rendimientos razonables en comparación con los homogéneos en la reacción de transesterificación. En particular, el SrO da un buen rendimiento de conversión en la transesterificación del aceite de girasol. Estos catalizadores pueden ser fácilmente inmovilizados en membranas poliméricas durante su preparación y los disolventes utilizados para ella, a pesar que pueden afectar morfológicamente el catalizador, no hacen variar su actividad de reacción. Las membranas catalíticas ofrecen reactividad para la reacción de transesterificación de aceite de girasol.

La permeabilidad de la membrana porosa se puede predecir a partir de su caracterización morfológica de una manera fácil y barata. Los datos morfológicos de membrana se pueden extraer con técnicas de microscopía y la interpretación de las imágenes.

Entonces, la permeación se puede calcular mediante el uso de estos datos con los modelos de Darcy y Hagen-Poiseuille. Varias técnicas pueden ser utilizadas para obtener los datos morfológicos de la membrana de: microscopía, porosímetro de mercurio, fisisorción, etc. Cada uno tiene sus propias limitaciones, que no proporciona resultados exactos. En cuanto a los modelos mencionados, la porosidad de la membrana y la media de tamaño de poro son las variables más sensibles, mientras que la tortuosidad es la que menos. En UF y NF sólo determinando el tamaño de poro de la superficie de la membrana selectiva y el espesor de la membrana es posible predecir su permeabilidad. Así que resulta ser un método barato, fácil y rápido de obtener la predicción.

UNIVERSITAT ROVIRA I VIRGILI
SEPARATION PROCESSES IN MICROALGAE BIOREFINING
Claudia Nurra

REFERENCES

[1] R. Harun, M. Singh, G.M. Forde, M.K. Danquah, Bioprocess engineering of microalgae to produce a variety of consumer products, Renew. Sust. Energ. Rev., 14 (2010) 1037-1047.

[2] T. Minowa, S. Sawayama, A novel microalgal system for energy production with nitrogen cycling, Fuel, 78 (1999) 1213-1215.

[3] S. Raposo, J. Pardão, M.E. Lima-Costa, Oleaginous microorganisms as sustainable feedstock for biodiesel production, New Biotechnol., 25, Supplement (2009) S276.

[4] P.J.l.B. Williams, L.M.L. Laurens, Microalgae as biodiesel & biomass feedstocks: Review & analysis of the biochemistry, energetics & economics, Energ. Environ. Sci., 3 (2010) 554-590.

[5] S. Amin, Review on biofuel oil and gas production processes from microalgae, Energy Convers. Manage., 50 (2009) 1834-1840.

[6] T.M. Mata, A.A. Martins, N.S. Caetano, Microalgae for biodiesel production and other applications: A review, Renew. Sust. Energ. Rev., 14 (2010) 217-232.

[7] J.N. Rosenberg, G.A. Oyler, L. Wilkinson, M.J. Betenbaugh, A green light for engineered algae: redirecting metabolism to fuel a biotechnology revolution, Curr. Opin. Biotechnol., 19 (2008) 430-436.

[8] M. Packer, Algal capture of carbon dioxide; biomass generation as a tool for greenhouse gas mitigation with reference to New Zealand energy strategy and policy, Energy Policy, 37 (2009) 3428-3437.

[9] X. Miao, Q. Wu, Biodiesel production from heterotrophic microalgal oil, Bioresour. Technol., 97 (2006) 841-846.

[10] Y. Chisti, Biodiesel from microalgae, Biotechnol. Adv., 25 (2007) 294-306.

[11] P. Sun, B. Wang, J. Yao, L. Zhang, N. Xu, Fast synthesis of biodiesel at high throughput in microstructured reactors, Ind. Eng. Chem. Res., 49 (2009) 1259-1264.

[12] X. Meng, J. Yang, X. Xu, L. Zhang, Q. Nie, M. Xian, Biodiesel production from oleaginous microorganisms, Renewable Energy, 34 (2009) 1-5.

[13] A. Demirbas, Progress and recent trends in biodiesel fuels, Energy Convers. Manage., 50 (2009) 14-34.

[14] N. Rossi, P. Jaouen, P. Legentilhomme, I. Petit, Harvesting of Cyanobacterium Arthrospira Platensis Using Organic Filtration Membranes, Food Bioprod. Process., 82 (2004) 244-250.

[15] F. Martinez, A. Martin, J. Malfeito, L. Palacio, P. Prádanos, F. Tejerina, A. Hernández, Streaming potential through and on ultrafiltration membranes: Influence of salt retention, J. Membr. Sci., 206 (2002) 431-441.

[16] C. Torras, X. Zhang, R. Garcia-Valls, J. Benavente, Morphological, chemical surface and electrical characterizations of lignosulfonate-modified membranes, J. Membr. Sci., 297 (2007) 130-140.

[17] M.I. Vazquez, C. Torras, R. Garcia-Valls, J. Benavente, A study on thermal effect on structure and transport properties of a composite lignosulfonated-polyamide/polysulfone membrane, Desalination, 245 (2009) 570-578.

[18] C. Torras, F. Ferrando, J. Paltakari, R. Garcia-Valls, Performance, morphology and tensile characterization of activated carbon composite membranes for the synthesis of enzyme membrane reactors, J. Membr. Sci., 282 (2006) 149-161.

[19] N. Sdrula, A study using classical or membrane separation in the biodiesel process, Desalination, 250 (2010) 1070-1072.

[20] N. Rossignol, L. Vandanjon, P. Jaouen, F. Quéméneur, Membrane technology for the continuous separation microalgae/culture medium: compared performances of cross-flow microfiltration and ultrafiltration, Aquacult. Eng., 20 (1999) 191-208.

[21] B. Petrusevski, G. Bolier, A.N. Van Breemen, G.J. Alaerts, Tangential flow filtration: A method to concentrate freshwater algae, Water Research, 29 (1995) 1419-1424.

[22] X. Zhang, Q. Hu, M. Sommerfeld, E. Puruhito, Y. Chen, Harvesting algal biomass for biofuels using ultrafiltration membranes, Bioresour. Technol., 101 (2010) 5297-5304.

[23] H. Choi, K. Zhang, D.D. Dionysiou, D.B. Oerther, G.A. Sorial, Influence of cross-flow velocity on membrane performance during filtration of biological suspension, J. Membr. Sci., 248 (2005) 189-199.

[24] B. Kwon, N. Park, J. Cho, Effect of algae on fouling and efficiency of UF membranes, Desalination, 179 (2005) 203-214.

[25] C. Torras, L. Pitol, R. Garcia-Valls, Two methods for morphological characterization of internal microcapsule structures, J. Membr. Sci., 305 (2007) 1-4.

[26] C. Torras, R. Garcia-Valls, Quantification of membrane morphology by interpretation of scanning electron microscopy images, J. Membr. Sci., 233 (2004) 119-127.

[27] N.A. Ochoa, P. Prádanos, L. Palacio, C. Pagliero, J. Marchese, A. Hernández, Pore size distributions based on AFM imaging and retention of multidisperse polymer solutes: Characterisation of polyethersulfone UF membranes with dopes containing different PVP, J. Membr. Sci., 187 (2001) 227-237.

[28] L.M. Vane, F.R. Alvarez, Full-scale vibrating pervaporation membrane unit: VOC removal from water and surfactant solutions, J. Membr. Sci., 202 (2002) 177-193.

[29] M.Y. Jaffrin, Dynamic shear-enhanced membrane filtration: A review of rotating disks, rotating membranes and vibrating systems, J. Membr. Sci., 324 (2008) 7-25.

[30] A. Brou, L. Ding, P. Boulnois, M.Y. Jaffrin, Dynamic microfiltration of yeast suspensions using rotating disks equipped with vanes, J. Membr. Sci., 197 (2002) 269-282.

[31] C. Torras, J. Pallares, R. Garcia-Valls, M.Y. Jaffrin, Numerical simulation of the flow in a rotating disk filtration module, Desalination, 235 (2009) 122-138.

[32] A. Demirbas, Comparison of transesterification methods for production of biodiesel from vegetable oils and fats, Energy Convers. Manage., 49 (2008) 125-130.

[33] Z. Qiu, L. Zhao, L. Weatherley, Process intensification technologies in continuous biodiesel production, Chemical Engineering and Processing: Process Intensification, 49 (2010) 323-330.

[34] L. Fjerbaek, K.V. Christensen, B. Norddahl, A review of the current state of biodiesel production using enzymatic transesterification, Biotechnol. Bioeng., 102 (2009) 1298-1315.

[35] I.M. Atadashi, M.K. Aroua, A.R.A. Aziz, N.M.N. Sulaiman, Refining technologies for the purification of crude biodiesel, Appl. Energ., 88 (2011) 4239-4251.

[36] M. Šoštarič, D. Klinar, M. Bricelj, J. Golob, M. Berovič, B. Likozar, Growth, lipid extraction and thermal degradation of the microalga Chlorella vulgaris, New Biotechnology, 29 (2012) 325-331.

[37] P.E. Wiley, J.E. Campbell, B. McKuin, Production of biodiesel and biogas from algae: A review of process train options, Water Environ. Res., 83 (2011) 326-338.

[38] Y. Li, M. Horsman, N. Wu, C.Q. Lan, N. Dubois-Calero, Biofuels from Microalgae, Biotechnol. Progr., 24 (2008) 815-820.

[39] H.M. Amaro, A.C. Guedes, F.X. Malcata, Advances and perspectives in using microalgae to produce biodiesel, Appl. Energ., 88 (2011) 3402-3410.

[40] B. Singh, A. Guldhe, I. Rawat, F. Bux, Towards a sustainable approach for development of biodiesel from plant and microalgae, Renew. Sust. Energ. Rev., 29 (2014) 216-245.

[41] P. Schenk, S. Thomas-Hall, E. Stephens, U. Marx, J. Mussgnug, C. Posten, O. Kruse, B. Hankamer, Second generation biofuels: high-efficiency microalgae for biodiesel production, Bioenerg. Res., 1 (2008) 20-43.

[42] I. Rawat, R. Ranjith Kumar, T. Mutanda, F. Bux, Biodiesel from microalgae: A critical evaluation from laboratory to large scale production, Appl. Energ., 103 (2013) 444-467.

[43] L. Brennan, P. Owende, Biofuels from microalgae—A review of technologies for production, processing, and extractions of biofuels and co-products, Renew. Sust. Energ. Rev., 14 (2010) 557-577.

[44] Y.-R. Hu, F. Wang, S.-K. Wang, C.-Z. Liu, C. Guo, Efficient harvesting of marine microalgae Nannochloropsis maritima using magnetic nanoparticles, Bioresour. Technol., 138 (2013) 387-390.

[45] C. Nurra, E. Clavero, J. Salvadó, C. Torras, Vibrating membrane filtration as improved technology for microalgae dewatering, Bioresour. Technol., 157 (2014) 247-253.

[46] R. Bhave, T. Kuritz, L. Powell, D. Adcock, Membrane-based energy efficient dewatering of microalgae in biofuels production and recovery of value added co-products, Environ. Sci. Technol., 46 (2012) 5599-5606.

[47] M.L. Gerardo, D.L. Oatley-Radcliffe, R.W. Lovitt, Minimizing the energy requirement of dewatering scenedesmus sp. by microfiltration: performance, costs, and feasibility, Environ. Sci. Technol., 48 (2013) 845-853.

[48] M.T. Hung, J.C. Liu, Microfiltration for separation of green algae from water, Colloids Surf. B. Biointerfaces, 51 (2006) 157-164.

[49] O. Morineau-Thomas, P. Jaouen, P. Legentilhomme, The role of exopolysaccharides in fouling phenomenon during ultrafiltration of microalgae (Chlorella sp. and Porphyridium purpureum): Advantage of a swirling decaying flow, Bioprocess Biosystems Eng., 25 (2002) 35-42.

[50] S.D. Rios, E. Clavero, J. Salvado, X. Farriol, C. Torras, Dynamic microfiltration in microalgae harvesting for biodiesel production, Ind. Eng. Chem. Res., 50 (2010) 2455-2460.

[51] N. Scharnagl, H. Buschatz, Polyacrylonitrile (PAN) membranes for ultra- and microfiltration, Desalination, 139 (2001) 191-198.

[52] S. Yang, Z. Liu, Preparation and characterization of polyacrylonitrile ultrafiltration membranes, J. Membr. Sci., 222 (2003) 87-98.

[53] W.W.Y. Lau, M.D. Guiver, T. Matsuura, Phase separation in polysulfone/solvent/water and polyethersulfone/solvent/water systems, J. Membr. Sci., 59 (1991) 219-227.

[54] L. Pitol, C. Torras, J.B. Avalos, R. Garcia-Valls, Modelling of polysulfone membrane formation by immersion precipitation, Desalination, 200 (2006) 427-428.

[55] S.K. Yong, J.K. Hyo, Y.K. Un, Asymmetric membrane formation via immersion precipitation method. I. Kinetic effect, J. Membr. Sci., 60 (1987) 219-232.

[56] P. Anadão, R.R. Montes, N.M. Larocca, L.A. Pessan, Influence of the clay content and the polysulfone molar mass on nanocomposite membrane properties, Appl. Surf. Sci., 275 (2013) 110-120.

[57] W. Zhao, Y. Su, C. Li, Q. Shi, X. Ning, Z. Jiang, Fabrication of antifouling polyethersulfone ultrafiltration membranes using Pluronic F127 as both surface modifier and pore-forming agent, J. Membr. Sci., 318 (2008) 405-412.

[58] S. Gogolewski, M. Jovanovic, S.M. Perren, J.G. Dillon, M.K. Hughes, Tissue response and in vivo degradation of selected polyhydroxyacids: Polylactides (PLA), poly(3-hydroxybutyrate) (PHB), and poly(3-hydroxybutyrate-co-3-hydroxyvalerate) (PHB/VA), J. Biomed. Mater. Res., 27 (1993) 1135-1148.

[59] R.M. Luciano, C.A.C. Zavaglia, E.A.R. Duek, M.C. Alberto-Rincon, Synthesis and characterization of poly(L-lactic acid) membranes: Studies in vivo and in vitro, J. Mater. Sci.: Mater. Med., 14 (2003) 87-94.

[60] M.P. Balanyà, Preparació i caracterització de compostos de PLA (àcid polilàctic), Ph.D. Dissertation, (2009).

[61] H. Sanaeepur, A. Ebadi Amooghin, A. Moghadassi, A. Kargari, S. Moradi, D. Ghanbari, A novel acrylonitrile–butadiene–styrene/poly(ethylene glycol) membrane: preparation, characterization, and gas permeation study, Polym. Adv. Technol., 23 (2012) 1207-1218.

[62] A.G. Boricha, Z.V.P. Murthy, Acrylonitrile butadiene styrene/chitosan blend membranes: Preparation, characterization and performance for the separation of heavy metals, J. Membr. Sci., 339 (2009) 239-249.

[63] K. Okano, T. Tanaka, C. Ogino, H. Fukuda, A. Kondo, Biotechnological production of enantiomeric pure lactic acid from renewable resources: recent achievements, perspectives, and limits, Appl. Microbiol. Biotechnol., 85 (2010) 413-423.

[64] N. Laura Alicia Manjarrez, C. Lourdes Ballinas, C. Alain, F. Vanessa, M. Vinicio Torres, D. Alejandro Camacho, L. José Román Torres, S. Guillermo González, Biopolymer-based nanocomposites: effect of lignin acetylation in cellulose triacetate films, Science and Technology of Advanced Materials, 12 (2011) 045006.

[65] L. Manjarrez Nevárez, L. Ballinas Casarrubias, O.S. Canto, A. Celzard, V. Fierro, R. Ibarra Gómez, G. González Sánchez, Biopolymers-based nanocomposites: Membranes from propionated lignin and cellulose for water purification, Carbohydr. Polym., 86 (2011) 732-741.

[66] C.d.S. Meireles, G.R. Filho, M. Fernandes Ferreira Jr, D.A. Cerqueira, R.M.N. Assunção, E.A.M. Ribeiro, P. Poletto, M. Zeni, Characterization of asymmetric membranes of cellulose acetate from biomass: Newspaper and mango seed, Carbohydr. Polym., 80 (2010) 954-961.

[67] G.R. Filho, S.F. da Cruz, D. Pasquini, D.A. Cerqueira, V.d.S. Prado, R.M.N. de Assunção, Water flux through cellulose triacetate films produced from heterogeneous acetylation of sugar cane bagasse, J. Membr. Sci., 177 (2000) 225-231.

[68] E. Tronc, C.A. Hernández-Escobar, R. Ibarra-Gómez, A. Estrada-Monje, J. Navarrete-Bolaños, E.A. Zaragoza-Contreras, Blue agave fiber esterification for the reinforcement of thermoplastic composites, Carbohydr. Polym., 67 (2007) 245-255.

[69] H. Strathmann, Production of microporous media by phase inversion processes, in: Materials Science of Synthetic Membranes, American Chemical Society, 1985, pp. 165-195.

[70] A. Seidel, Properties and Behavior of Polymers, John Wiley & Sons Ltd. Hoboken NJ, USA, 2 vol. set (2011) 1590.

[71] P.R. Walne, Studies on the food value of nineteen genera of algae to juvenile bivalves of the genera Ostrea, Crassostrea, Mercenaria, and Mytilus, Fishery Investigations, 26 (1970) 62

[72] N. Kawabata, K. Ohashi, T. Nishiyama, Releasing polyacrylonitrile from poor biodegradability by insertion of a highly biodegradable chemical structure into the main chain, J. Appl. Polym. Sci., 99 (2006) 852-857.

[73] T. Hwang, S.-J. Park, Y.-K. Oh, N. Rashid, J.-I. Han, Harvesting of Chlorella sp. KR-1 using a cross-flow membrane filtration system equipped with an anti-fouling membrane, Bioresource Technol., 139 (2013) 379-382.

[74] T.M. Mata, A.A. Martins, N.S. Caetano, Microalgae for biodiesel production and other applications: A review, Renew. Sust. Energ. Rev., 14 (2010) 217-232.

[75] R. Harun, M. Singh, G.M. Forde, M.K. Danquah, Bioprocess engineering of microalgae to produce a variety of consumer products, Renew. Sust. Energ. Rev., 14 (2010) 1037-1047.

[76] I. Rawat, R. Ranjith Kumar, T. Mutanda, F. Bux, Dual role of microalgae: Phycoremediation of domestic wastewater and biomass production for sustainable biofuels production, Applied Energy, 88 (2011) 3411-3424.

[77] D.-H. Kim, J.-H. Lee, Y. Hwang, S. Kang, M.-S. Kim, Continuous cultivation of photosynthetic bacteria for fatty acids production, Bioresource Technol., 148 (2013) 277-282.

[78] P.J.L. Williams, L.M.L. Laurens, Microalgae as biodiesel & biomass feedstocks: Review & analysis of the biochemistry, energetics & economics, Energy & Environmental Science, 3 (2010) 554-590.

[79] P.Y. Sun, B. Wang, J.F. Yao, L.X. Zhang, N.P. Xu, Fast Synthesis of Biodiesel at High Throughput in Microstructured Reactors, Industrial & Engineering Chemistry Research, 49 (2010) 1259-1264.

[80] S. Şirin, E. Clavero, J. Salvadó, Potential pre-concentration methods for Nannochloropsis gaditana and a comparative study of pre-concentrated sample properties, Bioresource Technol., 132 (2013) 293-304.

[81] J. Kim, G. Yoo, H. Lee, J. Lim, K. Kim, C.W. Kim, M.S. Park, J.-W. Yang, Methods of downstream processing for the production of biodiesel from microalgae, Biotechnology Advances, 31 (2013) 862-876.

[82] S. Babel, S. Takizawa, Microfiltration membrane fouling and cake behavior during algal filtration, Desalination, 261 (2010) 46-51.

[83] S.D. Ríos, J. Salvadó, X. Farriol, C. Torras, Antifouling microfiltration strategies to harvest microalgae for biofuel, Bioresour. Technol., 119 (2012) 406-418.

[84] W. Shi, M.M. Benjamin, Effect of shear rate on fouling in a Vibratory Shear Enhanced Processing (VSEP) RO system, Journal of Membrane Science, 366 (2011) 148-157.

[85] M.Y. Jaffrin, Dynamic shear-enhanced membrane filtration: A review of rotating disks, rotating membranes and vibrating systems, Journal of Membrane Science, 324 (2008) 7-25.

[86] R. Bott, T. Langeloh, E. Ehrfeld, Dynamic cross flow filtration, Chem. Eng. J., 80 (2000) 245-249.

[87] A. Martin, F. Martinez, J. Malfeito, L. Palacio, P. Pradanos, A. Hernandez, Zeta potential of membranes as a function of pH - Optimization of isoelectric point evaluation, Journal of Membrane Science, 213 (2003) 225-230.

[88] L. Palacio, Caracterización estructural y superficial de membranas microporosas, in: Departamento de Física Aplicada, Universidad de Valladolid, Valladolid, 1999.

[89] VSEP, membrane filtration of waste oil: A cost effective and environmentally sound processing solution". Vibratory Shear Enhanced Processing (VSEP)" New Logic Research Inc, . http://www.vsep.com/pdf/WasteOil.pdf (2011).

[90] X.L. Miao, Q.Y. Wu, Biodiesel production from heterotrophic microalgal oil, Bioresource Technol., 97 (2006) 841-846.

[91] K. Akutu, H. Kabashima, T. Seki, H. Hattori, Nitroaldol reaction over solid base catalysts, Applied Catalysis A: General, 247 (2003) 65-74.

[92] D.Y.C. Leung, X. Wu, M.K.H. Leung, A review on biodiesel production using catalyzed transesterification, Appl. Energ., 87 (2010) 1083-1095.

[93] S. Baroutian, M.K. Aroua, A.A.A. Raman, N.M.N. Sulaiman, A packed bed membrane reactor for production of biodiesel using activated carbon supported catalyst, Bioresour. Technol., 102 (2011) 1095-1102.

[94] D.E. López, J.G. Goodwin Jr, D.A. Bruce, E. Lotero, Transesterification of triacetin with methanol on solid acid and base catalysts, Applied Catalysis A: General, 295 (2005) 97-105.

[95] Y.-Y. Wang, H.-Y. Chou, B.-H. Chen, D.-J. Lee, Optimization of sodium loading on zeolite support for catalyzed transesterification of triolein with methanol, Bioresour. Technol., 145 (2013) 248-253.

[96] M.A. Dubé, A.Y. Tremblay, J. Liu, Biodiesel production using a membrane reactor, Bioresour. Technol., 98 (2007) 639-647.

[97] P. Cao, A.Y. Tremblay, M.A. Dubé, Kinetics of canola oil transesterification in a membrane reactor, Ind. Eng. Chem. Res., 48 (2009) 2533-2541.

[98] P. Cao, A.Y. Tremblay, M.A. Dubé, K. Morse, Effect of membrane pore size on the performance of a membrane reactor for biodiesel production, Ind. Eng. Chem. Res., 46 (2006) 52-58.

[99] C.M.L. Carvalho, P. Cunnah, M.R. Aires-Barros, J.M.S. Cabral, Performance of a membrane bioreactor for enzymatic transesterification: characterization and comparison with a batch stirred tank reactor, Biocatal. Biotransform., 18 (2000) 31-57.

[100] L. Giorno, R. Molinari, M. Natoli, E. Drioli, Hydrolysis and regioselective transesterification catalyzed by immobilized lipases in membrane bioreactors, J. Membr. Sci., 125 (1997) 177-187.

[101] W. Shi, B. He, J. Ding, J. Li, F. Yan, X. Liang, Preparation and characterization of the organic–inorganic hybrid membrane for biodiesel production, Bioresour. Technol., 101 (2010) 1501-1505.

[102] V. Nassehi, Modelling of combined Navier–Stokes and Darcy flows in crossflow membrane filtration, Chem. Eng. Sci., 53 (1998) 1253-1265.

[103] F.P. Cuperus, C.A. Smolders, Characterization of UF membranes: Membrane characteristics and characterization techniques, Adv. Colloid Interface Sci., 34 (1991) 135-173.

[104] M. Mulder, Basic principles of membrane technology, Springer-Verlag New York, LLC, 1996.

[105] C.J. Geankoplis, Transport Processes and Separation Process Principles : Includes Unit Operations / C.J. Geankoplis, in, Upper Saddle River, EUA : Prentice-Hall.

[106] C.E. Salmas, G.P. Androutsopoulos, A novel pore structure tortuosity concept based on nitrogen sorption hysteresis data, Ind. Eng. Chem. Res., 40 (2001) 721-730.

[107] L.T. Pinto, Um estudo do transiente da difusao gasosa em meios porosos, in: Chem. Eng., Universidade Federal do Rio de Janeiro, Rio de Janeiro, 1994, pp. 197.

[108] E. Uquiche, J.M. Del Valle, J. Ortiz, Supercritical carbon dioxide extraction of red pepper (Capsicum annuum L.) oleoresin, J. Food Eng., 65 (2004) 55-66.

[109] A.N. Anderson, J.W. Crawford, A.B. McBratney, On diffusion in fractal soil structures, Soil Sci. Soc. Am. J., 64 (2000) 19-24.

[110] M. Kutílek, Soil hydraulic properties as related to soil structure, Soil and Tillage Research, 79 (2004) 175-184.

[111] I. Lakatos, J. Lakatos-Szabó, Diffusion of H^+, H_2O and D_2O in polymer/silicate gels, Colloids Surf. Physicochem. Eng. Aspects, 246 (2004) 9-19.

[112] F.M. Jahnke, C.J. Radke, A radially perfused cell for measuring diffusion in compacted, highly sorbing media, Ind. Eng. Chem. Res., 28 (1989) 347-355.

[113] G.S. Armatas, P.J. Pomonis, A Monte Carlo pore network for the simulation of porous characteristics of functionalized silica: Pore size distribution, connectivity distribution and mean tortuosities, Chem. Eng. Sci., 59 (2004) 5735-5749.

[114] D. Tang, C. Kern, A. Jess, Influence of chemical reaction rate, diffusion and pore structure on the regeneration of a coked Al_2O_3-catalyst, Applied Catalysis A: General, 272 (2004) 187-199.

[115] C. Torras, R. Garcia-Valls, Quantification of membrane morphology by interpretation of scanning electron microscopy images, J. Membr. Sci., 233 (2004) 119-127.

[116] J.I. Calvo, A. Hernández, P. Prádanos, L. Martınez, W.R. Bowen, Pore size distributions in microporous membranes II. Bulk characterization of track-etched filters by air porometry and mercury porosimetry, J. Colloid Interface Sci., 176 (1995) 467-478.

[117] C. Torras, D. Puig, M. Ángel García, A new method to quantify parameters of membrane morphology from electron microscopy micrographs by texture recognition, Chem. Eng. Sci., 66 (2011) 4582-4594.

ANNEX 1

In this annex is detailed the function programmed with Matlab and presented in the chapter 5.

```
function SimC
% Generates porous membrane 2D cross-section images
%
%  SimC
%  Generates porous membrane 2D cross-section images
%
%  INPUT:
%  Type of correlation: linear, power, exponential
%  Minimum pore size
%  Maximum pore size
%  Width of the membrane
%  Simulate random macrovoids or not. If yes:
%    Place: random, big as the membrane width, at the top or bottom side
%    Number: few, large, medium
%
%  OUTPUT: 2D Image
%
%  BUG REPORT:
%  Please send your bug reports, comments and suggestions to
%  ctorras@irec.cat . Thanks.

%  Author:  Carles Torras
%           Bioenergy and Biofuels Division
%           Catalonia Institute for Energy Research
%           C/ Marcel·lí Domingo, 2. 43007 Tarragona - Catalonia - Spain
%           ctorras@irec.cat
%  Collaborators: C. Nurra, R. Carraud, D. Puig, M. A. García, S. Pertuz
%  Version: alpha       Revision: Sep. 10, 2014

correlacio = input('(1)-lineal, (2)-power, (3)-exp? ');
midamin = input('Mida mínima? ');
midamax = input('Mida màxima? ');
ample = input('Ample: (0) per defecte o n° desitjat: ');
gen = input('Vols generar macrovoids (1-si)? ');

if gen == 1
    tipus = input('(1)-aleatoris, (2)-totals, (3)-superiors, (4)-mig? ');
    quants = input('(1)-molts, (2)-pocs, (3)-mig? ');
end

if ample == 0
    ample = 30. * (midamin + midamax) / 2.;
end

llarg = ample;

if correlacio == 1
    % y = a + b * x
    b = (midamax - midamin) / ample;
    a = midamin;
elseif correlacio == 2
    % log y = log a + b * log x
    y = [midamin midamax];
    x = [0.0001 ample];
    p = polyfit(log(x),log(y),1);
    b = p(1);
    a = exp(p(2));
elseif correlacio == 3
    % y = a * exp (x * b)
    y = [midamin; midamax];
    x = [0.0001; ample];
```

```
    p = fit(x,y,'exp1');
    b = p.b;
    a = p.a;
end

figure(1);
clf;
axis equal;
axis off;
hold on;
posx = 0; posy = 0;
facpsep = 2.4;
while posx <= ample;
    if correlacio == 1
        mida = a + b * posx; %disp(mida);
    elseif correlacio == 2
        if posx == 0
            mida = midamin; %disp(mida);
        else
            mida = a * posx^b; %disp(mida);
        end
    elseif correlacio == 3
        if posx == 0
            mida = midamin; %disp(mida);
        else
            mida = a * exp(posx * b); %disp(mida);
        end
    end
    posx = posx + mida * facpsep;
    while posy <= llarg;
        posy = posy + mida * facpsep;
        DrawCircle(posx, posy, mida, 32, 'b-');
    end
    posy = 0;
end

if gen == 1
    if quants == 1
        num = 20;
    elseif quants == 2
        num = 2;
    else
        num = 8;
    end
    for i = 1:num
        if tipus == 1
            posx = ample * rand(1,1) * (1. - 0.);
            posy = llarg * rand(1,1) * (1. - 0.);
            f1 = ample * rand(1,1) * (0.1 - 0.);
            f2 = ample * rand(1,1) * (0.1 - 0.);
        elseif tipus == 2
            posx = ample * rand(1,1) * (1. - 0.);
            posy = llarg/100.;
            f2 = ample * 0.1;
            f1 = ample * rand(1,1) * (0.2 - 0.1);
        elseif tipus == 3
            posx = ample * rand(1,1) * (1. - 0.);
            posy = llarg / 100.;
            f2 = ample * 0.02;
            f1 = ample * rand(1,1) * (0.2 - 0.1);
        elseif tipus == 4
            posx = ample * rand(1,1) * (1. - 0.);
            posy = llarg/2.;
            f2 = ample * rand(1,1) * (0.1 - 0.);
            f1 = ample * rand(1,1) * (0.2 - 0.1);
        end
        i=0;
        for tetha = 1:0.01:360
            i = i + 1;
            matrix(i,2) = (f1 * (1. - sin(tetha)) * cos(tetha)) + posx;
            matrix(i,1) = (-f2 * 5. * (sin(tetha) - 1.)) + posy;
        end
```

```
        matrixx = sortrows(matrix,1);
        fill(matrixx(:,1),matrixx(:,2),'b');
    end
end

disp('');
disp(['Mida mínima: ' num2str(midamin)]);
disp(['Mida màxima: ' num2str(midamax)]);
disp(['Ample: ' num2str(ample)]);
disp(['Llarg: ' num2str(llarg)]);
print -dbmp -r1200 'figure.bmp';

end
```

```
function DrawCircle(x, y, r, nseg, S)
% Draw a circle on the current figure using ploylines
%
%  DrawCircle(x, y, r, nseg, S)
%  A simple function for drawing a circle on graph.
%
%  INPUT: (x, y, r, nseg, S)
%  x, y:    Center of the circle
%  r:       Radius of the circle
%  nseg:    Number of segments for the circle
%  S:       Colors, plot symbols and line types
%
%  OUTPUT: None
%
%  BUG REPORT:
%  Please send your bug reports, comments and suggestions to
%  pengtao@glue.umd.edu . Thanks.

%  Author:  Tao Peng
%           Department of Mechanical Engineering
%           University of Maryland, College Park, Maryland 20742, USA
%           pengtao@glue.umd.edu
%  Version: alpha       Revision: Jan. 10, 2006


theta = 0 : (2 * pi / nseg) : (2 * pi);
pline_x = r * cos(theta) + x;
pline_y = r * sin(theta) + y;

% plot(pline_x, pline_y, S);
fill(pline_x, pline_y, 'k');
```

UNIVERSITAT ROVIRA I VIRGILI
SEPARATION PROCESSES IN MICROALGAE BIOREFINING
Claudia Nurra

THESIS OUTPUTS

In this section are presented pubblications, posters and oral presentations borned from the work performed during the PhD studies and detailed in the previous chapters.

Journals

[1] **C. Nurra**, E. Clavero, J. Salvado, C. Torras. Vibrating membrane filtration as improved technology for microalgae dewatering. Bioresource Technology 157 (2014) 247−253.

[2] **C. Nurra**, C. Torras, E. Clavero, S. Rios, M. Rey, E. Lorente, X. Farriol, J. Salvado. Biorefinery concept in a microalgae pilot plant. Culturing, dynamic filtration and steam explosion fractionation. Bioresource Technology 163 (2014) 136−142.

[3] **C. Nurra**, E.A. Franco, M.L. Maspoch, J. Salvadó, C. Torras. Cheaper membrane materials for microalgae dewatering. Journal of Material Science (2014). DOI10.1007/s10853-014-8408-8.

[4] **C. Nurra**, E. Clavero, J. Salvado, C. Torras, Dynamic filtration and cheap membranes to decrease microalgae dewatering cost, 22nd European Biomass Conference and Exhibition, 23-26 June 2014, Hamburg, Germany.

<u>In progress</u>

[5] **C. Nurra**, L. Pitol-Filho, R. Carraud, S. Pertuz, D. Puig, M.A. García, J. Salvadó and C. Torras, Towards the prediction of porous membrane permeability from morphological data.

[6] **C. Nurra**, S. Abelló, J. Pasqualino, M. Makkee, J. Salvadó and C. Torras, Towards the characteristics of a catalytic membrane reactor for transesterification.

[7] T. Saucedo, **C. Nurra**, G. Gonzalez, L. Muñoz, C Torras, L. Ballinas, Membrane from sawdust of Pinus for microalgae filtration.

Oral presentations

[1] **C. Nurra**, E. Clavero, J. Salvadó, C. Torras, Membrane materials for microalgae concentration, Network young membranes (NYM 13) Enschede, July 21st 2011.

[2] **C. Nurra**, S. Abelló, J. Pasqualino, M. Makkee, J. Salvadó and C. Torras, Transesterification with heterogeneous catalyst in membrane reactors, CITEM2014, Santander, Spain, May 27th 2014.

[3] C. Torras, **C. Nurra**, E. Clavero, E. Lorente J. Salvadó and, Commissioning of a Microalgae Cultivation & Harvesting Pilot Plant and Development of a Feasibility Analysis Tool, 22nd Biomass Conference and Exhibition, Algae Event, Hamburg, Germany, June 25th 2014.

[4] **C. Nurra**, S. Ríos, E. Clavero, J. Salvadó and C. Torras, Dynamic Filtration and cheap membranes to decrease microalgae dewatering cost, 22nd Biomass Conference and Exhibition, Hamburg, Germany, 26th June 2014.

Poster presentations

[1] **C. Nurra**, E. Clavero, J. Salvadó, C. Torras, Membrane materials for microalgae concentration, International Congress of Membranes and Membrane Processes (ICOM 2011), July 26th 2011.

[2] **C. Nurra**, S.D. Rios, S. Şirin, J. Salvadó, C. Torras, Microalgae concentration in the biorefining process. VII Barcelona Global Energy Challenges, Barcelona, Spain, 28-29 June 2012.

[3] **C.Nurra**, Ester Clavero, Joan Salvadó, C. Totorras, Vibrating and conventional membrane filtration, 10th Doctoral day, URV Tarragona, Spain, 24th April 2013.

UNIVERSITAT ROVIRA I VIRGILI
SEPARATION PROCESSES IN MICROALGAE BIOREFINING
Claudia Nurra

ABOUT THE AUTHOR

Claudia Nurra was born on the 19th of September 1984 in Sassari, Italy. After finishing her high school in this city she moved to Lombardia to start Environmental Engineering at the University of Pavia, Italy. During those years she had the possibility to do an internship at the R&D section of VEOLIA EAU in Saint Malo, France.

She obtained her Msc degree in Environmental Engineering in 2010 and after it, on September 2010, she started her PhD thesis in the Bioenergy and Biofuels division of the Catalonia Institute for Energy Research (IREC) under the supervision of Dr. Carles Torras Font, in a project entitled “Separation processes in microalgae biorefining”. During this work she (co)supervised 3 Msc students for a research project in the laboratory. She participated on the design, construction (installations + equipment purchasing) and commissioning of IREC laboratories. She participated to the numerous European and National projects. She collaborated with several groups (national and international), with the opportunity of developing part of a work as guest student in the excellent research group of Delft University of Technology in the Catalysis Engineering section.

The results described in this Thesis and the multiple collaborations, with colleagues from the IREC and abroad, have led to 3 publications in international journals already published, other 3 ready for pubblication, and have been presented at numerous (international) conferences in the form of oral or poster presentations.

UNIVERSITAT ROVIRA I VIRGILI
SEPARATION PROCESSES IN MICROALGAE BIOREFINING
Claudia Nurra

ACKNOWLEDGEMENTS

First of all I would like to thank my supervisor Carles Torras for its constant support. Em vas donar la benvinguda a Catalunya, em vas donar confiança en la meva competència durant aquests quatre anys i em vas animar a fer-ho el millor possible. Em vas donar l'oportunitat d'aprendre un munt de nous concepte, tant durant les discussions científiques i en les experimentals. Jo mai t'agrairé prou l'orientació contínua, la paciència i tot l'esforç que vas fer perquè aquesta tesi sigui un èxit. Realment gràcies no només per la teva professionalitat com a supervisor, sinó també per donar-me sempre un dia somrient. Carles moltíssimes gràcies!

I would also like to thank the rest of the groups' staff Joan Salvadó, Esther Clavero, Daniel Montané, Sonia Abelló, Maria Rey, César Berrueco, Esther Lorente, Gloria Ramirez, Javier Recari, Francesc Valls, Sema Sirin, Jorgelina Pasqualino and Sergio Rios. I am thankful to all of you for the great moments, the shared situations and significant discussions. It has been a brilliant experience, working that close to you as a real team. I also want to thank Elena, Detta and David for the nice time passed together.

Besides, I would like to thank those who I have had the pleasure to collaborate with, even though their contribution is in this thesis or in common publications, I have learnt from everyone and shared interesting discussions. Among these people are Edgar Adrian Franco, Maria Lluïsa Maspoch, Luizildo Pitol-Filho, Said Pertuz, Domènec Puig, Miguel Ángel García and a special thanks to Lourdes Ballinas and Tania Saucedo for the good moments.

I also want to thank the Master students Najat, Raphaelle and Eduard, because at the same time they learnt they taught something to me.

I also want to thank the personal of the URV microscopy service Mercè, Mariana, Nuria, Rita and Lukas for their support and agreeable time passed together.

My collaboration abroad was at the University of Delft, Catalysis Engineering Department of the Faculty of Applied Sciences, where I am really thankful to Michiel Makkee for the excellent opportunity. I want to specially thank Tania Rodenas for showing me everything you had developed, and being a great company within Francesc Sastre and Maria Armiento. I also want to thank Freek Kaptejin and Jorge Gascon for the interesting comments and discussions. Kevin Mouthaan and Harrie Jansma for their technical help, but also the whole group for giving me a very pleasing stay.

I acknowledge the committee members of my PhD defense, Prof. Dr. J. Salvadó, Prof. Dr. Albert Ibarz, Prof. Dr. Ir. M. Makkee, Prof. Dr. Xavier Farriol, Prof. Dr. Jorge Gascon, Prof. Dr. Jordi Pagán-Gilabert and Prof. Dr. Clemens Posten. Thank you for accepting my invitation, even though some of you come from very far away, and for the attention you conferred to my thesis and all the valuable comments. Especially thanks to Michiel Makkee for his level of detail and his contributions to my work.

I am also grateful to the Catalonia Institute for Energy Research (IREC) for her PhD scholarship. This work was supported by the projects: ENE2011-22761 “Biorrefineria de microalgas: optimizacion de las etapas de cosechado y de obtencion de lipidos” funded by the Spanish Ministry of Science and Innovation; “Fuels from Biomass “(research program

funded by Excma. Diputacio Tarragona); “Demostracion del cultivo y procesado de algas en sistemas semicerrados con fertilizacion carbonica en el entorno de la refineria de Repsol en Tarragona”, funded by Spanish Ministry of Science and Innovation (Plan E) “Valorización do soro de leite mediante a produción de bioetanol e dun novo produto con propiedades anti-hipertensivas” funded by Vigo University and “Separation de peptides en suero mediante processos de filtration por membrane” funded by Queizúar SL. The research was also supported by the European Regional Development Funds (ERDF, FEDER Programa Competitividad de Catalunya 2007−2013).

Doing the PhD abroad makes you realize how important friends and family are. I want to thank all my friends in Spain; it is also because of them that I passed four great years in here. You were not only my friends but also my confidents and family in here. Le quiero dar las gracias especialmente a todos los amigos del aula Pont y en particular a Daniel y Judith por su afectuosa amistad, Kelly para sus fantásticas arepas, su bienvenida y su cariño desde que llegué, Carmen y Eloi para ser siempre presentes y en la primera línea en todos los momentos. También quiero darle las gracias a quien ha compartido conmigo sobretodo los primeros años de este camino como Luis y Romain y también Ester para estar conmigo compartirlo todo y ayudarme mucho desde mi llegada. Küçük karde ime te ekkürler Sema, because you are among the best people I have ever met and you will always have me as a friend.

Quiero darle las gracias a “los de la isla”, a Magda, Ramon, Brian, Jorge, Arturo, Sandra, Elena, Iliana, Andri, Janine y todos los demás Gracias para dar un pellizco de “salsa” a mis días. También gracias a Mari que me acogió en su “dent de rata” como si fuera mi casa y me regaló momentos de evasión en esta ultima tapa de mi tesis.

I also would like to thank my friends in Italy because even from far they could be present in my day life. Ringrazio tutti gli amici di Sennori la “house of lions” e la “house of lionesses” per la loro incondizionata amicizia e sostegno che mi accompagnerà sempre. In particolare ringrazio Sara, Lello e Aida che hanno sempre trovato il modo di starmi vicina, Alessio e Mariella con il loro coinvolgimento nei miei e loro progetti di vita, Giovanni che mi ha sempre regalato gioia e spronata ad essere me stessa, Stefano che mi ha sostenuta nelle mie scelte e incoraggiata a continuare. E gli amici di Pavia: Erika e Fabrizio per essere sempre presenti e per darmi tanta allegria, Daria che prende il primo volo disponibile per poter passare svariati fine settimana con me sin dal mio primo giorno qui a Tarragona, Sara con la sua positività, Mariam con la sua impetuosità, Valentina con la sua forza e dolcezza.

Camille, personne peut me donner le que tu as pu, ta capacité me soutenir et me donner sérénité a été très grande et importante pour moi. Merci pour toute ta compréhension avec moi et pour réussir me rendre une personne meilleure. Thomas merci pour ton continue itères et les précieuses idées sur les abeilles. Yohann, Marine, Maryse et Gilles pour votre soutien et votre positivité. Célestin pour la joie que tu as amené dans la famille.

Finally, I want to thank my family. Non potrò mai spiegare a parole quanto vi sono grata e quanto è importante per me il vostro amore, sostegno e il vostro esempio. Spero di poter fare lo stesso buon lavoro con i miei figli come voi l’avete fatto con me.
Voglio ringraziare anche tutti i miei zii per sostenermi, cugini e nipoti per darmi allegria. In particolare mio padrino e madrina Cicci e Uccia, che lo sono sempre stati inconsapevolmente, due guide sempre presenti per me. Voglio, inoltre scrivere due parole per le persone amate

che non ci sono più, ma che sono più che mai presenti nei miei ricordi e nelle mie azioni di ogni giorno e che sempre lo saranno.